Online Analytics of Pectic Compound Degradation in Small-Scale Using *Ustilago Maydis*

Online-Analytik des Abbaus von Pektinbestandteilen in Kleinkultur mittels *Ustilago Maydis*

Von der Fakultät für Maschinenwesen der Rheinisch-Westfälischen Technischen Hochschule
Aachen zur Erlangung des akademischen Grades eines Doktors der Naturwissenschaften
genehmigte Dissertation

vorgelegt von

Markus Jan Müller

Berichter: Universitätsprofessor Dr.-Ing. Jochen Büchs
Universitätsprofessor Dr. rer. nat. Michael Feldbrügge

Tag der mündlichen Prüfung: 28. November 2019

Diese Dissertation ist auf den Internetseiten der Universitätsbibliothek online verfügbar.

Danksagung

Die vorliegende Dissertation entstand während meiner Tätigkeit als wissenschaftlicher Mitarbeiter am Lehrstuhl für Bioverfahrenstechnik der RWTH Aachen University. Die Arbeit wurde im Rahmen des Projekts "PectiLyse" angefertigt, welches durch das NRW-Strategieprojekt BioSC gefördert wurde.

Mein besonderer Dank gilt Professor Jochen Büchs für die Betreuung meiner Arbeit und die Gelegenheit, im Rahmen meiner Promotion viele lehrreiche und spannende Jahre am Lehrstuhl zu verbringen. Seine Unterstützung, Ideen und Impulse waren entscheidend für das Gelingen dieser Arbeit. Professor Michael Feldbrügge möchte ich für die Übernahme des Koreferats, aber auch für die angenehme und aufgeschlossene Zusammenarbeit im Rahmen des Projekts danken. Professor Klaus Rademacher danke ich für die Übernahme des Prüfungsvorsitzes.

All meinen Projektpartnern im PectiLyse-Projekt danke ich für die gute Zusammenarbeit, insbesondere Kerstin Schipper und Peter Stoffels für ihren fachlichen Einsatz und die konstruktiven Diskussionen.

Ich bedanke mich bei allen Kollegen und Freunden der BioVT für die gemeinsame Zeit und den unkomplizierten Umgang miteinander. Die vielen fachlichen Diskussionen und Vorträge haben mich persönlich wie beruflich sehr vorangebracht. Insbesondere danke ich Christoph Scheeren, der mich gerade am Anfang meiner Zeit in der BioVT unterstützt und begleitet hat. Meinen Bürokollegen danke ich für die vielen Diskussionen, die angenehme Büroatmosphäre sowie die Kaffeepausen und andere willkommene Ablenkungen. Im Speziellen möchte ich mich bei Benedikt Heyman, Timm Keil, Judith Loogen, Sarah Stachurski, Bertram Geinitz und Nina Ihling für die Korrekturen und das Feedback zu Publikationen und dem Promotionsvortrag bedanken. Ein großes Dankeschön möchte ich auch allen Freunden für die zahlreichen Unternehmungen außerhalb des Lehrstuhls aussprechen.

Meinen fleißigen Studenten Elia Track, Charlotte Deffour, Isabel Bator, Eva Forsten, Carina Michel, Sarah Stachurski, Daniel Reibert und Nina Sonntag danke ich für ihren Einsatz und die

vielen eigenen Ideen, die das Projekt vorangebracht haben. Außerdem bedanke ich mich bei René Petri und Stefan Taubert für die Unterstützung im Laboralltag.

Besonders danke ich meiner Familie für ihren Rückhalt und ihre Unterstützung in all den Jahren. Insbesondere danke ich meinen Eltern und meinem Bruder, die immer an mich geglaubt und mich in meinen Entscheidungen bestärkt haben. Außerdem möchte ich meinen Großeltern danken, von denen ich viel lernen konnte und die mich mit zu dem Menschen gemacht haben, der ich heute bin. Elly und Herbert konnten die Zeit meiner Promotion leider nicht mehr miterleben, werden aber immer in meinem Herzen sein. Nina danke ich dafür, dass sie mich am Lehrstuhl gefunden und vom ersten Tag an unterstützt hat. Besonders in den letzten Wochen und Monaten danke ich dir dafür, dass du für mich da warst und mir Mut zugesprochen hast, wenn ich es am ehesten gebraucht habe. Ich bin glücklich darüber, dich an meiner Seite zu haben.

Funding, publications and contributions

This work was conducted during my time as a research assistant at the chair of biochemical engineering at RWTH Aachen University. Part of this work was performed within the project "PectiLyse – Activation of intrinsic enzymes for plant biomass breakdown", funded by the Strategieprojekt BioSC (No. 313/323-400-002 13). Funding is gratefully acknowledged.

By the time of submission, aspects of this thesis have been published or are prepared for submission.

- Müller Markus Jan, Stachurski Sarah, Stoffels Peter, Schipper Kerstin, Feldbrügge Michael and Büchs Jochen. Online evaluation of the metabolic activity of *Ustilago* maydis on (poly)galacturonic acid. Journal of Biological Engingeering (2018) 12:34.
- Stoffels Peter*, Müller Markus Jan*, Stachurski Sarah, Terfrüchte Marius, Schröder Sebastian, Ihling Nina, Wierckx Nick, Feldbrügge Michael, Schipper Kerstin, Büchs Jochen. Complementing the intrinsic repertoire of *Ustilago maydis* for degradation of the pectin backbone polygalacturonic acid. Journal of Biotechnology (2020) 307:148-163.
 - * Both authors contributed equally

Research in the field of biochemical engineering often depends on close collaboration with other institutes of cognate disciplines. All *Ustilago maydis* strains that were evaluated within this thesis were generated and provided by the Institute for Microbiology, Prof. Dr. Michael Feldbrügge, Heinrich-Heine University Düsseldorf. Chapter 3 [Stoffels, Müller, *et al.* prepared for submission] focusses on the generation and characterization of *U. maydis* strains expressing pectinolytic enzymes of different origin. For a comprehensive description of the microbiological background, some of the most relevant methods and results obtained at the Institute for Microbiology were included here. Bioinformatic evaluation, cloning and offline testing of recombinant *U. maydis* strains (Chapters 3.2.1 - 3.2.8) were performed by P. Stoffels (Institute of Microbiology, Heinrich-Heine University Düsseldorf). Within these chapters, S. Schröder cloned and tested the strains expressing bacterial polygalacturonase

Zusammenfassung

Im Sinne einer nachhaltigen Bioökonomie stellen pektinreiche Biomasseströme ein wertvolles Substrat dar. Besonders pektinhaltig sind z.B. Zitrusschalen, Apfeltrester oder Zuckerrübenschnitzel. Für einen effizienten Abbau muss der angewandte Organismus eine Vielzahl von Enzymen produzieren. Dies ist entscheidend für eine effiziente Verwertung der Pektinfraktion. Pektin besteht zum Großteil aus Galakturonsäure-Monomeren. Es kann nicht von etablierten Organismen wie *Saccharomyces cerevisiae* metabolisiert werden. Daher ist ein Mikroorganismus erforderlich, der gleichzeitig Pektin metabolisieren und hochwertige Produkte herstellen kann. Aufgrund seiner Komplexität ist die Analyse von Pektin jedoch herausfordernd. Daher sind neue Online-Überwachungssysteme für Bioprozesse erforderlich.

Zunächst wurde ein Verfahren zur Bestimmung der verbleibenden Galakturonsäurekonzentration während des Wachstums von *Ustilago maydis* im Schüttelkolben entwickelt. Die Konzentration während der Kultivierung wurde basierend auf dem online gemessenen Gesamtsauerstoffverbrauch ermittelt und durch Offline-Probenahmen verifiziert. Anschließend wurde diese Methode auf komplexere, schwer zu quantifizierende Substrate ausgeweitet. Es wurde der Einfluss der Expression einer Exo-Polygalakturonase aus *Aspergillus tubingensis* auf das Wachstum auf Polygalakturonsäure untersucht. Durch Hinzufügen von Endo-Polygalakturonase exprimierenden *U. maydis*-Stämmen wurden anschließend Co-Kulturen untersucht. Auf Pektin und Zuckerrübenschnitzel wurden Co-Kulturen mit externen Enzymen supplementiert.

Die Vorhersage der Restsubstratkonzentration basierend auf dem Gesamtsauerstoffverbrauch wurde etabliert und im Kleinkulturmaßstab validiert. Basierend auf dieser Methode wurde eine Co-Kultur von *U. maydis*-Stämmen identifiziert, die Endo- und Exo-Polygalakturonasen exprimieren und Polygalakturonsäure effizient metabolisieren kann. Durch die Supplementierung mit externen Enzymen konnte eine Metabolisierung von Zuckerrübenschnitzeln erreicht werden. Die vorgestellte Methode kann angewendet werden, um die verbleibende Konzentration von Komplexsubstraten abzuschätzen, die derzeit schwierig zu quantifizieren sind. Dies wird die Entwicklung konsolidierter Bioprozesse unterstützen.

II Abstract

Abstract

In the spirit of a circular bioeconomy, pectin-rich biomass waste streams represent a valuable substrate for a biorefinery process. Particularly rich in pectin are, e.g., citrus peel, apple pomace or sugar beet pulp. For efficient degradation, the applied organism should produce a diverse mixture of cellulases, hemicellulases and pectinases. This is essential for efficient and economic valorization of the pectin fraction. Pectin is mainly composed of galacturonic acid monomers. It is not metabolized by well-established organisms, such as *Saccharomyces cerevisiae*. Thus, a microbial production system capable of metabolizing pectin and producing high-value products is required. However, due to its complexity, analysis of pectin is challenging. Thus, new online monitoring tools for bioprocesses are required.

A method for the online determination of residual substrate was developed for the growth of *Ustilago maydis* on pectic compounds. Cultivations were carried out in shake flasks with online monitoring of the respiration activity. The residual galacturonic acid concentration during cultivation was predicted based on the overall oxygen consumption and verified by offline sampling. Afterwards, this method was extended towards polygalacturonic acid, pectin and sugar beet pulp, which are challenging to quantify. The influence of heterologous expression of an exo-polygalacturonase on *U. maydis* growth on polygalacturonic acid was investigated. Co-cultivation of *U. maydis* strains expressing endo- and exo-polygalacturonases were conducted on polygalacturonic acid and compared to axenic cultivation. Co-cultivations on pectin and sugar beet pulp were supplemented with external cellulases and pectinases.

Prediction of the residual substrate concentration based on the overall oxygen consumption was established and validated in small-scale. Based on this method, a co-culture of *U. maydis* strains expressing fungal endo- and exo-polygalacturonases was identified to be highly efficient in the metabolization of polygalacturonic acid. On pectin or sugar beet pulp, cultures required supplementation with external enzymes to convert half of the complex substrates. The introduced method can be applied to estimate the amount of consumed complex substrates which are currently challenging to quantify. This will support the development of consolidated bioprocesses.

Contents

Zusar	mmenfassung	I
Abstr	ract	II
Conte	ents	III
Abbr	eviations	VI
Symb	ools	III
List o	f Figures and Tables	VIII
List o	f Appendix Figures and Tables	X
1 Intr	oduction	1
1.1	Consolidated bioprocessing of pectin-rich biomass	1
1.2	Pectin structure and analytics	2
1.3	Enzymatic pectin degradation	3
1.4	Ustilago maydis as potent model organism for CAZyme production	4
1.5	Online monitoring of biomass hydrolysis	6
1.6	Objectives and overview	7
	ine evaluation of the metabolic activity of Ustilago maydis on galacture	
poly	galacturonic acid	9
2.1	Introduction	9
2.2	Materials and methods	10
	2.2.1 Microorganisms	10
	2.2.2 Cultivation media and cultivation conditions	10
	2.2.3 Cultivation with online monitoring and offline sampling	11
	2.2.4 Offline analysis	12
	2.2.4.1 Optical density	12
	2.2.4.2 pH value	12

IV Contents

	2.2.4.3 Ammonia	12
	2.2.4.4 Quantification of carbon sources	12
	2.2.4.5 Cell dry weight	13
	2.2.4.6 Enzymatic activity via reducing sugar assay (DNS assay)	13
2.3	Online monitoring of <i>U. maydis</i> growth on GalA	14
2.4	Correlation of oxygen uptake with consumed GalA	18
2.5	Characterization of growth on PolyGalA	22
	2.5.1 Influence of initial glucose concentration on enzyme expression	25
	2.5.2 Investigation of enzyme stability by substrate pulsing	29
2.6	Conclusion	32
3 Con	aplementing the intrinsic repertoire of <i>Ustilago maydis</i> for degradation of the	ρ
	in backbone polygalacturonic acid	
3.1	Introduction	
3.2	Material and methods	
	3.2.1 Plasmids, strains and media	
	3.2.2 Microscopic analyses	
	3.2.3 Bioinformatic evaluation	38
	3.2.4 Preparation of cell extracts	39
	3.2.5 Protein precipitation from culture supernatants	39
	3.2.6 SDS-Page and Western blot analysis	39
	3.2.7 Protein deglycosylation	40
	3.2.8 Offline polygalacturonase activity assay	40
	3.2.9 Online measurement of the metabolic activity	41
	3.2.10 Offline analytics	41
	3.2.11 Determination of liberated GalA during RAMOS cultivations	42
3.3	Inventory of intrinsic enzymes for pectin degradation and metabolization	42
3.4	Activation of an intrinsic endo-polygalacturonase	46
3.5	Complementation with unconventionally secreted, heterologous, bacterial	
	polygalacturonases	47
3.6	Complementation with conventionally secreted heterologous fungal	
	polygalacturonases	50

3.7	Following the physiological parameters during growth on PolyGalA using	
	RAMOS	53
3.8	Characterizing co-fermentations using RAMOS	56
3.9	Conclusion	61
4 Ann	olication of online measurement tools for the investigation of microbial and	
	ymatic pectin degradation	63
4.1	Introduction	
4.2	Material and methods	
1,2	4.2.1 Microorganisms	
	4.2.2 Pectin and sugar beet pulp composition	
	4.2.3 Cultivation media, external enzymes and cultivation conditions	
	4.2.4 Cultivation with online monitoring in the RAMOS or μRAMOS device	
4.3	Simultaneous cultivation on multiple different pectic sugars	
4.4	Estimation of correlation factors for oxygen consumption and consumption of	
	complex pectic substrates	71
4.5	Growth on pectin	
	4.5.1 Influence of pectin characteristics	
	4.5.2 Influence of external enzyme additions	
4.6	Growth on sugar beet pulp	
4.7	Conclusion	
5 Sun	nmary and outlook	87
Biblio	ography	i
Appe	ndix	xix
Appe	ndices for Chapter 2	xix
Appe	ndices for Chapter 3	xxiii
Annei	ndices for Chanter 4	vvvi

VI Abbreviations

Abbreviations

Abbreviation	Description
A. aculeatus	Aspergillus aculeatus
A. niger	Aspergillus niger
A. tubingensis	Aspergillus tubingensis
AP-he	high esterified apple pectin
AP-le	low esterified apple pectin
CAZyme	carbohydrate-active enzyme
Cbx	carboxin
CM-Glc	complex medium, supplemented with 10 g/L glucose
c-Tr	cellulase from T. reesei
DNA	deoxyribonucleic acid
DNS	3,5-dinitrosalicylic acid
DTT	dithiothreitol
E. coli	Escherichia coli
EDTA	ethylenediaminetetraacetic acid
ER	endoplasmic reticulum
f.c.	final concentration
GalA	galacturonic acid
$GalA_0$	galacturonic acid at cultivation start
HRP	horseradish peroxidase
IgG	immunoglobulin G
MES	2-(N-morpholino)ethanesulfonic acid
MOPS	3-(N-morpholino)propanesulfonic acid
Nat	nourseothricin
NCBI	National Center for Biotechnology Information
P. carotovorum	Pectobacterium carotovorum
p-Aa	pectinase from A. aculeatus
p-An	pectinase from A. niger
PCR	polymerase chain reaction
PMSF	phenylmethylsulfonylfluorid
PolyGalA	polygalacturonic acid
PVDF	polyvinylidene fluoride
RAMOS	respiration activity monitoring system
S. cerevisiae	Saccharomyces cerevisiae
SDS	sodium dodecyl sulphate
SHH	Strep-tripleHA(hemagglutinin)-decahistidine
sp.	species
SP-he	high esterified sugar beet pectin
T. reesei	Trichoderma reesei
TCA	trichloric acid
U. maydis	Ustilago maydis
C. mayais	Simago mayans

Symbols

Symbols

Abbreviation	Description	Unit
An	absorption at n nm	-
CF	correlation factor	mmol/g
cS	molar concentration of substrate S	mol/L
CTR	carbon dioxide transfer rate	mmol/L/h
E	enzyme activity	U/mL
GalA0	galacturonic acid concentration at cultivation start	g/L
(Poly)GalAcalc	calculated residual (poly)galacturonic acid concentration	g/L
GalAcon	concentration of overall consumed GalA	g/L
GalAlib	liberated amount of GalA	g/L
GalAsup	concentration of GalA in culture supernatant	g/L
KI	kinetic inhibition coefficient	mol/L
mCF	mixed correlation factor	mmol/g
MW	molecular weight	g/mol
OD600	optical density at 600 nm	-
OT	overall oxygen consumption	mmol/L
OTR	oxygen transfer rate	mmol/L/h
OTR*	oxygen transfer rate at plateau phase	$\mu mol/mL/min$
pKa	logarithmic acidity constant	-
RQ	respiratory quotient	-
RQtheo	theoretical (calculated) RQ	-
T	temperature	$^{\circ}\mathrm{C}$
VL	filling volume (liquid fraction)	mL
X	biomass	
YXS	yield coefficient (biomass per substrate)	gX/gS
ν	stoichiometric coefficient	-

List of Figures and Tables

Figure 1-1 Schematic structure of the most abundant pectin classes (homogalacturonan and	
rhamnogalacturonan I) and relevant enzymes for degradation.	4
Figure 1-2: Process scheme of PolyGalA degradation.	7
Figure 2-1: Cultivation of <i>U. maydis</i> AB33P5ΔR on GalA	. 16
Figure 2-2: Cultivation of <i>U. maydis</i> AB33P5ΔR/AtPgaX with varying GalA and buffer concentrations.	. 19
Figure 2-3: Correlation of overall oxygen consumption and produced biomass to initial GalA concentration.	. 21
Figure 2-4: Cultivation of <i>U. maydis</i> AB33P5ΔR and AB33P5ΔR/AtPgaX on (Poly)GalA	. 24
Figure 2-5: Cultivation of <i>U. maydis</i> AB33P5ΔR/AtPgaX on PolyGalA with varying initial glucose concentrations.	
Figure 2-6: Comparison of enzymatic activity determined from offline (DNS) and online (OTR) measurements	. 28
Figure 2-7: Influence of PolyGalA pulses on the cultivation of <i>U. maydis</i> AB33P5ΔR/AtPgaX	. 31
Figure 3-1: Conservation of a putative endo-polygalacturonase of <i>U. maydis</i> .	. 44
Figure 3-2: Metabolization of GalA. Conservation of the GalA catabolic pathway between <i>A. niger</i> and <i>U. maydis</i>	. 45
Figure 3-3: Activation of an intrinsic endo-polygalacturonase.	. 47
Figure 3-4: Complementation with bacterial endo- and exo-polygalacturonases.	. 49
Figure 3-5: Complementation with fungal endo- and exo-polygalacturonases	. 51
Figure 3-6: Co-fermentations of fungal endo- and exo-polygalacturonases.	. 53
Figure 3-7: Cultivation of the UmPgu1 (endo-polygalacturonase) overexpression strain on GalA and PolyGalA	
Figure 3-8: RAMOS cultivation of axenic cultures and co-fermentations on PolyGalA	. 57

Figure 3-9: Co-fermentation of AtPgaX (fungal exo-polygalacturonase) and AaPgu1 (fungal endo-
polygalacturonase) overexpression strains with different inoculation ratios on PolyGalA.
Figure 3-10: GalA liberation rate during co-fermentation of AtPgaX (fungal exo-polygalacturonase)
Figure 3-10: GalA liberation rate during co-fermentation of AtPgaX (fungal exo-polygalacturonase) and AaPguI (fungal endo-polygalacturonase) overexpression strains (inoculation ratio 5:1) on PolyGalA
Figure 4-1: Overview of evaluated process parameters. 64
Figure 4-2: Axenic cultivation of U . $maydis$ AB33P5 Δ /AtPgaX and AB33P5 Δ /AaPgu1 on GalA 67
Figure 4-3: Substrate preference of an <i>U. maydis</i> co-fermentation for different pectic sugars
Figure 4-4: Comparison of <i>U. maydis</i> co-fermentation growth on different pectins
Figure 4-5: Influence of external enzymes on <i>U. maydis</i> co-fermentation on sugar beet pectin SP-he.78
Figure 4-6: Influence of external pectinase on <i>U. maydis</i> axenic and co-fermentation on high esterified
apple pectin AP-he80
Figure 4-7: Influence of external enzymes on <i>U. maydis</i> co-fermentation on sugar beet pulp
Table 2-1: List of applied microorganisms and their origin
Table 2-2: Stoichiometric coefficients and RQ _{theo} for carbon balance
Table 3-1: DNA oligonucleotides used in this chapter
Table 3-2: <i>U. maydis</i> strains used in this chapter
Table 4-1: Composition and characteristics of pectin and sugar beet pulp
Table 4-2: Experimentally determined correlation factors (CFs) for oxygen and sugar consumption. 72
Table 4-3: Experimentally determined mCFs for oxygen and pectin / sugar beet pulp consumption 73

List of Appendix Figures and Tables

Figure A1: Exemplary calibration curve for offline DNS assay on reducing groups	xix
Figure A2: Comparison of <i>U. maydis</i> AB33P5ΔR cultivation in modified Verduyn medium wi without vitamin supplementation	
Figure A3: RQ during the cultivation of <i>U. maydis</i> AB33P5ΔR on GalA (same cultivation as single Figure 2-1).	
Figure A4: Development of the pH value during the cultivation of <i>U. maydis</i> AB33P5ΔR/AtPg GalA (same cultivation as shown in Figure 2-2).	
Figure A5: Control cultivation of <i>U. maydis</i> AB33P5ΔR/AtPgaX on glucose and PolyGalA	xxii
Figure A6: Conservation of putative pectin lyase and pectin methylesterase of <i>U. maydis</i>	xxiii
Figure A7: Exemplary definition of (Poly)GalA consumption phase during co-fermentation of <i>U. maydis</i> on PolyGalA.	
Figure A8: The morphology of strains overexpressing pectinases is not disturbed	xxv
Figure A9: Biological duplicates of axenic culture and co-fermentations on PolyGalA	xxvi
Figure A 10: Axenic cultivation of <i>U. maydis</i> AB33P5Δ on different pectic sugars	xxxi
Figure A 11: Axenic cultivation of <i>U. maydis</i> AB33P5ΔR/AaPgu1 and AB33P5ΔR/AtPgaX or SP-he.	•
Figure A 12: Axenic cultivation of <i>U. maydis</i> on pectin AP-he	xxxiii
Figure A 13: Axenic and co-fermentation of <i>U. maydis</i> on differently pretreated sugar beet pul	p. xxxiv
Table A1: Validation of complete glucose consumption.	xxvi
Table A2: Intrinsic repertoire for pectin degradation	xxvii

Chapter 1

Introduction

1.1 Consolidated bioprocessing of pectin-rich biomass

The microbial fermentation of biomass waste streams originating from agriculture and forestry provides a huge potential for a sustainable and value-added bioeconomy [Kamm and Kamm 2004]. The sugars required as a carbon source for fermentation usually originate from lignocellulosic biomass that has for example been thermochemically pretreated and enzymatically hydrolyzed [Edwards and Doran-Peterson 2012, Klement, *et al.* 2012, Rinaldi, *et al.* 2010]. The main fractions of all biomasses are cellulose, hemicellulose and lignin. However, the share of the fractions depends on the origin of the biomass [Anders, *et al.* 2015, Rivas, *et al.* 2008]. A fourth fraction, often not taken into account, is pectin. Very little is known about the pectin content in wooden biomass. It is assumed to be neglectable with about 1-4% [BeMiller 2001]. Other biomass such as apple pomace, citrus peel or sugar beet pulp are rich in pectin with a content of up to 30% [Doran, *et al.* 2000, Edwards and Doran-Peterson 2012, Rafiq, *et al.* 2016]. The efficient utilization of those biomasses in consolidated bioprocessing requires hydrolysis and consumption of pectin. A chemical 2-step hydrolysis process already enabled ethanol formation of *Saccharomyces cerevisiae* on orange peel [Oberoi, *et al.* 2010]. However, the pectin fraction remained unused in that study.

Sugar beet pulp is an abundant but low-value by-product of the sugar industry. During industrial processing of 1 t of sugar beet, 250 kg of sugar beet pulp are produced [Pfeifer & Langen, personal communication]. Europe alone produces around 20 million tons of wet sugar beet pulp per year, with a dry matter content of 6-12% [Joanna, *et al.* 2018]. Most of the dried, fiber-rich sugar beet pulp is used as animal feed [Feedimpex 2019]. However, the economic profit is limited due to drying costs [Edwards and Doran-Peterson 2012]. Hence, up-cycling of sugar beet pulp would be advantageous. One approach is the utilization for production of high-value products in a consolidated bioprocess. Therefore, the respective microorganisms must be able to enzymatically hydrolyze the (pretreated) pectin-rich pulp to release fermentable sugars and, at the same time, produce a value-added product.

1.2 Pectin structure and analytics

Pectin is well-known as industrial gelling agents. It is commonly used in the food and cosmetic industry [May 1990, Willats, et al. 2006]. In plants, pectin reinforces the primary cell wall and is a major component of the middle lamella [Carpita 1996]. From a chemical perspective, pectin is a complex and branched heteropolysaccharide that can be divided in four structural classes [Glass, et al. 2013, Lampugnani, et al. 2018, Mohnen 2008]: homogalacturonan (Figure 1-1. left), rhamnogalacturonan I (Figure 1-1, right), rhamnogalacturonan II and xylogalacturonan. With about 60% (w/w), homogalacturonan is the most abundant polymer in pectin [Caffall and Mohnen 2009]. It consists of linear, α-(1,4)-linked galacturonic acid (GalA) units that are partially methylated or acetylated [Levigne, et al. 2002, Pedrolli, et al. 2009]. Polygalacturonic acid (PolyGalA) is a region in homogalacturonan lacking the esterifications. Rhamnogalacturonan I, rhamnogalacturonan II and xylogalacturonan consist of a heteropolymer backbone and several different side chains including numerous different sugars [Glass, et al. 2013]. As a result, a diverse set of hydrolytic enzymes is required for full enzymatic conversion of pectin-rich biomasses and waste streams [Glass, et al. 2013, Jayani, et al. 2005].

Analytics of polysaccharides usually requires acid hydrolysis for generation of sugar monomers or shorter oligomers [Anders, *et al.* 2015]. In case of pectic polymers, the degradation by acid hydrolysis is unfavorable for several reasons: Even harsh and elongated treatments do not

completely degrade the pectic polymers [Garna, et al. 2004]. In addition, the hydrolysis rate strongly depends on pH, temperature and the degree of methylation of the hydrolyzed pectin [Krall and McFeeters 1998]. Finally, GalA monomers irreversibly form lactones under the conditions of hydrolysis disabling the subsequent analysis of the released sugars [Blake and Richards 1968]. Consequently, methods for complete degradation of pectic polymers usually combine physical and enzymatic hydrolysis with high-performance anion-exchange chromatography [Daas, et al. 1999, Emaga, et al. 2012].

1.3 Enzymatic pectin degradation

The complete breakdown of biomass as carbon source for microbial fermentation requires numerous carbohydrate-active enzymes (CAZymes, [Lombard, et al. 2014]) for each component [Glass, et al. 2013, Jäger, et al. 2011, J Zhang, et al. 2018]. Since commercial enzyme cocktails represent the main running cost of a biorefinery, the importance of screening for and microbial production of hydrolytic enzymes for biomass breakdown has increased in the last decades [Jäger, et al. 2011, Mühlmann, et al. 2017, Ortiz, et al. 2017, J Zhang, et al. 2018].

Regarding enzymatic pectin degradation, a large set of CAZymes is needed for efficient pectin degradation due to its complex structure. [Jayani, *et al.* 2005]. Figure 1-1 shows some of the enzymes acting on homogalacturonan. Complete homogalacturonan degradation requires the efficient interplay of exo- and endo-polygalacturonases that in concert hydrolyze the PolyGalA backbone. Alternatively, pectate and pectin lyases can break the β-1-4 bonds by a transelimination mechanism yielding unsaturated (methyl)oligogalacturonates [Yadav, *et al.* 2009]. In addition, methyl-esterifications and *O*-acetylations of the PolyGalA backbone result in the additional need for pectin methylesterases and pectin acetylesterases [Senechal, *et al.* 2014]. Hydrolysis of other structural classes containing, among others, arabinose, rhamnose, galactose, fucose and xylose moieties, requires additional other hydrolytic enzymes [Glass, *et al.* 2013].

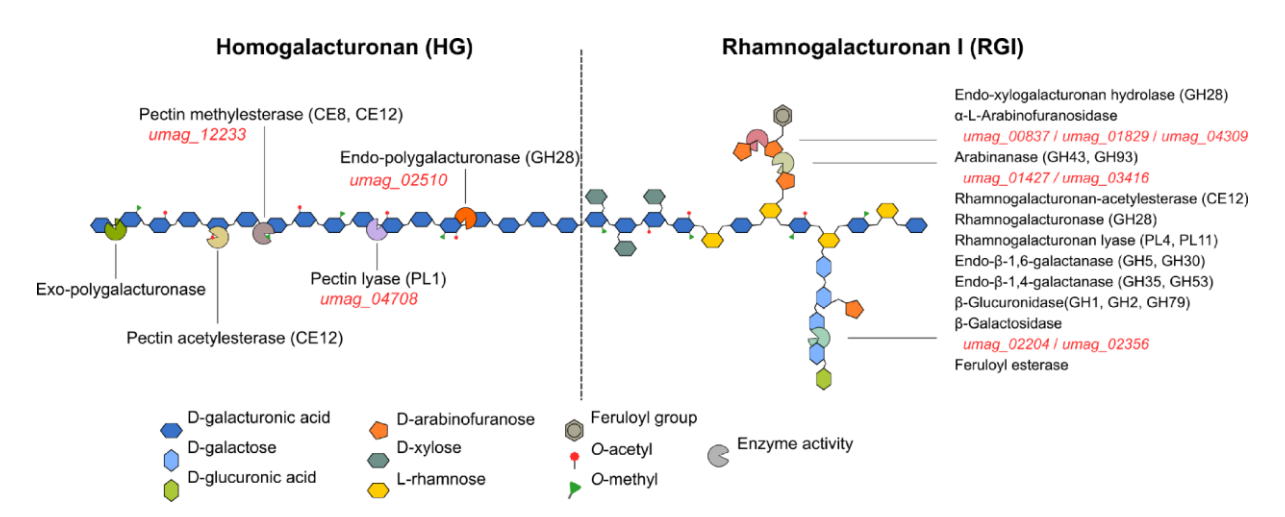


Figure 1-1 Schematic structure of the most abundant pectin classes (homogalacturonan and rhamnogalacturonan I) and relevant enzymes for degradation. Enzymes required for degradation of the two major pectin classes and their sites of action are depicted. Corresponding enzymatic domains according to CAZy database are provided in brackets. Glycoside hydrolase domain (GH), polysaccharide lyase domain (PL), carbohydrate esterase domain (CE) [AFMB 2018]. The *U. maydis* genome encodes some putative pectinolytic enzymes (corresponding *umag* identifiers indicated in red), especially for decomposition of the PolyGalA backbone in homogalacturonan and the arabinose side-chains of rhamnogalacturonan I.

1.4 *Ustilago maydis* as potent model organism for CAZyme production

A multitude of such pectinolytic enzymes is produced by filamentous fungi [de Vries 2003] and various bacteria [Jayani, et al. 2005]. S. cerevisiae is the workhorse for bioethanol production from lignocellulosic biomass [Branco, et al. 2018]. However, it does not produce intrinsic CAZymes for biomass degradation and does not naturally grow on many of the pectin components. Thus, recent research focused on extending it into a host for bioethanol production from pectin [Benz, et al. 2014, Biz, et al. 2016, Glauche, et al. 2017]. Filamentous fungi like Trichoderma reesei, Aspergillus niger or Neurospora crassa are promising alternatives as some of them are naturally equipped for pectin degradation [Glass, et al. 2013, Lara-Marquez, et al. 2011]. However, suitable high-value products are lacking and efficient culturing in bioreactors remains a challenge [Klement, et al. 2012, Papagianni, et al. 1998]. Utilization of Ustilago maydis is a further promising alternative to compete with current CAZyme production organisms that circumvents the drawbacks of filamentous fungi [Elena Geiser, et al. 2014, Paulino, et al. 2017]. U. maydis is the best-characterized member of the family of Ustilaginaceae. Originally, it was isolated as a phytopathogenic fungus, which provokes corn

smut disease. During the nonpathogenic stage, *U. maydis* grows in a yeast-like, unicellular form by budding with a haploid genome [Banuett and Herskowitz 1994]. This is the biotechnologically relevant form of *U. maydis*. In response to plant cues, *U. maydis* cells fuse and grow as dikaryotic filaments which invade the maize tissue [Garrido, et al. 2004, Hartmann, et al. 1999, Vollmeister, et al. 2012]. For efficient invasion, the fungus encodes a distinct set of hydrolytic enzymes that are required for traversing the plant cell wall (including among others xylanases, endoglucanases and β-glucosidases) [Cano-Canchola, et al. 2000, Couturier, et al. 2012, Doehlemann, et al. 2008, E. Geiser, et al. 2016]. Hence, it would be perfectly suited for pectin valorization. However, the CAZymes are mainly produced during the infections stage in the plant and not during the biotechnologically relevant yeast phase [Doehlemann, et al. 2008]. Hartmann, et al. [1999] addressed this problem and activated several CAZymes in the yeast phase by exchanging the native promoters of the respective genes by a strong artificial promoter. This enabled the detection of active enzymes during yeast-like growth and resulted in degradation of simple biomass-related substrates like cellobiose [E. Geiser, et al. 2016]. Additionally, as a proof of principle, itaconic acid was produced using cellobiose as sole carbon source [E. Geiser, et al. 2016].

Over the last decades, *U. maydis* has developed into a fungal model organism that is prominent for research on host-pathogen interaction, cell and RNA biology as well as homologous recombination and unconventional secretion [Djamei and Kahmann 2012, Vollmeister, *et al.* 2012]. Handling of *U. maydis* is well established. A versatile toolset for efficient genetic manipulation yielding genetically stable strains is available [Brachmann, *et al.* 2004, Khrunyk, *et al.* 2010, Schuster, *et al.* 2016, J. Stock, *et al.* 2012, Terfrüchte, *et al.* 2014]. Yeast-like growing cells are very robust and can easily be cultivated in submerged culture, including large-scale cultivation in bioreactors under elevated hydromechanical stress [Klement, *et al.* 2012]. The fungus can easily be transformed into a non-infectious, safe-to-use form [Feldbrügge, *et al.* 2013, Kahmann, *et al.* 1995]. In addition, it is innocuous to humans and infected plant parts are even relished as a delicacy called *Huitlacoche* in Central America [Feldbrügge, *et al.* 2013, Valverde, *et al.* 1995]. *U. maydis* does not only harbor the conventional secretion pathway for protein export via the endomembrane system but also an unconventional secretion route [Dimou and Nickel 2018, Reindl, *et al.* 2019]. This, unconventional secretion circumvents the endomembrane system and consequently the cognate post-translational modifications. This can

be essential for secretion of bacterial proteins coincidentally containing detrimental eukaryotic *N*-glycosylation sites [Koepke, *et al.* 2011, J. Stock, *et al.* 2012]. Export of heterologous proteins via unconventional secretion using the endochitinase Cts1 as a carrier has been established a few years ago [Sarkari, *et al.* 2014, J. Stock, *et al.* 2012, Terfrüchte, *et al.* 2017].

Consolidated bioprocesses implement not only biomass degradation but also formation of a valuable product. Thus, a favorable production organism is capable of both, production of hydrolytic enzymes and product formation in a single process [Olson, et al. 2012, Singh, et al. 2017]. In this context, *U. maydis* is promising, because it naturally produces valuable secondary metabolites that can serve as valuable products, including organic acids like itaconic acid and malate as well as the glycolipids ustilagic acid and mannosylerythrytol lipids [Bölker, et al. 2008, Elena Geiser, et al. 2014, Khachatryan, et al. 2015]. Overall, this organism is able to break down complex carbohydrate polymers and, simultaneously, convert the liberated sugars into high value products.

1.5 Online monitoring of biomass hydrolysis

The Respiration Activity Monitoring System (RAMOS) enables the online monitoring of oxygen transfer rate (OTR), carbon dioxide transfer rate (CTR) and respiratory quotient (RQ) in eight parallel shake flask cultivations [T. Anderlei and Büchs 2001, Tibor Anderlei, *et al.* 2004]. This technique can be applied to monitor the metabolic activity of CAZyme producing organisms. The production of CAZymes enables the expressing organism to grow on the corresponding polymeric substrate [Antonov, *et al.* 2016, E. Geiser, *et al.* 2016]. Thus, the metabolic activity of the organism grown on those polymeric substrates indicates the CAZyme activity. This principle is illustrated in Figure 1-2 for the degradation of PolyGalA by *U. maydis*.

During cultivation, the overall oxygen consumption (OT) can be determined by integrating the OTR. The OT is thereby a measure of the overall consumed oxygen and, due to the stoichiometric coupling, the carbon source. Antonov, *et al.* [2016] analyzed the digestibility of different types of cellulose by online monitoring of the respiration activity of *T. reesei* Rut-C30. Alternative cellulase producers were subsequently investigated using this methodology,

demonstrating its high potential [Antonov, et al. 2017]. Thus, the RAMOS technology provides a powerful tool for the characterization of CAZyme producing strains based on their metabolic activity on complex substrates in shake flask scale.

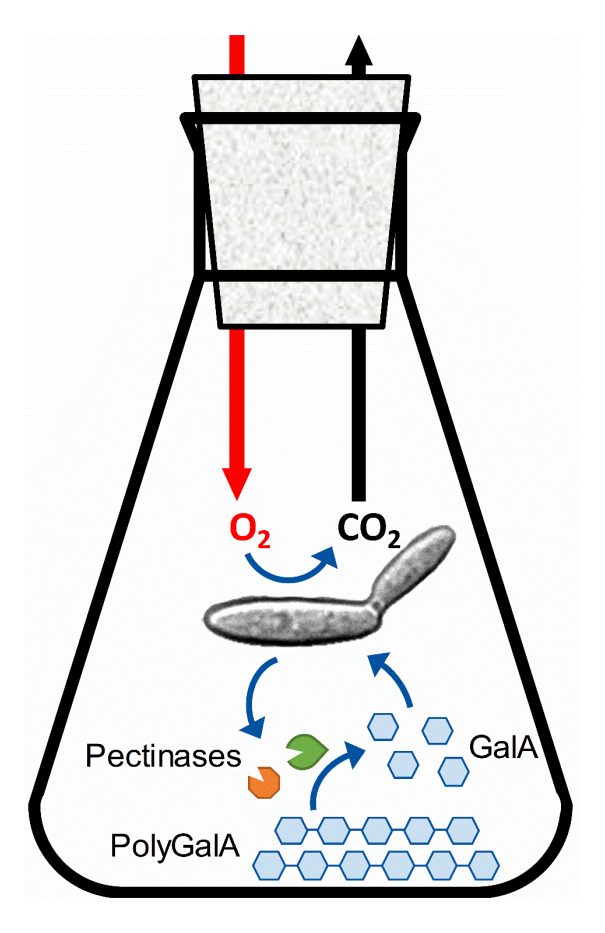


Figure 1-2: Process scheme of PolyGalA degradation. *U. maydis* produces pectinases that degrade dissolved PolyGalA to monomeric GalA. GalA and oxygen are consumed in a fixed stoichiometric ratio while carbon dioxide is released. Oxygen consumption and carbon dioxide release are measured online. This concept enables the investigation of PolyGalA degradation by pectinolytic enzymes based on online monitoring of the metabolic activity.

1.6 Objectives and overview

An important methodological challenge during the optimization of bioprocesses using plant derived biomass is to measure the substrate conversion. This verifies the respective enzyme activities in the culture broth. The present thesis addresses this hurdle. It aims to characterize growth of *U. maydis* on pectin-derived substrates with increasing complexity. Reaching that goal will facilitate process development towards utilization of sugar beet pulp. The

quantification of substrate conversion is a challenge during process development. Thus, online-monitoring of the respiration activity in small-scale is used to evaluate the metabolic activity of the organism. This way, conclusions on the substrate utilization can be drawn.

In Chapter 2, growth of *U. maydis* on galacturonic acid (GalA), which is the main pectin sugar unit, is characterized. A detailed investigation of the respiration profile is applied to formulate a stoichiometric coupling of oxygen consumption, GalA consumption and biomass formation. Based on this, a calculation model to estimate residual GalA in the culture broth is developed. This calculation model is applied to the cultivation of a recombinant *U. maydis* strain expressing an exo-polygalacturonase from *Aspergillus tubingensis*. This enzyme enables growth on the polygalacturonic acid (PolyGalA). The calculation model is moreover used to quantify the enzymatic activity in the culture broth.

In Chapter 3, novel *U. maydis* strains, that constitutively express several endo- and exopolygalacturonases, are characterized on glucose and GalA. The investigated enzymes are from intrinsic, fungal and bacterial origins. Bacterial enzymes are expressed via an unusual secretion pathway that bypasses the endomembrane system. Thereby, N-glycosylation, which might affect enzyme activity, is prevented. The generated strains are tested in axenic cultures and cofermentations using the RAMOS device. The developed methodology for estimation of the residual substrate amount in the culture broth guides the classification process of the tested endo-polygalacturonases. Co-fermentations are demonstrated to be beneficial for the growth of CAZyme expressing *U. maydis* strains on PolyGalA.

In Chapter 4, more complex substrates are utilized. Hydrolysis of three different pectins, varying in their origin and degree of esterification, is evaluated. The effect of an addition of external pectinases and cellulases on the total substrate consumption evaluated. Finally, the established co-fermentation is grown using sugar beet pulp as a model substrate for a biorefinery process. With addition of external enzymes, significant consumption of this complex substrate is achieved.

Chapter 2

Online evaluation of the metabolic activity of Ustilago maydis on galacturonic acid and polygalacturonic acid

2.1 Introduction

Ustilago maydis has the potential to compete the established carbohydrate-active enzyme (CAZyme) production hosts as has been described in Chapter 1.4. Regarding a bioprocess that converts pectin-rich sugar beet pulp into fermentable sugars, few pectinolytic enzymes (including endo-polygalacturonase, pectin lyase and pectin methylesterase) have been annotated in the *U. maydis* genome [Doehlemann, *et al.* 2008, Kämper, *et al.* 2006]. However, few is known about the growth of *U. maydis* on galacturonic acid (GalA), one of the main sugar fractions in sugar beet pulp [Micard, *et al.* 1996].

Therefore, the metabolic activity of *U. maydis* during growth on GalA is evaluated in detail in this Chapter. During the cultivation, the respiration profile (oxygen transfer rate, OTR; carbon dioxide transfer rate, CTR and respiratory quotient, RQ) is investigated in detail. The RQ can be used to clearly separate the consumption phases of GalA and glucose, which is added to the medium as a starter carbon source. Stoichiometric coupling of oxygen consumption, GalA consumption and biomass formation is tested by applying different GalA concentrations. Overall consumed oxygen (OT) analysis of those cultivations forms a calculation model for the

estimation of residual GalA in the culture broth based on the consumed oxygen during GalA metabolization. This calculation model is applied on the cultivation of the recombinant $U.\ maydis$ strain AB33P5 Δ R/AtPgaX. The strain produces an exo-polygalacturonase originating from $Aspergillus\ tubingensis$ that enables growth on polygalacturonic acid (PolyGalA). Moreover, the enzymatic activity in the culture broth can be determined by the derivative of the calculated residual PolyGalA concentration. The effect of different initial glucose concentrations on the enzyme production level is tested. Finally, the enzyme stability is evaluated giving substrate pulses at distinct stages of the cultivation.

2.2 Materials and methods

2.2.1 Microorganisms

The strains used in this Chapter are specified in Table 2-1. The genetic modification of $U.\ maydis\ AB33P5\Delta R$ was performed by homologous recombination of a linearized plasmid containing the codon-optimized exo-polygalacturonase gene pgaX originating from $A.\ tubingensis$ under control of the constitutive strong promoter P_{oma} [Flor-Parra, $et\ al.\ 2006$, Hartmann, $et\ al.\ 1999$, Kester, $et\ al.\ 1996$, Sarkari, $et\ al.\ 2014$, Zarnack, $et\ al.\ 2006$]. The construct was inserted in the ip locus mediating carboxin (Cbx) resistance [J. Stock, $et\ al.\ 2012$].

Table 2-1: List of applied microorganisms and their origin

Strain number	Description	Vector used for modification	Resistance	Progenitor	Manipula- ted Locus	References
UMa1391	AB33P5∆R		Phleo	AB33		[Sarkari, <i>et al.</i> 2014]
UMa2106	AB33P5ΔR/AtPgaX	pUMa3108	Phleo, Cbx	UMa1391	ip	Chapter 3

2.2.2 Cultivation media and cultivation conditions

U. maydis strains were cultivated in 250 mL shake flasks with a filling volume of $V_L = 20$ mL (shaking diameter 50 mm, shaking frequency 300 rpm, T = 30 °C). All cultivations were performed in modified Verduyn medium [Verduyn, *et al.* 1992]. The exact composition was

4 g/L NH₄Cl, 0.5 g/L KH₂PO₄, 0.2 g/L MgSO₄ · 7 H₂O, 0.01 g/L FeSO₄ · 7 H₂O and 1 mL/L trace element solution. The trace element solution includes 15 g/L ethylenediaminetetraacetic acid (EDTA), 4.5 g/L ZnSO₄ · 7 H₂O, 0.84 g/L MnCl₂, 0.3 g/L CoCl₂ · 6 H₂O, 0.3 g/L CuSO₄ · 5 H₂O, 0.4 g/L Na₂MoO₄ · 2 H₂O, 4.5 g/L CaCl₂ · 2 H₂O, 3 g/L FeSO₄ · 7 H₂O, 1 g/L B(OH)₃, 0.1 g/L KI. The medium was buffered either with 39.04 g/L (0.2 M) 2-(N-morpholino)ethanesulfonic acid (MES) or with 41.86 g/L (0.2 M)3-(N-morpholino)propanesulfonic acid (MOPS), depending on the applied carbon source. The pH of the medium without carbon source and trace element solution was set to 6.5 with NaOH, if not stated otherwise. The corresponding carbon source (glucose, GalA or PolyGalA) was dissolved separately at higher concentrations (glucose 500 g/L, GalA 200 g/L, PolyGalA 40 g/L). For acidic substrates, the pH was adjusted with NaOH. Finally, the dissolved carbon source was added to the medium at varying concentrations. GalA was purchased from Sigma-Aldrich (St. Louis, USA). PolyGalA was purchased form Carl Roth (Karlsruhe, Germany) at a purity of ≥ 85%. All other chemicals were of analytical grade. Glucose, GalA, FeSO₄ and buffer solutions were sterile-filtered using 0.2 µm cut-off filters (Acrodisc 32 mm, Pall, Dreieich, Germany). The other solutions were separately autoclaved (121°C, 20 min).

2.2.3 Cultivation with online monitoring and offline sampling

All cultivations were performed in 250 mL shake flasks, modified for usage in an in-house built RAMOS device [T. Anderlei and Büchs 2001, Tibor Anderlei, *et al.* 2004]. Commercial versions of the device are available from Kühner AG (Birsfelden, Switzerland) or HiTec Zang GmbH (Herzogenrath, Germany). The flasks were filled with 20 mL medium and shaken with a shaking frequency of 300 rpm at a shaking diameter of 50 mm.

For precultures, Verduyn medium with 20 g/L glucose was inoculated with 500 μ L cell suspension from a cryostock culture. The cells were grown 16 to 24 h until the carbon source was depleted. After determination of the optical density using a spectrophotometer (Genesys 20, Thermo Fischer Scientific, Waltham, USA), the required volume of culture broth was harvested by centrifugation and the main cultures were inoculated at a defined OD₆₀₀ between 0.2 and 0.65.

For offline samples, cotton plug-sealed shake flasks were cultivated in parallel to the RAMOS flasks under identical cultivation conditions using identical inocula.

2.2.4 Offline analysis

2.2.4.1 Optical density

Biomass during cultivation in non-turbid media (without PolyGalA) was determined by measuring the optical density at 600 nm (OD_{600}) with a spectrophotometer using 1.5 mL micro cuvettes (PS, Plastibrand, Roth, Karlsruhe, Germany). If necessary, samples were diluted with 0.9% (w/v) NaCl solution to a final $OD_{600} < 0.3$. NaCl solution was used as blank. Each sample was measured in duplicates.

2.2.4.2 pH value

The pH value of unfiltered culture broth was measured at room temperature using a pH-meter (HI2211 pH, Hanna Instruments, Vöhringen, Germany) equipped with a pH-electrode (InLab Easy pH, Mettler-Toledo, Giessen, Germany).

2.2.4.3 Ammonia

The ammonium concentration of culture supernatant was determined after dilution to appropriate concentrations using the Spectroquant test kit (N° 114544, Merck KGaA, Darmstadt, Germany). The samples were measured using a photometer (Nova 60, Merck KGaA, Darmstadt, Germany)

2.2.4.4 Quantification of carbon sources

Glucose and GalA concentrations were determined from cell-free supernatant by HPLC. After sterile filtration with 0.2 µm filters (Rotilabo syringe filters Mini-Tip cellulose acetate membrane, N° PP52.1, Carl Roth, Karlsruhe, Germany), the samples were separated in the HPLC (Prominence, Shimadzu AG, Kyoto, Japan) using an organic acid resin column

(250 x 8 mm, CS-Chromatographie Service GmbH, Langerwehe, Germany). The separation was achieved with 1 mM H₂SO₄ at 75°C at a flow rate of 0.8 mL/min. The column was coupled to a refractometer (Shodex RI-101, Showa Denk Europe, Munich, Germany) and the data was analyzed by the software Chromeleon 6.2 (Dionex, Germering, Germany).

2.2.4.5 Cell dry weight

For determination of the cell dry weight, 2 mL culture broth were collected in a dry reaction tube, centrifuged and the supernatant was discarded. After drying the cell pellet for 48 h at 80 °C, it was weighted using an analytical balance (LA 254i, VWR International GmbH, Darmstadt, Germany). All samples were measured as technical triplicates.

2.2.4.6 Enzymatic activity via reducing sugar assay (DNS assay)

Culture broth was collected, centrifuged, and subsequently used for offline determination of the enzymatic activity. 4 g/L PolyGalA solution in 0.1 M MES buffer, pH 6.0 was used as substrate. The assay was performed in one 2 mL reaction tube per time point incubated in a thermoshaker at 30°C and 800 rpm over a period of 24 h. At each sampling point, one reaction tube was heated up to 95 °C for 5 min to inactivate the enzyme. After the last sampling point, the concentration of reducing groups was determined by 3,5-dinitrosalicylic acid (DNS) assay [Miller 1959]. All samples were mixed with DNS solution (10 g/L DNS, 404 g/L potassium sodium tartrate tetrahydrate, 16 g/L NaOH) at equal volumes. The colorimetric reaction was carried out for 10 min in a thermoshaker at 95 °C and 800 rpm. Finally, the samples were cooled on ice and transferred to a 96-well microplate with a filling volume of 300 µL per well. All samples were measured in technical triplicates. The absorption at 540 nm (A₅₄₀) was measured in a plate reader (Synergy 4, Biotek, Winooski, USA). As internal control for turbid samples, the A₆₃₀ was measured as well as described previously [Nishi and Elin 1985]. The final DNSbased absorbance was determined as A₅₄₀-A₆₃₀. Calibration curves were prepared using GalA at concentrations between 0 and 20 mM. An exemplary calibration curve is shown in Figure A1. The enzymatic activity was calculated from the increase of reducing groups during the first 4 h. The monomeric GalA concentration at the beginning of the reaction was determined from the measured reducing groups at the reaction start.

2.3 Online monitoring of *U. maydis* growth on GalA

The applied measurement principle for growth of *U. maydis* on PolyGalA is shown in Figure 1-2 (Chapter 1.5). *U. maydis* is grown in RAMOS shake flasks with PolyGalA as carbon source. If pectinases are available to degrade the polymeric substrate to monomers, monomeric GalA is consumed by *U. maydis*. The consumption of GalA correlates with the uptake of oxygen and the release of carbon dioxide in a specific molar ratio. Thus, by online measurement of the OTR and CTR, the pectinolytic activity of the produced enzymes in the culture broth can be determined. Furthermore, the relation between the amount of overall consumed oxygen and the residual substrate concentration in the culture supernatant was investigated. The resulting method for prediction of the residual substrate concentration was applied for monomeric GalA but, more importantly, also for PolyGalA that cannot be quantified easily by offline measurement.

As first step, the growth of the protease deficient strain U. maydis AB33P5 ΔR on GalA was characterized by online monitoring of the metabolic activity. AB33 is known to grow in a stable unicellular state making it applicable up to fermenter scale [Brachmann, et al. 2001]. Furthermore, the strain produces less lipids compared to other U. maydis strains like MB215 [Hewald, et al. 2006]. This provides the potential to achieve high carbon fluxes towards a desired product. The specific quintuple protease deletion strain, previously generated by Sarkari, et al. [2014], was chosen to gain a higher enzyme stability in the culture supernatant.

The mineral medium described by E. Geiser, et al. [2016] was adapted for the cultivation on pectic substrates. Nitrogen limitation is known to induce itaconic acid production in certain *U. maydis* strains, but significantly reduces growth [Klement, et al. 2012, Maassen, et al. 2014, Voll, et al. 2012, Zambanini, et al. 2017]. As this study focuses on the growth on complex substrates, the ammonium chloride concentration was elevated from 0.8 to 4.0 g/L to prevent a secondary substrate limitation. The vitamin solution was omitted, as no advantageous effect was visible during the cultivation (see Figure A2). Low amounts of glucose have previously been used to achieve an exponential growth of the culture before entering the second growth phase on the main carbon source [Antonov, et al. 2016]. Therefore, 4 g/L glucose and 20 g/L GalA were used as carbon sources. The pH value was expected to increase when *U. maydis*

consumes an acidic carbon source. To prevent a strong pH shift towards basic values, the originally reported 0.1 M MES buffer was replaced with 0.2 M MOPS buffer. MOPS buffer (pKa = 7.2) provides a larger buffer capacity towards higher pH values compared to MES buffer (pKa = 6.1).

Figure 2-1A shows the OTR and CTR over time of an *U. maydis* AB33P5ΔR cultivation in the modified mineral medium containing glucose (4 g/L) and GalA (20 g/L) as carbon sources. In each experiment, biological duplicates of the cultivation conditions were investigated. The variation between the duplicates was very low, indicating a high reproducibility. The first exponential growth phase of *U. maydis* AB33P5ΔR was characterized by consumption of glucose as preferred carbon source. The maximal OTR of 10 mmol/L/h was reached after 10.5 h. With the depletion of glucose, the OTR decreased to 3.5 mmol/L/h at 11.5 h, indicating a metabolic adaption of the organisms for the second growth phase. Depletion of glucose was also verified by offline sampling as depicted in Figure 2-1B (first vertical grey dashed line). During the first growth phase, no GalA was consumed. The optical density increased from 0.2 to 2.8. The pH slightly decreased from 6.52 to 6.25 due to ammonia consumption [Christensen and Eriksen 2002, Philip, *et al.* 2018].

During the second growth phase, the culture consumed GalA until substrate depletion after 43 h (second vertical grey dashed line). The OTR increased at a lower rate when compared to growth on glucose, indicating a poorer metabolization rate of GalA. This slow growth on GalA is characteristic for *U. maydis* and these results are consistent with previous reports [Cano-Canchola, *et al.* 2000]. The OTR increased towards a maximal OTR of 11.8 mmol/L/h after 41 h. The finally measured optical density was 9.0. The end of the cultivation was characterized through a steep descent of the OTR after 43 h. At this point, all GalA was consumed. The pH increased during the GalA consumption phase to 7.1. This behavior is typical during the consumption of acidic carbon sources as they cross the cell membrane only in their protonated form [Kreyenschulte, *et al.* 2018]. At the end of the cultivation, 1.45 g/L ammonium chloride remained in the culture supernatant, indicating that the elevated concentration of 4 g/L ammonium chloride was sufficient to prevent nitrogen limitation.

The RQ describes the ratio of CTR to OTR. It is known as a central parameter to characterize the metabolic activity of microorganisms during growth on multiple substrates of different

degree of reduction [Tibor Anderlei, *et al.* 2004]. Figure A3B shows the RQ over time for the cultivation on GalA. During growth on glucose, OTR and CTR are identical, which results in a RQ of about 1. Similar RQ values were obtained by others for the growth of *U. maydis* and yeasts while growing on glucose [Tibor Anderlei, *et al.* 2004, Klement, *et al.* 2012]. During the growth on GalA, the CTR values are higher than the OTR, resulting in an RQ of 1.3 to 1.4. Finally, after depletion of GalA, the RQ drops below 1, indicating that for maintenance internal reduced storage compounds like, e.g., lipids are consumed.

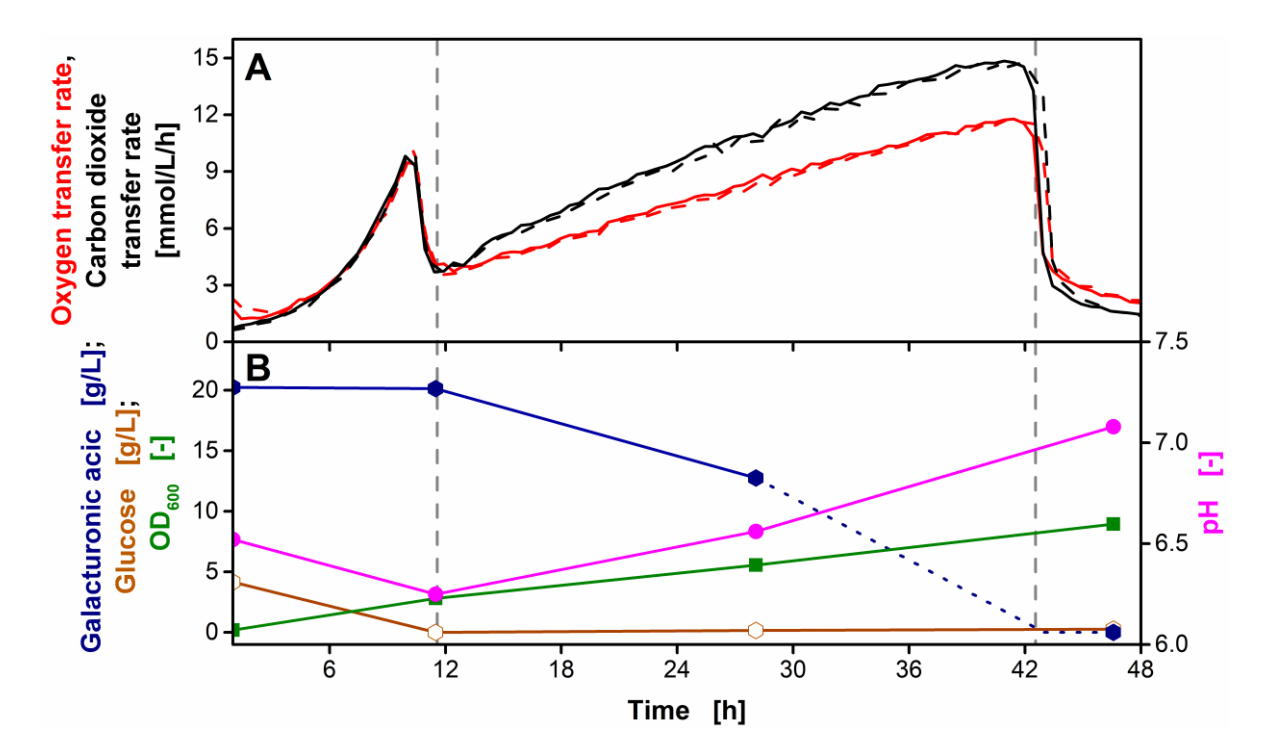


Figure 2-1: Cultivation of *U. maydis* **AB33P5AR on GalA.** The strain was grown on glucose (4 g/L) and GalA (20 g/L) as carbon sources. Vertical grey dashed lines indicate depletion of glucose (11.5 h) and GalA (43 h). **A** Biological duplicates of OTR and CTR, represented each as line and dashed line. **B** Concentrations of GalA and glucose, OD_{600} and pH. The blue dotted line represents the assumed course of GalA concentration since the OTR indicates GalA depletion after 43 h. Culture conditions: modified Verduyn medium, 0.2 M MOPS, initial pH 6.5, 250 mL flask, filling volume 20 mL, shaking frequency 300 rpm, shaking diameter 50 mm, initial $OD_{600} = 0.2$, T = 30 °C.

To understand the different distinct levels of the RQ, a carbon balance was developed for the cultivation on glucose and GalA. Assuming pure biological combustion of GalA for energy metabolism, GalA is oxidized to carbon dioxide and water as described by Equation (1).

$$v_S C_6 H_{10} O_7 + v_O O_2 \rightarrow v_C CO_2 + v_H H_2 O$$
 (1)

ν: stoichiometric coefficients for substrate GalA (S), oxygen (O), carbon dioxide (C) and water (H)

The corresponding theoretical RQ value (RQ_{theo}) can be calculated from the stoichiometric coefficients as described by Equation (2). They are 1.0 and 1.2 for glucose and GalA respectively as listed in Table 2-2.

$$RQ_{\text{theo}} = \frac{v_{\text{C}}}{v_{\text{O}}} \tag{2}$$

RQ_{theo}: theoretical respiratory quotient [-]

However, to represent conditions that are more realistic, Equation (1) has to be extended with the formation of biomass and the consumption of ammonia as described in Equation (3).

$$\nu_{\rm S} \, {\rm C}_6 {\rm H}_{10} \, {\rm O}_7 + \nu_{\rm N} \, {\rm NH}_3 + \nu_{\rm O} \, {\rm O}_2 \rightarrow \nu_{\rm X} \, {\rm X} + \nu_{\rm C} \, {\rm CO}_2 + \nu_{\rm H} \, {\rm H}_2 {\rm O}$$
 (3)

 ν : stoichiometric coefficients for ammonia (N) and biomass (X)

Balancing of Equation (3) requires the stoichiometric coefficient v_X . The elemental composition of *U. maydis* under N-unlimited conditions was previously determined to be $CH_{1.826}O_{0.579}N_{0.145}$ [Klement, *et al.* 2012]. Based on the determination of the cell dry weight and measurement of the residual substrate concentration by HPLC, a yield coefficient for biomass formation ($Y_{X/S}$) of 0.51 and 0.27 g_{X/g_S} was calculated according to Equation (4) for glucose and GalA, respectively. The results are listed in Table 2-2.

$$Y_{XS} = \frac{\Delta X}{\Delta S} \tag{4}$$

 Y_{XS} : yield coefficient $[g_X/g_S]$

 ΔX , ΔS : change of biomass (X) or substrate (S) concentrations between sampling points [g/L]

 Y_{XS} was used to define v_X as described in Equation (5).

$$v_{X} = Y_{XS} \frac{MW_{X}}{MW_{S}} \tag{5}$$

MW_X, MW_S: molecular weight of biomass (X) or substrate (S) [g/mol]

Using the experimental value for v_X in Equation (3) results in stoichiometric coefficients and the RQ_{theo} values for combined combustion and biomass formation as given in Table 2-2. The calculated RQ_{theo} values of 1.10 and 1.38 for glucose and GalA, respectively, matched the experimentally determined data (Figure A3B). This indicates that no relevant carbon fluxes other than combustion to carbon dioxide for energy generation and cell growth occur. Thus, the carbon balance is closed for the cultivation on glucose and GalA.

Table 2-2: Stoichiometric coefficients and RQ_{theo} **for carbon balance.** Carbon sources glucose (Glc) and GalA are compared with or without biomass formation.

Conditions	C- source	Sum formula	$\nu_{\rm S}$	$ u_{ m N}$	ν_0	$\nu_{\rm X}$	$ u_{C}$	$ u_{\mathrm{H}}$	RQ _{theo}	$Y_{X/S}$
Pure combustion	Glc	C ₆ H ₁₂ O ₆	1	-	6	-	6	6	1.00	-
Pure combustion	GalA	C ₆ H ₁₀ O ₇	1	-	5	-	6	5	1.20	-
Combustion and biomass formation	Glc	C ₆ H ₁₂ O ₆	1	0.53	2.13	3.65	2.35	3.46	1.10	0.51
Combustion and biomass formation	GalA	C ₆ H ₁₀ O ₇	1	0.29	2.92	1.97	4.06	3.63	1.38	0.27

2.4 Correlation of oxygen uptake with consumed GalA

One aim of this study is to provide a method for predicting the residual concentration of GalA from the OT during the GalA consumption phase. The correlation developed in this Chapter will later be applied on the growth of U. maydis AB33P5 Δ R/AtPgaX on PolyGalA. For

consistence with the later application, this strain was already used for the development of the correlation introduced within this chapter.

For experimentally developing a correlation of the OT with the GalA supplemented in the medium, the concentration of GalA was varied from 0 to 34.6 g/L. As the pH is increasing during the consumption of GalA, the buffer concentration was increased in proportion to the substrate concentrations with a minimal buffer concentration of 0.1 M.

Figure 2-2A shows the OTR over time of U. maydis AB33P5 Δ R/AtPgaX in media containing glucose (4 g/L) and varied concentrations of both, GalA (0 to 34.6 g/L) and MOPS buffer (0.1 to 0.4 M).

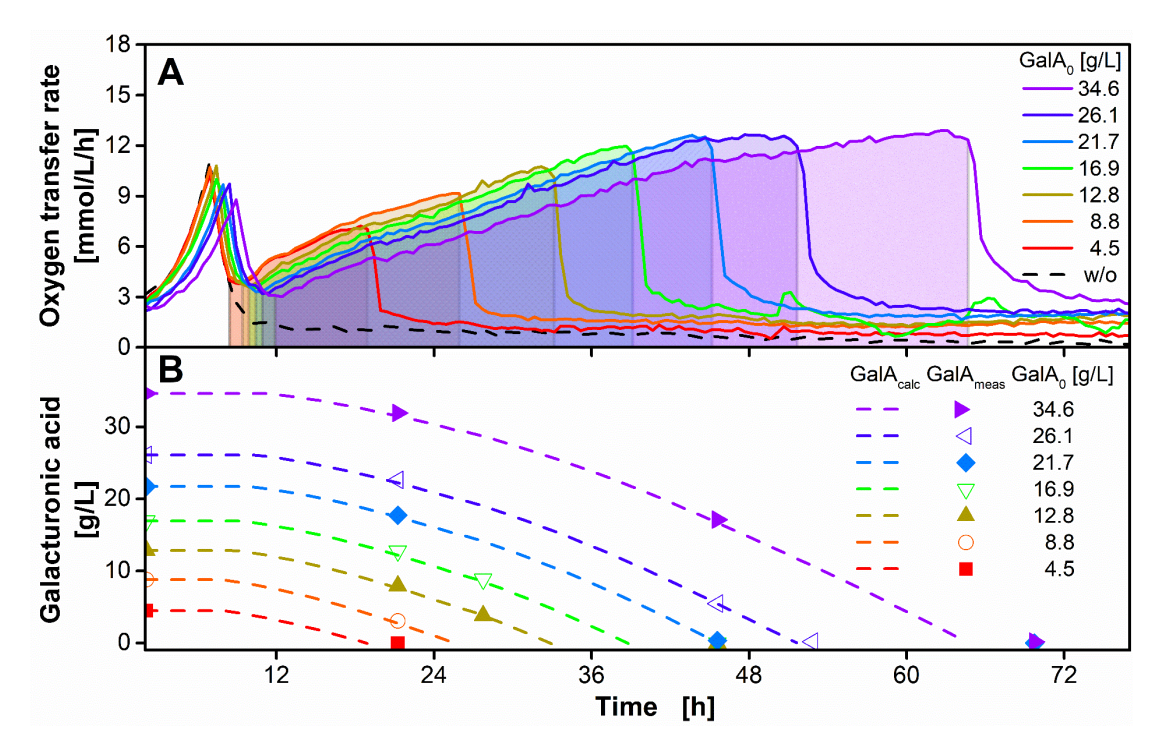


Figure 2-2: Cultivation of *U. maydis* AB33P5 Δ R/AtPgaX with varying GalA and buffer concentrations. The medium was supplemented with glucose (4 g/L) and varying amounts of initial GalA (GalA₀) and MOPS buffer. 0, 4.5, 8.8, 12.8, 16.9, 21.7, 26.1 and 34.6 g/L GalA₀ was supplemented with 0.1, 0.1, 0.1, 0.15, 0.2, 0.25, 0.3 and 0.4 M MOPS, respectively. **A** OTR. The GalA consumption phase is indicated by the shaded area below the OTR curve for each cultivation. **B** Dashed lines represent the predicted residual substrate concentration in the culture medium (GalA_{calc}) according to Equation (6). Symbols represent offline measured values (GalA_{meas}). Culture conditions: modified Verduyn medium, initial pH 6.5, 250 mL flask, filling volume 20 mL, shaking frequency 300 rpm, shaking diameter 50 mm, initial OD₆₀₀ = 0.65, T = 30 °C.

Compared to Figure 2-1A, the same two growth phases on glucose (lasting for 10 to 12 h) and GalA can be distinguished. The growth on glucose was only slightly slowed down at elevated GalA and buffer concentrations due to increased osmolarity. In line with this, previous studies reported the high robustness of *U. maydis* under elevated osmolarities while not remaining totally unaffected [Klement, *et al.* 2012, Salmerón-Santiago, *et al.* 2011]. As expected, the OTR of the control cultivation without GalA dropped down to a basal level already after 10 h. All other cultivations showed the typical two-stage growth behavior. GalA was depleted after different cultivation times, according to the initially supplemented substrate concentration. The corresponding OTs for the GalA consumption phases are indicated in Figure 2-2A by the shaded areas under the curves.

In Figure 2-3 (squares), the OT during the GalA consumption phase (see also shaded areas in Figure 2-2A) was plotted against the initial GalA concentration. The linear regression of the data points (red dashed line) demonstrates the excellent correlation of the two parameters. Thus, the reciprocal value of the experimental calibration factor $\frac{v_0}{v_s}$ can be used to predict the residual substrate concentration GalAcalc during the entire cultivation according to Equation (6).

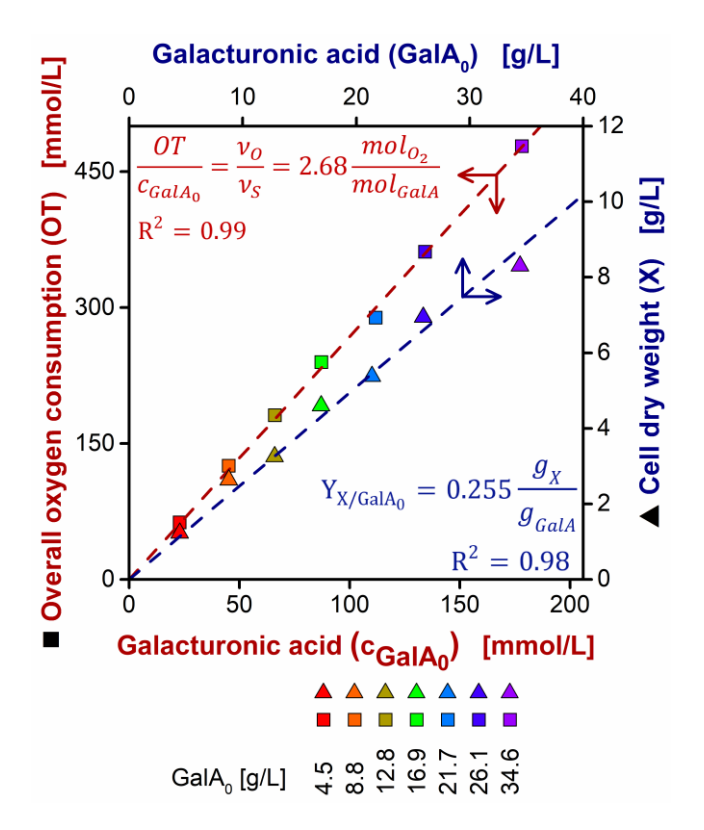


Figure 2-3: Correlation of overall oxygen consumption and produced biomass to initial GalA concentration.

Overall oxygen consumption (OT, squares, red axes) is correlated to the molar initial GalA concentration (c_{GalA_0}), produced biomass (X, triangles, blue axes) to the initial GalA mass concentration ($GalA_0$). The colored data points correspond to the equally colored cultivations shown in Figure 2-2. The GalA concentrations were determined via offline measurement. The OT is considered for the GalA consumption phase. A linear fit was plotted (dashed lines, arrows indicate corresponding axes). The reciprocal value of $\frac{v_0}{v_S}$ can be substituted in Equation (6). The calibration factors and coefficients of determination are specified in the plot.

$$(Poly)GalA_{calc} = MW_{(Poly)GalA}(c_{(Poly)GalA_0} - \frac{v_S}{v_O} OT)$$
 (6)

(Poly)GalA_{calc}: calculated residual (Poly)GalA concentration [g/L]

MW_{(Poly)GalA}: molecular weight of (Poly)GalA [g/mol]

 $c_{(Poly)GalA_0}$: initial (Poly)GalA concentration [mol/L]

OT: overall oxygen consumption during (Poly)GalA consumption phase [mol/L]

GalA_{calc} is shown for all cultivations in Figure 2-2B (dashed lines). The predicted GalA_{calc} is in very good agreement with offline measured concentrations of GalA (GalA_{meas}, Figure 2-2B, symbols). This verifies the high reliability of the predicted concentrations. Furthermore, the predicted depletion of substrate correlates well with the sharp drop in the OTR.

The carbon balancing introduced in the previous chapter requires experimental values for $Y_{X/S}$. Online monitoring of the metabolic activity (OTR) enabled sampling right after glucose was depleted and shortly after depletion of GalA. Figure 2-3 (triangles) shows the data that was used to calculate the yield coefficient $Y_{X/S}$ as described by Equation (4). Compared to the yield coefficient on glucose, determined from the first growth phase with $Y_{X/S} = 0.51 \text{ gx/gs}$, U. maydis does produce less biomass from GalA ($Y_{X/S} = 0.27 \text{ gx/gs}$). This can partially be explained by the degree of reduction as a parameter for the energy content of the substrate. For GalA, the degree of reduction is 3.33 per carbon atom. Compared to that, glucose shows a degree of reduction of 4 per carbon atom. Thus, the energy content of GalA is lower than of glucose. This is also in accordance with the lower growth rate on GalA compared to glucose, as the increase of the OTR during growth on GalA is not exponential (Figure 2-1A) [Cano-Canchola, et al. 2000].

Comparing the different OTR profiles in Figure 2-2A, it should be noted that the increase in the OTR becomes less steep for the cultivation with 34.6 g/L GalA towards the end of the cultivation. This might be associated with a slight shift in the cultivation pH (final pH: 7.3, see also Figure A4). *U. maydis* is usually cultivated at pH values of 5.5 to 6.5 [Elena Geiser, *et al.* 2014]. Cultivations above that optimal range can reduce the specific growth rate.

2.5 Characterization of growth on PolyGalA

To achieve metabolization of PolyGalA, *U. maydis* AB33P5ΔR/AtPgaX was applied. Two reference cultivations of this strain are shown in Figure A5. In one cultivation, 20 g/L glucose was added as single carbon source (black) while in the other cultivation 20 g/L PolyGalA without supplemented glucose was provided (green). No growth was observed for the cultivation with pure PolyGalA, indicating that PolyGalA is not sufficient as a sole carbon source. As the strain grows exponentially on glucose, the medium containing PolyGalA was supplemented with 4 g/L glucose as a starter carbon source. Such supplementation of the culture medium with 4 g/L glucose was already used in Chapters 2.3 and 2.4 for the cultivation on monomeric GalA to enhance the cell density at the beginning of the second growth phase. For the cultivation on PolyGalA, the glucose supplementation additionally enables the microbial production and secretion of hydrolytic enzymes from glucose. Previous studies on the regulatory elements of the implemented P_{oma} promoter indicate a strong influence of the applied carbon source on the expression of the target protein [Hartmann, et al. 1999]. The strongest expression was achieved when glucose, fructose, sucrose or arabinose were provided as carbon source while significantly lower expression rates were achieved on xylose, maltose or glycerol [Hartmann, et al. 1999]. Assuming a similar decreased activity of the Poma promoter on (Poly)GalA could explain the lack of metabolic activity for the *U. maydis* cultivation on PolyGalA as sole carbon source.

To determine the ability of the new strain to grow on monomeric GalA, a second reference cultivation on glucose and GalA was conducted. Figure 2-4A shows the OTR over time for the cultivation of AB33P5 Δ R/AtPgaX (blue) and its progenitor strain AB33P5 Δ R (olive green) on 4 g/L glucose and 20 g/L monomeric GalA. Both strains showed a similar pattern of the OTR course demonstrating their comparability during the cultivation. In contrast to AB33P5 Δ R

lacking the exo-polygalacturonase, AB33P5\Delta R/AtPgaX also showed metabolic activity when cultivated on PolyGalA (black). However, in comparison to the cultivation on monomeric substrate, the cultivation on PolyGalA behaved differently. Similar OTR patterns were previously observed for cultivations of *T. reesei* on cellulose and divided into three different phases [Antonov, et al. 2017, Antonov, et al. 2016]. The cultivation of AB33P5ΔR/AtPgaX on PolyGalA could be divided into the same phases. The first phase during GalA consumption (13-18 h) could be described by an identical OTR for both cultivations, with PolyGalA (black) and monomeric GalA (blue) as main carbon source. This indicates an unlimited growth on the monomer in both cases. The corresponding RQ (Figure 2-4B) showed a characteristic pattern with an RQ of 1.1 during the glucose consumption phase (< 10 h), a short kink after glucose depletion (10-12 h) and an increase to 1.3-1.4 at the beginning of the GalA consumption phase (< 12 h). After 18 h, the OTR of the cultivation on PolyGalA entered the second phase. A plateau of OTR = 5.7 mmol/L/h was reached (18-26 h). This indicates a substrate limitation. The current enzymatic activity in the culture supernatant led to a constant liberation rate of GalA monomers. The RQ remained on a high level of 1.3-1.4, verifying that all hydrolyzed sugar units are immediately consumed. Using the method for prediction of the residual substrate concentration described by Equation (6) enabled the calculation of the PolyGalA concentration (PolyGalA_{calc}). In this case, the molar concentration refers to the monomeric GalA without considering the degree of polymerization. As the OTR of the cultivation shown in Figure 2-4A (black curve) remained constant, no new exo-polygalacturonase is produced by the strain. This plateau in the OTR correlates with the linear decrease of PolyGalAcalc depicted in Figure 2-4C (black curve). Thus, during this phase, the culture is limited due to enzymatic activity in the supernatant, meaning that a higher enzymatic activity would lead to a higher OTR. After 26 h, the cultivation on PolyGalA entered a third phase. The OTR starts to decrease towards a basal level. After 42 h, the OTR of both cultures, with polygalacturonic and monomeric GalA, ran in parallel. Previously, a decreasing OTR during the cultivation of *T. reesei* on cellulose was annotated with a decreased accessibility of the substrate [Antonov, et al. 2016]. In that context, the last phase (26 to 42 h) is likely to show a decreasing accessibility of PolyGalA resulting in a lower liberation rate of monomeric GalA. The RQ deceased during this third phase towards the level of pure combustion indicating a decreasing biomass formation and increasing cell maintenance. During this last phase, the cultivation could be characterized as substrate limited. In this case, more substrate would lead to a higher OTR.

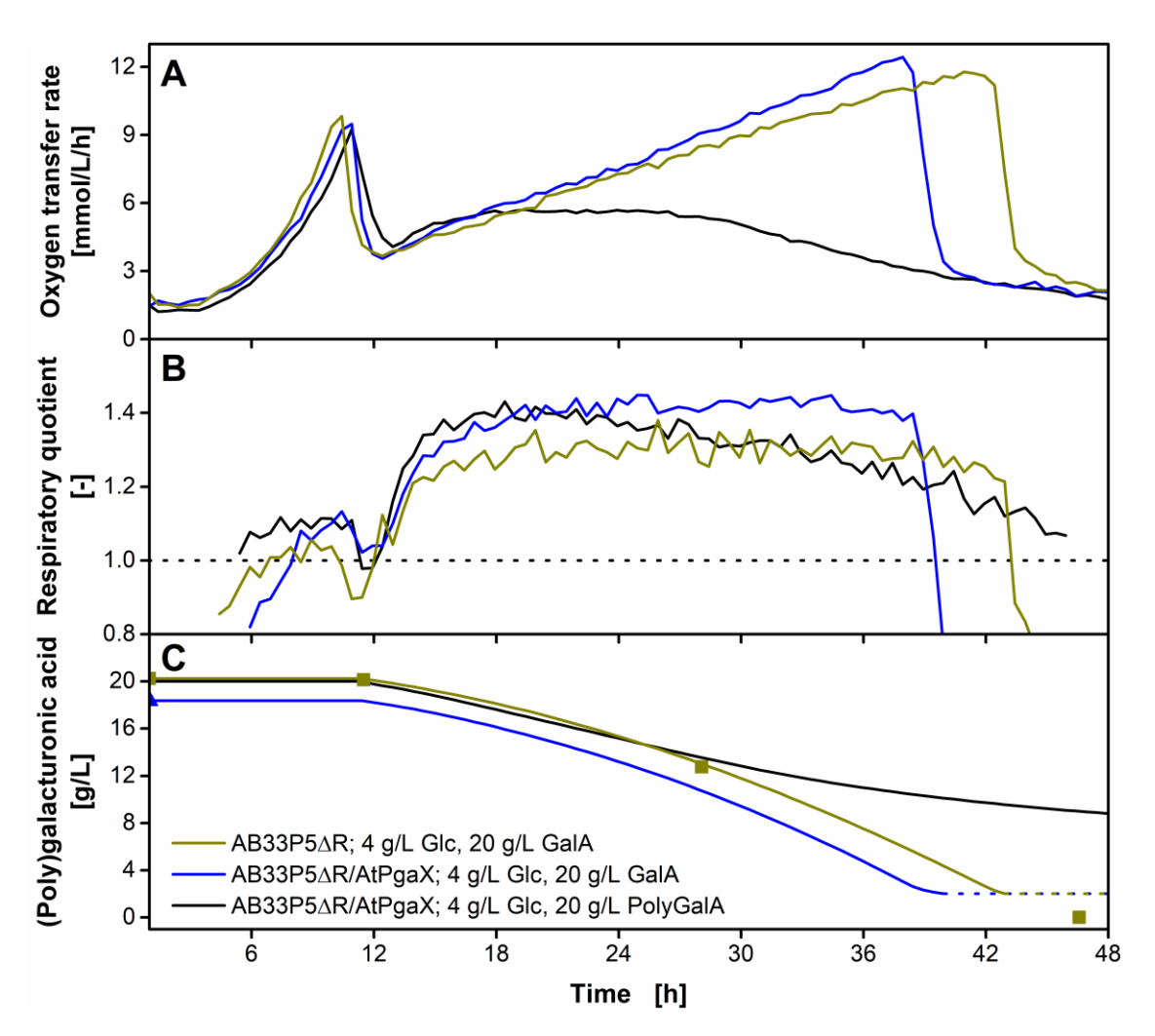


Figure 2-4: Cultivation of *U. maydis* AB33P5ΔR and AB33P5ΔR/AtPgaX on (Poly)GalA. The strains were grown on glucose (4 g/L) and GalA or PolyGalA (20 g/L) as carbon sources. A Mean value of duplicates of OTR. B Mean value of duplicates of the RQ. The dotted horizontal line represents RQ = 1. C Predicted residual substrate concentration in the culture medium (GalA_{calc} or PolyGalA_{calc}) according to Equation (6). The RQ drops below 1 after 40 and 44 h, respectively, indicating depletion of GalA. Thus, the line for GalAcalc in Figure 2-4C is dotted from that time point on. Symbols represent offline-measured values. The mean values of biological duplicates are shown for online measurements for better clarity. Culture conditions: modified Verduyn medium, 0.2 M MOPS, initial pH 6.5, 250 mL flask, filling volume 20 mL, shaking frequency 300 rpm, shaking diameter 50 mm, initial OD₆₀₀ = 0.2, temperature 30 °C.

During the second phase of limitation by the enzymatic activity, the OTR level during the linear decrease of PolyGalAcalc could be applied as a read-out for online determination of the enzymatic activity. The constant plateau in the OTR indicates the enzymatic hydrolysis as growth-limiting parameter of the cultivation. All liberated monomeric GalA is immediately consumed. Equation (7) describes the calculation of the enzymatic activity of the culture supernatant from the plateau level OTR*. One unit of enzyme activity is defined as the amount of enzyme required to liberate 1 µmol of GalA per minute.

$$E = OTR^* \frac{v_S}{v_O}$$
 (7)

E: enzymatic activity [U/mL]

OTR*: oxygen transfer rate at plateau [µmol/mL/min]

The determined enzymatic activity in the culture supernatant was 35.1 mU/mL. This method has several advantages over offline enzymatic assays. It is possible to measure even low activities that are hard to detect via offline enzymatic assays. Additionally, the method is not affected by possible product inhibition of the enzyme, a known issue for several pectinases or cellulases [Bélafi-Bakó, *et al.* 2007, Teugjas and Väljamäe 2013]. Finally, the determination is conducted under cultivation conditions and, thus, more reliable with regard to a later process scale-up compared to artificial conditions in offline enzyme assays.

2.5.1 Influence of initial glucose concentration on enzyme expression

As discussed above, exo-polygalacturonase is exclusively produced during the growth on glucose. Elevated glucose concentrations elongate the enzyme production phase and should consequently lead to an increased enzymatic activity. After glucose depletion, during the growth on PolyGalA, an increased enzymatic activity should therefore correlate with a higher plateau of the OTR. To test this assumption, the glucose concentration during cultivations on PolyGalA was varied between 4 and 20 g/L. The corresponding OTR profiles are depicted in Figure 2-5A. All cultivations started to grow equally on glucose. After 8.5, 13.5 and 16.0 h, glucose (4, 12 and 20 g/L) was depleted, respectively, as indicated by the drop in the OTR. After a slight increase while growing unlimited on GalA, a plateau was reached at an OTR of 5.4, 11.9 and 15.4 mmol/L/h for 4, 12 and 20 g/L glucose, respectively. The elevated OTR plateau for higher initial glucose concentrations indicates a higher enzymatic activity as hypothesized above. This is most probably due to increased enzyme concentrations, as the cultivations with higher glucose concentrations experienced a longer enzyme production phase. The higher OTR plateau is consistent with a higher liberation and consumption rate of GalA. Thus, a shorter duration of the OTR plateau can be observed with 10 h for 20 g/L initial glucose or 12.5 h for 12 g/L initial glucose, when compared to 28.5 h for 4 g/L initial glucose. However, the overall consumed substrate does not differ substantially between the different cultivations (Figure 2-5C). This is independent of elongated cultivation times or the enzyme concentration in the media and underlines the high comparability in terms of substrate accessibility.

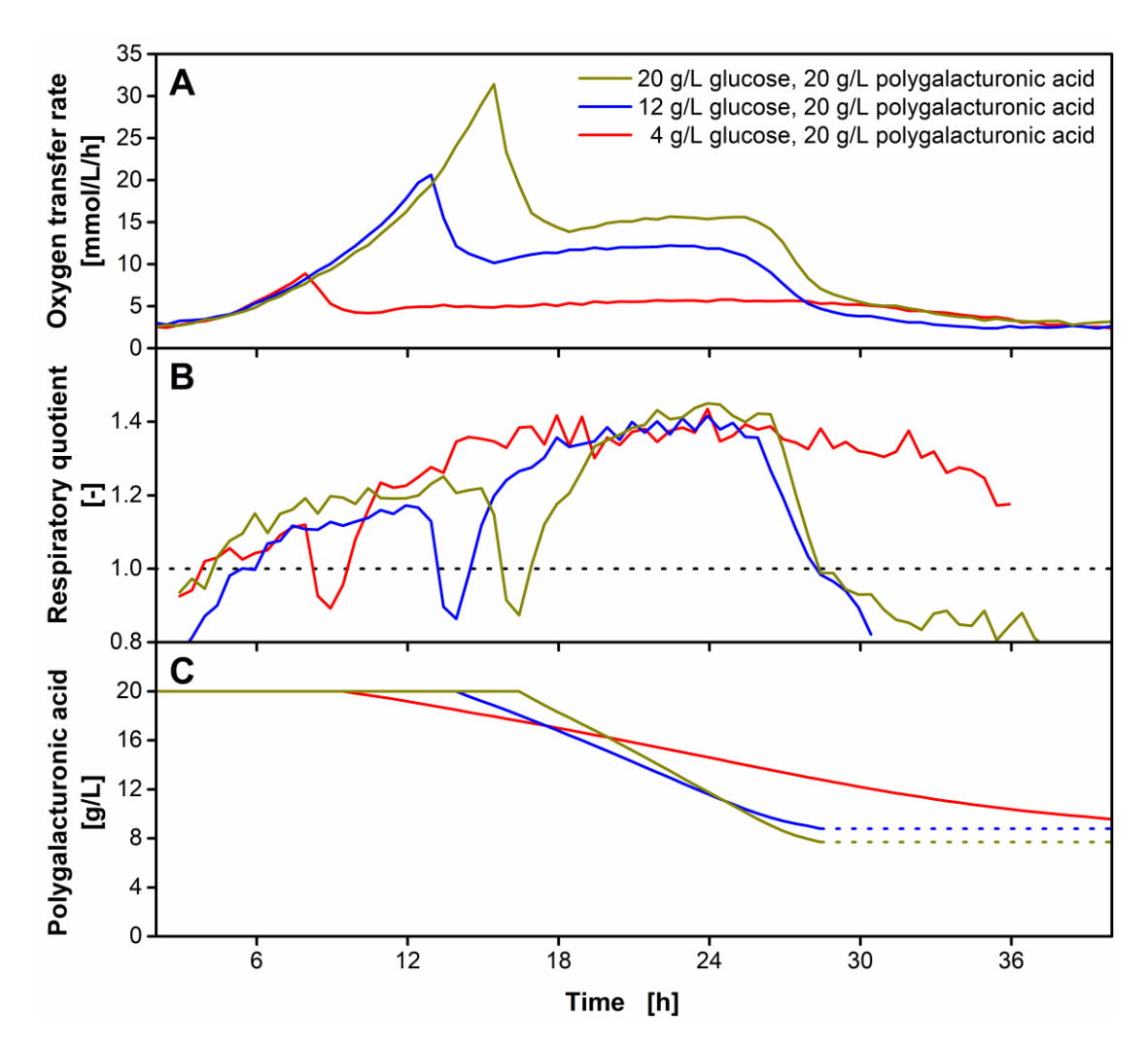


Figure 2-5: Cultivation of *U. maydis* AB33P5ΔR/AtPgaX on PolyGalA with varying initial glucose concentrations. The strain was grown on glucose (4, 12 and 20 g/L) and PolyGalA (20 g/L) as carbon sources. A Mean value of biological duplicates of RQ. The dotted horizontal line represents RQ = 1. C Predicted residual PolyGalA concentration in the medium (PolyGalA_{calc}) according to Equation (6). The RQ drops below 1 after 29 h, indicating depletion of accessible PolyGalA. Thus, the line for PolyGalA_{calc} in Figure 2-5C is dotted from that time point on. The mean values of biological duplicates are shown for better clarity. Culture conditions: modified Verduyn medium, 0.1 M MOPS and 0.1 M MES, initial pH 6.0, 250 mL flask, filling volume 15 mL, shaking frequency 350 rpm, shaking diameter 50 mm, initial OD₆₀₀ = 0.6, temperature 30 °C

Obviously, the accessibility of the polymeric substrate decreases during the cultivation due to single modified GalA residues. Esterified repeating units in the PolyGalA chain may remain unconsumed in the fermentation. As the exo-polygalacturonase is specifically acting on the

non-reducing end and can hydrolyze only unesterified residues, a single modification in the backbone may block the degradation of the entire PolyGalA chain [Abbott and Boraston 2007, Kester, *et al.* 1996, Trindade, *et al.* 2016]. A small degree of impurities in the substrate also explains the incomplete metabolization of PolyGalA, as 8 g/L of initially 20 g/L substrate remain in the medium at the end of the cultivation.

To validate the introduced method for online determination of the enzymatic activity, samples of culture supernatant were drawn after 17 and 23 h of the cultivations on 4, 12 and 20 g/L glucose and 20 g/L PolyGalA shown in Figure 2-5. The enzymatic activities determined from offline measurement are clearly different from the online-determined measurements as can be seen in Figure 2-6. Offline activities are in the range of 23 to 33 mU/mL for all glucose concentrations at both time points (Figure 2-6, blue bars). For the lowest glucose concentration, the online-determined enzymatic activities were in the same order of magnitude (Figure 2-6, red bars). However, the online-determined activities for 12 and 20 g/L glucose were up to 4fold higher than the offline-determined values. This discrepancy between the online and offline enzymatic activity can be explained by examining the enzyme kinetics. The enzyme kinetics for the tested exo-polygalacturonase have been reported to be very susceptible to product inhibition [Kester, et al. 1996]. The enzyme can be competitively inhibited by monomeric GalA with a kinetic inhibition coefficient of $K_I = 0.3$ mM. As the GalA concentration at the beginning of the assay reaction is > 2 mM for all offline assays (Figure 2-6, hatched blue bars), it is probable that the enzyme is inhibited during the entire offline assay. That would explain the constant outcome for enzymatic activity. The activities determined from online measurement are highly reliable as the product is constantly consumed and the enzyme is not affected by product inhibition. Thus, in case of a product inhibition, the offline determination of enzymatic activities underestimates the real enzymatic activity. Previous reports on product inhibited CAZymes also recommend to set-up consolidated bioprocessing in order to prevent high sugar accumulation by constant consumption of the released sugars [Andrić, et al. 2010, E. Geiser, et al. 2016, Kumar, et al. 2008].

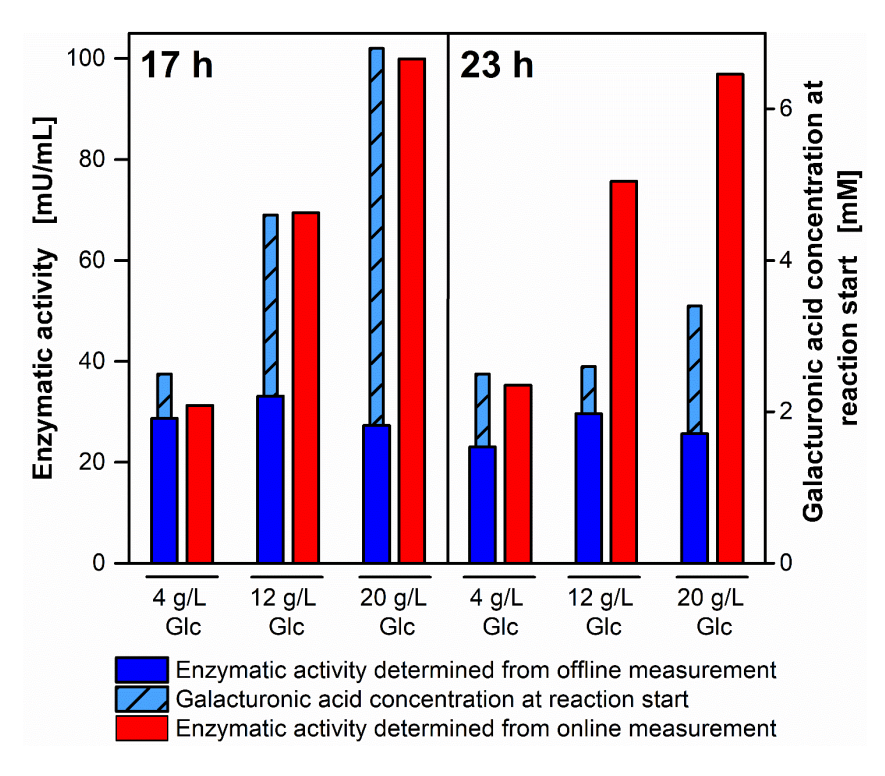


Figure 2-6: Comparison of enzymatic activity determined from offline (DNS) and online (OTR) measurements. The hydrolytic enzymatic activity on PolyGalA was determined by offline DNS assays (blue bars) or by online determination of the linear substrate consumption shown in Figure 2-5 (red bars). Samples of culture supernatant were taken and analysed after cultivation times of 17 and 23 h. For offline assays, the reaction time was 4 h and the PolyGalA concentration 4 g/L. Light blue bars show the GalA concentration at the beginning of the offline assay.

The online determination of enzymatic activities for product inhibited CAZymes provides reliable results, even at low total enzymatic activities. However, two prerequisites have to be fulfilled for the introduced method. First, the expressed enzymes have to liberate fermentable sugar units. If for example endo-enzymes simply degrade the polymeric substrates into shorter oligomers that cannot be further converted, the organism shows no metabolic activity and, thus, fails to grow on the hydrolysis products. An *U. maydis* strain producing the intrinsic endopolygalacturonase would, thus, show no growth on PolyGalA. Secondly, too high activities of the hydrolytic enzyme would lead to a completely unlimited growth on the liberated fermentable sugar units and, thus, the substrate consumption rate never equals the liberation rate. Under those conditions, no linear decrease of the substrate concentration, as shown in Figure 2-5C, could be calculated.

2.5.2 Investigation of enzyme stability by substrate pulsing

A consolidated bioprocess for degradation of plant biomass requires highly stable CAZymes. For this study, a haploid *U. maydis* strain, in which five proteases were deleted, was used to prevent degradation of the secreted pectinases. This strain was previously successfully used to produce heterologous single-chain antibodies in *U. maydis* [Sarkari, *et al.* 2014]. To prove the enzyme stability of the secreted exo-polygalacturonase and to verify the understanding of the three phases during the growth on PolyGalA discussed previously, PolyGalA was pulsed at different time points as depicted in Figure 2-7.

The first time point for a PolyGalA pulse during the unlimited growth phase on GalA was after 17.5 h (Figure 2-7A, red curve). The OTR plateau at 7 mmol/L/h is slightly higher compared to the reference cultivation without pulse (black curve, 6 mmol/L/h). This increase might be associated to more available total PolyGalA substrate. During the plateau phase, the cultures run in parallel until the substrate accessibility decreases in the reference cultivation after about 24 h. The OTR plateau of the pulsed culture continues its level of 7 mmol/L/h until the substrate accessibility decreases here as well after about 28 h. The course of the RQ (Figure 2-7B) shows again a clear separation between the growth phases on glucose (< 17 h) and GalA (> 17 h), as well as the depletion of GalA. A similar behavior was observed when the pulse was added in the OTR plateau phase after 19 h (Figure 2-7A, blue curve). After the pulse, the OTR slightly increased from 6 to 7 mmol/L/h and runs in parallel to the cultivation with the earlier pulse until the end of the experiment.

The reference cultivation (Figure 2-7A, black curve) reached a basal level in the OTR after 28 h. Adding a pulse in that cultivation after 39 h (Figure 2-7A, olive green curve) results in an immediate increase of the OTR to 6 mmol/L/h, the level of the first plateau. This clearly demonstrates the stability of the enzymes in culture supernatant. Even under starvation of the cells, the enzyme remains functional.

All previously pulsed cultivations were supplemented with a second pulse after 70 h (Figure 2-7A, arrows). This pulse resulted in a similar response in all cases. The cultivations reached a similar OTR level. As described for the pulse after 39 h, the OTR started to decrease right after

the maximal OTR was reached. The RQ values remained below those values obtained during the first OTR plateau. This indicates a stronger maintenance metabolism due to starvation.

Figure 2-7C shows the OT. The pulsed cultivations reach comparable final values of 315 mmol/L. The reference cultivation shows a lower final OT of 200 mmol/L. The method for prediction of the residual substrate concentration was applied to compare the overall consumption of the supplemented polygalacturonic (Figure 2-7D). After the PolyGalA consumption, the reference culture consumed 50% of the supplemented PolyGalA. All pulsed cultivations also ended up at 50% substrate consumption after 60 h and even after consumption of the second substrate pulse (84 h). Thus, even under different cultivation conditions, the percentage of convertible PolyGalA remains constant. The sharp increase in the OTR after the pulses at 39 and 70 h indicates that the presented cultivation system is tolerant towards short starvation times and the secreted exo-polygalacturonase is neither degraded nor inhibited by secreted metabolites of the cells or by other media components.

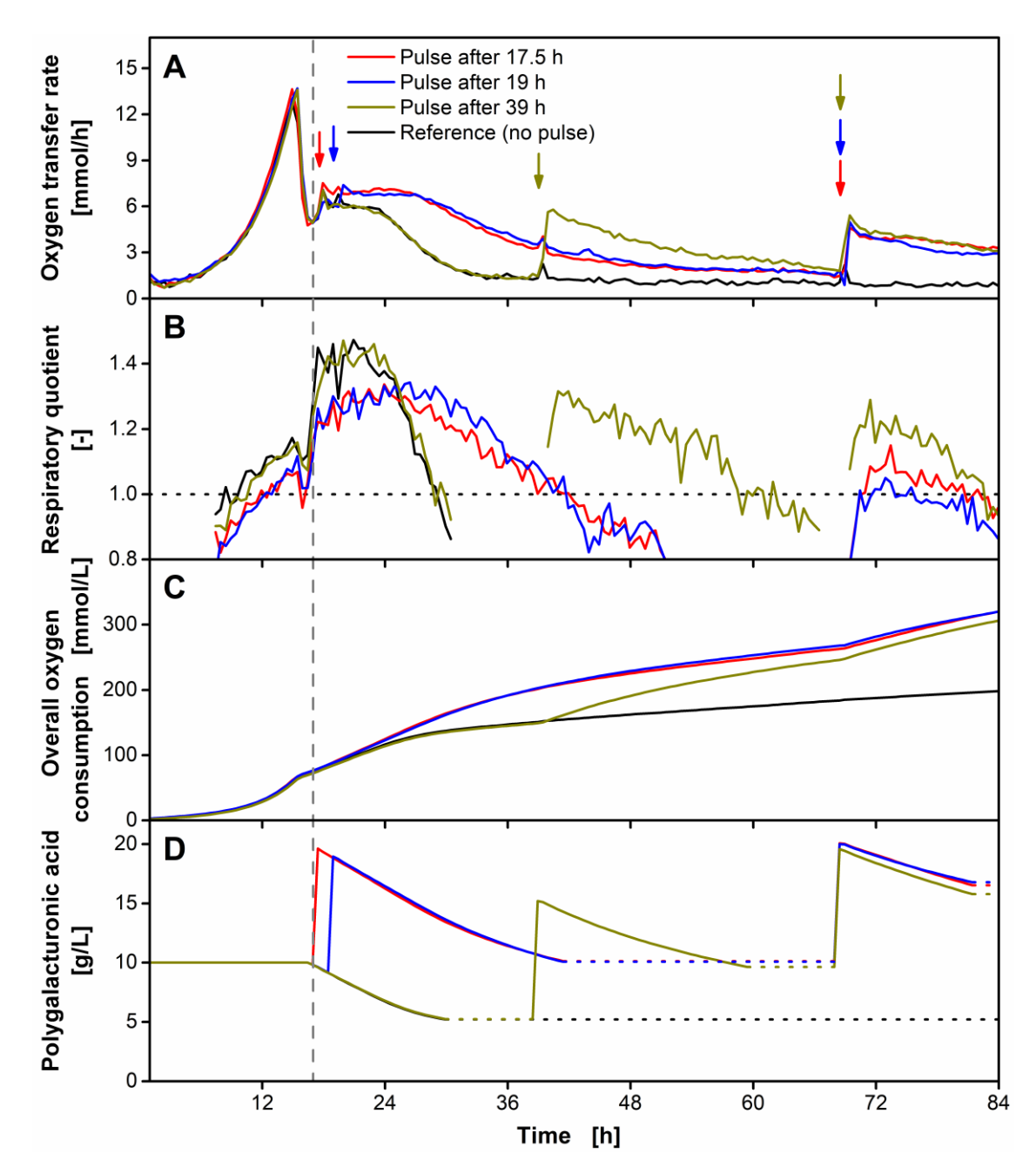


Figure 2-7: Influence of PolyGalA pulses on the cultivation of *U. maydis* **AB33P5**Δ**R**/**AtPgaX**. The strain was grown on glucose (6.5 g/L) and PolyGalA (10 g/L) as carbon sources. Pulses of PolyGalA were added at indicated time points (arrows). At 68.5 h, all cultures except the reference received a second substrate pulse. The values for the OTR, the OT and the predicted residual PolyGalA concentration (PolyGalA_{calc}) refer to the initial filling volume. The vertical dashed line represents the beginning of PolyGalA consumption. **A** Mean value of biological duplicates of the OTR. **B** Mean value of biological duplicates of RQ. The dotted horizontal line represents RQ = 1. For clarity, the RQ is only shown for OTR > 2 mmol/L/h. **C** Mean value of duplicates of the OT. **D** PolyGalA_{calc} according to Equation (6). The RQ drops below 1 during consumption of PolyGalA, indicating depletion of accessible substrate. Thus, the line for PolyGalA_{calc} in Figure 2-7D is dotted during that time. The mean values of biological duplicates are shown for better clarity. Culture conditions: modified Verduyn medium, 0.2 M MOPS, initial pH 6.5, 250 mL flask, initial filling volume 20 mL, shaking frequency 300 rpm, shaking diameter 50 mm, initial OD₆₀₀ = 0.2, temperature 30 °C. The mass of PolyGalA in one pulse equals the initial mass supplemented in the medium. Pulses of 5 mL PolyGalA solution (40 g/L) were added.

2.6 Conclusion

This chapter described the metabolic activity of *U. maydis* growing on GalA, the main component of pectin, by application of online monitoring tools. The growth behavior was reproducible and enabled closed carbon balancing for the growth on glucose and GalA. The overall consumed oxygen was successfully correlated with the consumed amount of substrate. A method for the prediction of the residual substrate concentration was developed. The production of the heterologous exo-polygalacturonase PgaX in *U. maydis* activated this strain to grow on PolyGalA. The developed method was applied to calculate the enzymatic activity during the growth of this activated *U. maydis* strain on PolyGalA. A comparison with offline determined enzymatic activities showed that online measurements prevented an underestimation of the enzymatic activity due to inhibition by accumulated product. Thus, the newly introduced method for online determination of the enzymatic activity is highly favorable in case of product inhibited hydrolytic enzymes. Finally, the stability of secreted enzymes was proven over the entire course of fermentation by pulsing substrate at distinct times of the cultivation.

To complete the concept of consolidated bioprocessing, the complexity of digestible substrate has to be further increased. For growth on pectin, sugar beet pulp, or other pectin-rich waste streams, a high number of different enzymes such as hydrolases or monooxygenases is required [Cragg, *et al.* 2015]. Co-fermentations seem to be promising in a consolidated bioprocess as this concept mimics nature in terms of microbial cooperation on degradation of plant biomass [Alcantara, *et al.* 2017, Bader, *et al.* 2010].

Further efforts must be made to increase the overall consumption rate of PolyGalA. This might be achieved by implementation of other pectinases. For example, an endo-polygalacturonase would be beneficial which can cleave PolyGalA chains with esterified residues at the non-reducing ends that cannot be hydrolyzed by exo-polygalacturonases. By an intra-chain cleavage, new active sites for the exo-polygalacturonase are provided. With such two-enzyme system, more complex substrates might be addressed, like pectin or pectin-rich biomass wastestreams. The next chapter will therefore deal with online monitoring *U. maydis* cofermentations to detect synergistic effects of the expressed enzymes on PolyGalA degradation.

Chapter 3

Complementing the intrinsic repertoire of *Ustilago* maydis for degradation of the pectin backbone polygalacturonic acid

3.1 Introduction

Chapter 2 showed that *Ustilago maydis* is able to grow on monomeric galacturonic acid (GalA), the most abundant sugar in pectin. This has been proven by application of the respiration activity monitoring system (RAMOS) device, enabling the development of a methodology for the online quantification of consumed GalA (Chapter 2.4). This methodology is based on the stoichiometric linkage between GalA consumption, oxygen consumption and carbon dioxide release. Extension of this methodology towards the estimation of residual polygalacturonic acid (PolyGalA) resulted in the determination of enzymatic activities for an *U. maydis* strain producing a heterologous exo-polygalacturonase. However, not all PolyGalA present in the medium was consumed during the cultivation.

This Chapter focusses on the evaluation of various alternative endo- and exopolygalacturonases to increase the overall metabolization of PolyGalA. Enzymes of intrinsic, fungal and bacterial origin are tested in constitutive production hosts. A combination of genetic and bioprocess engineering is used to establish PolyGalA decomposition and consumption. Online monitoring tools are used to assess the hydrolytic activity of three different endopolygalacturonases. *U. maydis* strains expressing endo- and exo-polygalacturonase are therefore co-cultivated on PolyGalA.

3.2 Material and methods

3.2.1 Plasmids, strains and media

All plasmid vectors were generated using standard molecular cloning methods including Golden Gate cloning [Green and Sambrook 2012, Terfrüchte, *et al.* 2014]. Plasmids were propagated in *Escherichia coli* Top10 cells. The vector for intrinsic gene activation with the strong P_{oma} promoter was assembled by Golden Gate cloning [E. Geiser, *et al.* 2016, Terfrüchte, *et al.* 2014] using approximately 1 kb flanking regions in the 5' region of the intrinsic open reading frame thereby deleting the putative region for the native promoter of about 1 kb. Genomic DNA of *U. maydis* strain UM521 [Kämper, *et al.* 2006] was used as a template for flank generation by polymerase chain reaction (PCR). Heterologous genes were inserted in the *ip* locus using integrative vectors mediating carboxin resistance [J. Stock, *et al.* 2012] or in the modified *upp3* locus of strain AB33P5 Δ R, in which five proteases including *upp3* had previously been sequentially deleted [Sarkari, *et al.* 2014]. Heterologous genes were specifically codon-optimized for expression in *U. maydis* using an online tool [Haag, *et al.* in press, Zhou, *et al.* 2018] and produced by chemical gene synthesis (Integrated DNA Technologies, Leuven, Belgium). Oligonucleotides used for molecular cloning are listed in Table 3-1.

Table 3-1: DNA oligonucleotides used in this chapter.

Designation	Nucleotide sequence (5´- 3´)	
oMB425	ACAGCTCTTCCGTGCATTTAAATACCTCGAAGCACAACGTACG	
oMB426	ACAGCTCTTCCGGCCCACCCGAGGCACCGTCTTTATGC	
oMB427	ACAGCTCTTCCCCTATGGCCTGCCTTTTGCTGGTTGG	
oMB428	CGCGCTCTTCCGACATTTAAATACCCGACAATTTGATGTTGG	
oMF502	ACGACGTTGTAAAACGACGGCCAG	
oMF503	TTCACACAGGAAACAGCTATGACC	

pUMa2822 (pDest_Poma:umag_02510_NatR) for in locus promoter exchange of umag_02510 was generated by SapI-mediated Golden Gate cloning. The reaction included the up- and downstream flanks generated on UM521 gDNA using the primer combinations MF425xMF426 and MF427xMF428, respectively, the storage vector pUMa2443 [Aschenbroich, et al. 2018] containing a nourseothricin resistance cassette (NatR) and the Poma promoter, as well as the destination vector pUMa2074 [Aschenbroich, et al. 2018]. The integrative plasmids for locus pUMa3108 (pRabX1_Poma_pgaX_CbxR), pUMa3400 insertion the (pRabX1_Poma_pguB-cts1_CbxR), pUMa3401 (pRabX1_Poma_peh1-cts1_CbxR), pUMa3403 (pRabX1_Poma_pga1_CbxR) were generated by standard restriction-ligation cloning. The corresponding codon-optimized heterologous genes were synthetized with cognate flanking restriction sites. Heterologous fungal genes included their N-terminal native signal peptides for entry of the endoplasmic reticulum (ER) whereas the signal peptides of bacterial genes were eliminated for export of the corresponding protein by Cts1-mediated unconventional secretion (signal peptides predicted with SignalP5.0;) [Nielsen 2017]. pUMa2113 [Sarkari, et al. 2014] seved as backbone for insertion of bacterial genes via NcoI/SpeI or BamHI/SpeI sites, thereby replacing the gus gene, resulting in translational Cts1 fusions. For insertion of fungal genes, pUMa2113 was modified removing cts1 via NotI/SfiI and NcoI/SfiI hydrolysis creating an intermediate vector carrying the P_{oma} promoter [Hartmann, et al. 1999] and the gus gene fused to a Strep-tripleHA-decahistidine (SHH)-tag encoding sequence [Sarkari, et al. 2014]. Via restriction with BamHI/SfiI the gus gene was removed from the intermediate vector and replaced by the respective heterologous fungal gene upstream (in frame) of the shh sequence [Sarkari, et al. 2014]. Plasmid sequences and detailed cloning strategies will be provided upon request.

 $U.\ maydis$ strains applied or generated in this study are listed in Table 3-2. Genomically stable strains were obtained by homologous recombination using the parental strain AB33P5 Δ R [Sarkari, et al. 2014]. All plasmids were linearized at the flank borders or within the ip^R allele using unique restriction endonucleases [Bosch, et al. 2016, Terfrüchte, et al. 2014]. Excised linear constructs were used to transform $U.\ maydis$ protoplasts [Bosch, et al. 2016]. Each genetic modification was verified by Southern blot analysis using digoxigenin labeled probes (PCR Dig Labeling Mix, Roche, Basel, Switzerland). Mutants transformed with integrative plasmids were selected for harboring a single plasmid copy in the ip locus by Southern blot

analysis using a probe generated by PCR using primer combination MF502/MF503 and the template pUMa260 [Loubradou, *et al.* 2001]. For *in locus* modifications the complete flanking regions were used as probes.

Table 3-2: *U. maydis* strains used in this chapter.

Strain	Relevant genotype, resistance	UMa ¹	Refe- rence	Plasmid trans- formed	Manipulated locus ²	Progenitor (Uma) ¹ [Reference]
AB33P5Δ R	FRT5[$um04400 \Delta$] FRT3[$um11908\Delta$] FRT2[$um00064\Delta$] FRTwt[$um02178\Delta$] FRT1[$um04926\Delta$] PhleoR	1391	[Sarkar i, et al. 2014]	detailed strain description in Sarkari, et al. [2014]	ip (cbx), umag_04400, umag_11908, umag_00064, umag_2178, umag_04926	AB33 [Brachmann, et al. 2001] AB33P5ΔR
AB33P5Δ R /UmPgu1	FRT5[um04400 Δ] FRT3[um11908Δ] FRT2[um00064Δ] FRTwt[um02178Δ] FRT1[um04926Δ] P02510::umag_02510:: Poma::um02510 PhleoR, NatR	2030	This chap- ter.	Poma:umag _02510_Nat R (pUMa2822)	umag_02510	(UMa1391) [Sarkari, et al. 2014]
AB33P5Δ R /AtPgaX	FRT5[$um04400 \Delta$] FRT3[$um11908\Delta$] FRT2[$um00064\Delta$] FRTwt[$um02178\Delta$] FRT1[$um04926\Delta$] ip^r [$PomaAtPgaX$: SHH] ip^s PhleoR, CbxR	2106	Chap- ter 2	pRabX1_ Poma_pgaX _SHH_ CbxR (pUMa3108)	ip (cbx)	AB33P5ΔR (UMa1391) [Sarkari, <i>et al.</i> 2014]

Strain	Relevant genotype, resistance	UMa ¹	Refe- rence	Plasmid trans- formed	Manipulated locus ²	Progenitor (Uma) ¹ [Reference]
AB33P5Δ R /AaPgu1 ³	FRT5[um04400 Δ] FRT3[um11908Δ] FRT2[um00064Δ] FRTwt[um02178Δ] FRT1[um04926Δ] ipf [PomaAaPgul: SHH] ips PhleoR, CbxR	2416	This chap- ter.	pRabX1_ Poma_AaPg u1_SHH_ CbxR (pUMa3403)	ip (cbx)	AB33P5ΔR (UMa1391) [Sarkari, <i>et al.</i> 2014]
AB33P5Δ R /PcPeh1 ⁴	FRT5[$um04400 \Delta$] FRT3[$um11908\Delta$] FRT2[$um00064\Delta$] FRTwt[$um02178\Delta$] FRT1[$um04926\Delta$] ip^r [PomaPcPeh1: SHH: cts1] ip^s PhleoR, CbxR	2402	This chap-ter.	pRabX1_ Poma_Peh1 -SHH-Cts1_ CbxR (pUMa3401)	ip (cbx)	AB33P5ΔR (UMa1391) [Sarkari, <i>et al.</i> 2014]
AB33P5Δ R /KpPguB ⁴	FRT5[um04400 Δ] FRT3[um11908Δ] FRT2[um00064Δ] FRTwt[um02178Δ] FRT1[um04926Δ] ip' [PomaKpPguB: SHH: cts1] ip' PhleoR, CbxR	2401	This chapter.	pRabX1_Po ma_PguB- SHH-Cts1_ CbxR (pUMa3400)	ip (cbx)	AB33P5ΔR (UMa1391) [Sarkari, <i>et al.</i> 2014]

¹ Internal strain collection number

For strain generation *U. maydis* strains were grown at 28 °C in complex medium (CM) supplemented with 10 g/L glucose (CM-Glc) [Holliday 1974]. For determination of enzyme activities indicated strains were grown in modified Verduyn mineral medium as described in

² Sequences available on NCBI or PEDANT [IBIS 2019, NCBI 2019]

³ The intrinsic signal peptide encoding sequences of the enzymes were kept

⁴ The intrinsic signal peptide encoding sequences predicted by SignalP 4.1 were removed to allow for unconventional secretion [CBS 2019]

Chapter 2.2.2 using 0.1 M MES, pH 6.5 as buffer. The modified Verduyn mineral medium was supplemented with 1% (w/v) glucose unless stated otherwise.

3.2.2 Microscopic analyses

For microscopy, cells were immobilized on agarose patches (2% final concentration (f. c.)). A wide-field microscope setup from Visitron Systems, Axio Imager M1 equipped with a CCD camera and the objective lens Plan Neofluar (63 x, NA 1.25) was used. The microscopic system was controlled by the MetaMorph software (Molecular Devices, version 7, Sunnyvale, USA). The program was also used for image processing, including the adjustment of brightness and contrast.

3.2.3 Bioinformatic evaluation

To identify *U. maydis* orthologues to *Aspergillus niger* Gaa enzymes proposed to function in GalA catabolism respective amino acid sequences were subjected to BlastP analyzes on the National Center for Biotechnology Information (NCBI) server against the reference protein dataset *Ustilago maydis* 521 (taxid:237631). Amino acid identities over the whole length of homologous sequences were determined by amino acid alignments using the program CloneManager 12 (Sci-Ed Software).

Putative enzyme functions and glycoside hydrolase domains of pectinolytic enzymes were derived from BlastP analyzes against the full reference protein database (refseq_protein) on NCBI. Well-characterized proteins upon the top hits were used for amino acid alignments and conservation of functional residues was determined based on available literature information. N-terminal signal sequences for prediction of conventional secretion were determined by SignalP4.1 [Nielsen 2017]. *U. maydis* amino acid (umag) sequences were retrieved from the PEDANT *U. maydis* genome homepage. The amino acid alignment has been assembled using Clustal Omega [EMBL-EBI 2019, Sievers, *et al.* 2011] and the program ESPript 3.0 [Robert and Gouet 2014]. Identical amino acids are depicted with a black background.

3.2.4 Preparation of cell extracts

U. maydis cell extracts were prepared as described in Stock et al. 2016 [Janpeter Stock, et al. 2016] using denaturing sodium phosphate buffer (0.1 M Na₂HPO₄/NaH₂PO₄, 8 M Urea, 0.01 M Tris/HCl, pH 8.0) supplemented with inhibitor mix protease (1 mM phenylmethylsulfonylfluorid (PMSF), 10 mM dithiothreitol (DTT), 2.5 mM benzamidine hydrochloride hydrate, 5 × cOmplete Protease EDTA-free Protease Inhibitor Cocktail (Sigma-Aldrich, now Merck, Darmstadt, Germany). Cell pellets of 2 mL cultures were mixed with 500 μL denaturing sodium phosphate buffer and 100 μL of glass beads (0.25-0.5 mm; Carl Roth, Karlsruhe, Germany). The cell disruption was performed in a ball mill (Retsch, Haan, Germany) at 30 Hz for 5 min. The mixture was centrifuged at $16,000 \times g$ for 30 min. $400 \,\mu$ L of the supernatant were transferred to a new 1.5 mL reaction tube and stored on ice. The protein concentration of the supernatant was determined via Bradford assay. 10 ng of protein was incubated with 1 × denaturing Laemmli-buffer [Laemmli 1970] in a volume of 20 µL at 95°C for 10 min. For subsequent deglycosylation of cell extracts, the denaturation of the protein was performed in $1 \times$ glycoprotein reaction buffer (Chapter 3.2.7).

3.2.5 Protein precipitation from culture supernatants

To precipitate proteins, cell free culture supernatants were harvested by centrifugation $(16,000 \times g, 10 \text{ min})$ and supplemented with 10% (v/v) trichloric acid (TCA). After overnight incubation at 4°C, precipitates were pelleted by centrifugation $(16,000 \times g, 30 \text{ min}, 4°C)$ and washed twice with ice-cold acetone (precooled to -20°C). The protein pellets were then resuspended in $15 \mu L$ of $3 \times \text{denaturing Laemmli-buffer [Laemmli 1970]}$ (protein concentration factor about $60 \times$) and the pH was neutralized with $2 \mu L$ 1 M NaOH. For sodium dodecyl sulfate (SDS)-Page analysis, the samples were boiled for 10 min. After centrifugation $(22,000 \times g, 5 \text{ min})$ the supernatants were used for SDS-Page.

3.2.6 SDS-Page and Western blot analysis

SDS-Page was used to separate proteins by their molecular masses. Proteins from gels were transferred to methanol-activated polyvinylidene fluoride (PVDF) membranes using semi-dry

Western blotting. Tagged proteins were detected using primary anti-HA antibodies (Sigma-Aldrich, now Merck, Darmstadt, Germany; 1:3,000 dilution) and secondary anti-mouse IgG-horseradish peroxidase (HRP) conjugates (Promega, Mannheim, Germany; 1:4,000 dilution). Blots were developed using AceGlow Western blotting detection reagent (PeqLab, now VWR, Erlangen, Germany) and a LAS4000 chemiluminescence imager (GE LifeScience/VWR, Erlangen, Germany). To visualize protein loading, the PVDF membranes were stained with Coomassie Brilliant Blue by incubation in the staining solution for several minutes (0.05% Coomassie Brilliant Blue R250, 15% (v/v) acetic acid, 15% (v/v) methanol), followed by a short rinse in water and subsequent drying.

3.2.7 Protein deglycosylation

Proteins in cell extracts or precipitated culture supernatants were treated with the PNGaseF deglycosylation kit (New England Biolabs, Frankfurt am Main, Germany) to remove the sugar moieties of N-glycosylations. 10 μ g of cell extracts or protein pellets obtained by TCA precipitation were dissolved in 10 μ L 1 \times glycoprotein reaction buffer and denatured by incubation at 95 °C for 10 min. 2 μ L 10% (w/v) NP-40, 2 μ L 10 \times GlycoBuffer II and 1 μ L PNGaseF were added and the volume adjusted to 20 μ L with H₂O. Reaction mixes were incubated for 4 h at 37 °C and subsequently analyzed by SDS-Page and Western blot analysis.

3.2.8 Offline polygalacturonase activity assay

For polygalacturonase production, shake flask cultures of respective strains were inoculated in modified Verduyn mineral medium containing 10 g/L glucose at an OD₆₀₀ of 0.5 and incubated for 24 h (200 rpm, 28 °C). After this time, glucose was completely consumed, which was additionally verified by DNS assays (Table A1) or roughly estimated by glucose test strips (Macherey-Nagel, Düren; Germany). 200 μ L cell-free culture supernatant were mixed with 800 μ L PolyGalA solution (0.5% (w/v) in 0.1 M sodium acetate buffer, pH 5.5) and incubated at 30°C and 600 rpm. 60 μ L samples were taken at 0, 6 and 24 h and incubated at 95°C for 10 min to deactivate the respective enzymes. Samples were stored at -20°C until the DNS assay was performed. Determination of the reducing group concentration was done via DNS assay as described in Chapter 2.2.4.6. Transparent polystyrene 96-well microtiter plates (Greiner Bio-

One, Frickenhausen, Germany) were used for absorption measurement using a Tecan 200 plate reader (Tecan, Männerdorf, Switzerland). GalA standard curves were recorded using standard solutions with concentrations of 0, 0.625, 1.125, 2.5, 5.0, 10.0 and 20.0 mM of GalA. Initial values (0 h) were subtracted to remove background.

3.2.9 Online measurement of the metabolic activity

Online monitoring of the oxygen transfer rate (OTR), the carbon dioxide transfer rate (CTR) and the respiratory quotient (RQ) enabled determining the metabolic activity of cultures. Cultivations were performed as described in Chapter 2.2.3. The flasks were filled with 20 mL modified Verduyn mineral medium (Chapter 2.2.2) that was inoculated to an initial OD₆₀₀ of 0.6 with an over-night grown pre-culture. As carbon sources, the medium was supplemented with 4 g/L glucose and varying amounts of (Poly)GalA. Consumption of (Poly)GalA leads to an increasing pH. To prevent alkalization during growth on those acid substrates, the medium was buffered with 0.2 M MOPS, pH 6.0.

Based on the RQ, cultivation phases with glucose and (Poly)GalA consumption were identified, as described in Chapter 2.5. PolyGalA consumption started after the OTR and RQ drop due to glucose depletion. The end of PolyGalA consumption was defined as the time point where a linear fit of the RQ reached a value of 1.0. Figure A7 depicts an exemplary fit of the RQ during the cultivation represented in Figure 3-8. The overall consumed oxygen (OT) during consumption of (Poly)GalA was used to estimate the respective residual substrate concentration as described in Chapter 2.4. The enzymatic activity in the culture supernatant was determined from the linear decrease of the calculated concentration of residual (Poly)GalA over time as described in Chapter 2.5.

3.2.10 Offline analytics

Offline sampling and analytics were performed as described in Chapter 2.2.4.

PolyGalA was precipitated prior to HPLC measurement as the polymer can block the chromatographic column. Therefore, cell-free culture broth supernatant was treated as described by Spiro, *et al.* [1993].

3.2.11 Determination of liberated GalA during RAMOS cultivations

The overall liberated amount of GalA was determined using Equation (8).

$$GalA_{lib} = GalA_{sup} + GalA_{con}$$
 (8)

GalA_{lib}: concentration of overall liberated GalA from PolyGalA [g/L]

 $GalA_{sup}$: concentration of GalA in the culture supernatant, measured by HPLC [g/L]

 $GalA_{con}$: concentration of the overall consumed GalA [g/L], determined from the OT as described by Equation (6)

The time specific liberation rate of GalA between two sampling time points (t_1 and t_2) can be calculated by Equation (9).

$$\frac{\Delta GalA_{lib}}{\Delta t} = \frac{GalA_{lib,2} - GalA_{lib,1}}{t_2 - t_1}$$
(9)

This liberation rate was plotted against $t = \frac{t_1 + t_2}{2}$.

3.3 Inventory of intrinsic enzymes for pectin degradation and metabolization

Earlier studies suggest that some pectinolytic enzymes are present in *U. maydis* [Cano-Canchola, *et al.* 2000, Doehlemann, *et al.* 2008, Kämper, *et al.* 2006, Mueller, *et al.* 2008]. To inspect its natural abilities to degrade pectin in more detail, a list of potentially relevant enzymes was carefully re-evaluated bioinformatically. Therefore, the presence of enzymatic domains,

especially of the glycoside hydrolase domain and conserved domains of other CAZyme families was checked [CAZypedia Consortium 2018]. Furthermore, it was screened for conventional N-terminal secretion signals (SignalP5.0; [CAZypedia Consortium 2018]), and well-characterized orthologues were identified by BlastP analysis to compare enzyme architectures and the presence of active site residues (Figure 1-1, Table A2).

The analysis confirmed that several potential secreted pectinolytic enzymes with conserved hydrolytic domains are encoded in the *U. maydis* genome. These include a putative endopolygalacturonase, pectin lyase and pectin methylesterase. These enzymes are potentially acting on the PolyGalA backbone in homogalacturonan (Figure 1-1, Figure A6 and Table A2). For example, the putative endo-polygalacturonase shows homology to well-characterized endopolygalacturonases like the ones from *Fusarium moniliforme* and *Aspergillus aculeatus*. Remarkable are conserved substrate binding sites and residues involved in proton donation to the glycosidic oxygen and activation of H₂O for the nucleophilic attack (Figure 3-1) [Abdulrachman, *et al.* 2017, Federici, *et al.* 2001]. In addition, it carries a predicted N-terminal signal peptide for secretion via the conventional endomembrane system (Figure 3-1, Table A2), which is in line with its putative extracellular function.

In addition to the enzymes acting on homogalacturonan, three putative arabinofuranosidases and two arabinases were detected in the U. maydis genome. Those enzymes break down arabinofuranose or arabino-oligosaccharides from rhamnogalacturonan I and II side chains. Finally, other enzymes were identified which act on less abundant sugar residues (for example, β -galactosidase; Figure 1-1, Table A2).

Most enzymes acting on the homogalacturonan backbone release GalA, the main sugar unit in pectin. GalA also represents the major component of pectin hydrolysates [Caffall and Mohnen 2009]. Therefore, the metabolization of this monosaccharide is a prerequisite for growth on pectin. In Chapter 2.3, it was shown that *U. maydis* is able to grow on GalA.

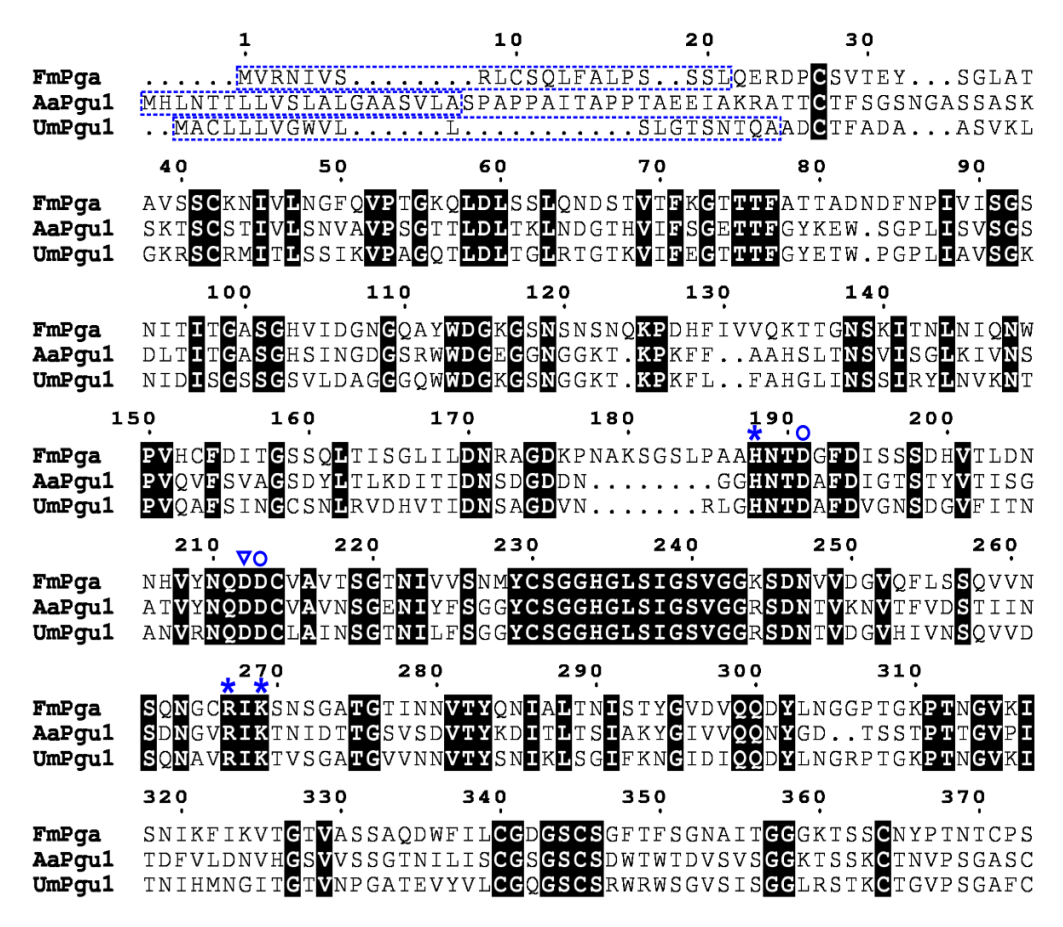


Figure 3-1: Conservation of a putative endo-polygalacturonase of *U. maydis.* Amino acid alignment showing the conservation of important functional residues between the well-characterized *Fusarium moniliforme* Pga (FmPga; accession number **Q07181.1**), *A. aculeatus* Pgu1 (AaPgu1; accession number **Q74213.1**) and the putative endo-polygalacturonase Pgu1 present in *U. maydis* (UmPgu1; accession number **KIS69158.1**). Blue asterisks depict residues involved in substrate binding; the blue triangle marks the aspartate residue that presumably donates protons to the glycosidic oxygen and the circles mark residues involved in activating H₂O for the nucleophilic attack [Federici, *et al.* 2001]. The predicted N-terminal signal peptides for conventional secretion are indicated by the blue dashed boxes.

To evaluate the pathway for GalA metabolization in *U. maydis*, the bioinformatics survey was extended. A conserved catabolic pathway of GalA has been described in *A niger* and other filamentous fungi (Figure 3-2, [E. S. Martens-Uzunova and Schaap 2009]). It involves enzymes that convert GalA into pyruvate and L-glyceraldehyde in three enzymatic steps. L-glyceraldehyde is subsequently reduced to glycerol. Homologs in *U. maydis* were identified by BlastP analyses using the enzyme amino acid sequences from *A. niger* [Elena S. Martens-Uzunova and Schaap 2008] as queries. Homologs of all four enzymes are encoded in the *U. maydis* genome, ranging between 38 and 60% amino acid identity (Figure 3-2). This suggests that *U. maydis* can catabolize GalA via a similar pathway like *A. niger*.

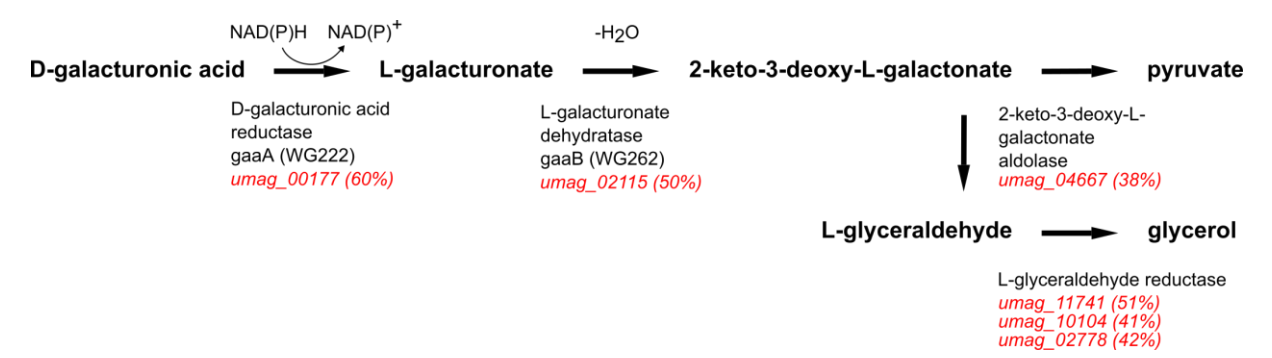


Figure 3-2: Metabolization of GalA. Conservation of the GalA catabolic pathway between A. niger and U. maydis. Numbers indicate the percentage of overall amino acid conservation. umag numbers (red font) correspond to respective gene identifiers found on PEDANT Ustilago maydis genome database or NCBI. Figure adapted from Elena S. Martens-Uzunova and Schaap [2008].

In summary, the bioinformatic analyses indicated that *U. maydis* contains enzymes to hydrolyze some of the enzymatic bonds in pectin molecules. However, the present enzyme set is clearly not sufficient to completely degrade the complex polymer into its monomers, because essential players are lacking for homogalacturonan degradation, for example exo-polygalacturonase and pectin acetylesterase (Figure 1-1). Moreover, the enzymes are mainly secreted during plant infection and not during the biotechnologically relevant yeast stage [Doehlemann, *et al.* 2008]. This finding is in line with the earlier observation that in the yeast form the fungus is not even able to grow naturally on the PolyGalA backbone of pectin. An earlier study reported contradictory growth of *U. maydis* in the yeast form on PolyGalA [Cano-Canchola, *et al.* 2000]. These findings were not supported by other publications why both, activation of intrinsic enzymes and supplementation with heterologous enzymes were aimed within this chapter to allow for PolyGalA metabolization.

Other fungi like the filamentous growing ascomycetes *Aspergillus oryzae* or *Aspergillus fumigatus* harbor large enzyme sets for pectin degradation with up to 50 representatives, often occurring in multiple copies [Doehlemann, *et al.* 2008, Martinez, *et al.* 2008]. The reduced set of *U. maydis* could be attributed to its biotrophic lifestyle that relies on the colonization of living plant tissue [Brefort, *et al.* 2009, Martinez, *et al.* 2008, Schipper and Doehlemann 2012]. Although the fungus must avoid destroying plant cells completely, it still needs to enter and spread in the plant tissue. The present enzymes could be used to loosen the recalcitrant structure of the plant cell walls for penetration [Doehlemann, *et al.* 2008]. However, deletion of the genes for predicted endo-polygalacturonase, pectin lyase or pectin methyl-esterase did not even impair virulence, suggesting that the function of the enzymes during plant infection is negligible

[Doehlemann, et al. 2008]. In this context, it is surprising that the bioinformatic survey suggested that *U. maydis* can metabolize GalA in the yeast phase. Importantly, this ability was confirmed by the studies described in Chapter 2.3. This indicates that yeast-like growing cells may encounter GalA monomers in a plant-associated environment, for example in the soil, and use it for nutrition.

3.4 Activation of an intrinsic endo-polygalacturonase

The activation of intrinsic enzymes remarked a first step towards degradation of pectins PolyGalA backbone. To activate enzyme production during the yeast phase, an overexpression strain was generated. This strain expressed one of the most important intrinsically encoded enzymes acting on pure PolyGalA: the predicted endo-polygalacturonase (UmPgu1, encoded by umag_02510, Figure 1-1 and Figure 3-1). The established promoter exchange strategy was used, in which the native promoter of the respective gene is replaced by the strong, constitutive P_{oma} promoter (Figure 3-3A) [E. Geiser, et al. 2016]. The construct was stably introduced in the protease-deficient strain AB33P5ΔR. This strain lacks a total of five proteases and has a significantly reduced proteolytic activity in the culture supernatant, thus, avoiding extensive extracellular degradation of, e.g., secreted enzymes [Sarkari, et al. 2014]. The morphology of the engineered strain was not impaired (Figure A8). To check for enzyme activity, cell-free culture supernatant of the expression strain AB33P5ΔR/UmPgu1 was incubated with the substrate PolyGalA. The release of reducing sugars after 6 and 24 h was detected by DNS assay (Figure 3-3B). In contrast to the progenitor strain, the supernatant of the activated strain released significant amounts of reducing sugars from PolyGalA, confirming that the bioinformatics prediction was correct and UmPgu1 is indeed secreted as an active polygalacturonase (Figure 3-3B).

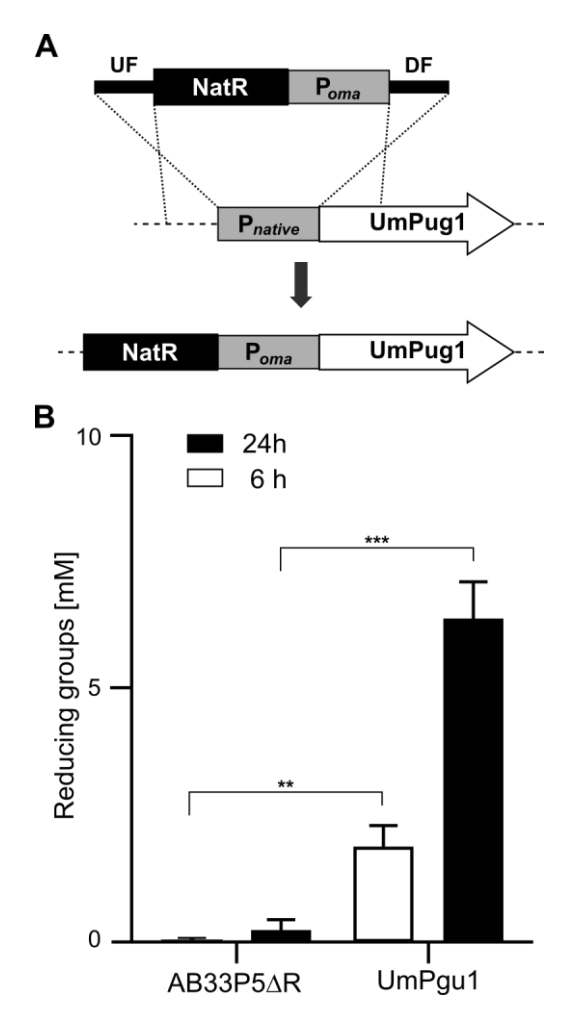


Figure 3-3: Activation of an intrinsic endo-polygalacturonase. A Schematic representation of the applied gene-activation strategy [E. Geiser, et al. 2016]. The native promoter of the corresponding gene umpgu1 ($umag_02510$) was replaced by the strong constitutive promoter P_{oma} (grey). A nourseothricin resistance cassette (NatR, black) was inserted for selection. **B** DNS assay depicting enzymatic activity of constitutively expressed intrinsic endo-polygalacturonase on PolyGalA. The progenitor strain AB33P5 Δ R served as control, exhibiting no significant activity. Upon incubation with PolyGalA, the activated strain AB33P5 Δ /UmPgu1 showed a strongly enhanced release of reducing sugars. The graph represents the results of three biological replicates. Error bars depict standard deviation. **: p value < 0.01; ***: p value 0.001 (two sample *t*-test).

3.5 Complementation with unconventionally secreted, heterologous, bacterial polygalacturonases

Since the genome of *U. maydis* does not encode a complete enzyme set for pectin degradation and especially lacks any obvious exo-polygalacturonase homologue for release of monomeric GalA from PolyGalA, complementation with potent heterologous enzymes was aimed. The ability to secrete potent bacterial enzymes is a unique opportunity of the system published by Jayani, *et al.* [2005]. It is only feasible because of the existence of the unconventional secretion

pathway, which circumvents the endomembrane system and, thus, potentially harmful posttranslational modifications (Figure 3-4A) [J. Stock, *et al.* 2012].

The bacterial exo-polygalacturonase PguB from *Klebsiella sp. CGMCC 4433* (KpPguB; accession number JQ388228.1; GH28) was tested first [Ibrahim, *et al.* 2017]. To this end, a strain was generated, in which a codon-optimized version of the respective gene was expressed as translational fusion with the carrier Cts1 for unconventional secretion (Figure 3-4B) [J. Stock, *et al.* 2012]. Of note, the sequence for the native signal peptide present in the bacterial gene was eliminated to redirect it to the unconventional secretion pathway. A sequence coding for a protein tag (SHH-tag) was inserted in between the two genes to allow for detection and purification of the fusion protein. The tag consisted of OneStrep, 3 × HA and 10 × His [Sarkari, *et al.* 2014]. The construct was inserted at the *ip* locus, which is an established locus for the expression of heterologous genes [J. Stock, *et al.* 2012].

Western blot analyses demonstrated that the fusion protein is synthetized and secreted into the culture supernatant (Figure 3-4C, D). Notably, the prediction of N-glycosylation sites revealed the presence of three potential motifs in KPguB (Figure 3-4B). Therefore, exporting this bacterial enzyme via the conventional secretion pathway in eukaryotes would very likely lead to artificial *N*-glycosylation, which might interfere with its activity. Applying the unconventional secretion pathway avoids these post-translational modifications [J. Stock, *et al.* 2012]. DNS assays using culture supernatants and PolyGalA as a substrate confirmed that no relevant amounts of reducing sugars are released by supernatants of the progenitor strain AB33P5ΔR that was used as a control (Figure 3-4E). By contrast, supernatants yielded from the strain producing KpguB clearly depicted enzyme activity. The amount of released reducing sugars after 6 h was negligible, while after 24 h low amounts of about 0.5 mM reducing sugars had been released (Figure 3-4E). These concentrations were detectable but clearly lower compared to the concentration of reducing ends produced by the intrinsic endopolygalacturonase (Figure 3-3B).

A similar strategy was followed to test a bacterial endo-polygalacturonase, using Peh1 from *Pectobacterium carotovorum* (PcPeh1; accession number M83222.1; GH28) [Yuan, *et al.* 2012]. This protein even contains up to six predicted *N*-glycosylation motifs (Figure 3-4B), again suggesting that unconventional secretion is a valuable tool to secrete the protein while

avoiding potentially deleterious post-translational modifications. Western blot analysis and DNS assays confirmed secretion and activity with about 1 mM released reducing sugars after 24 h (Figure 3-4C-E).

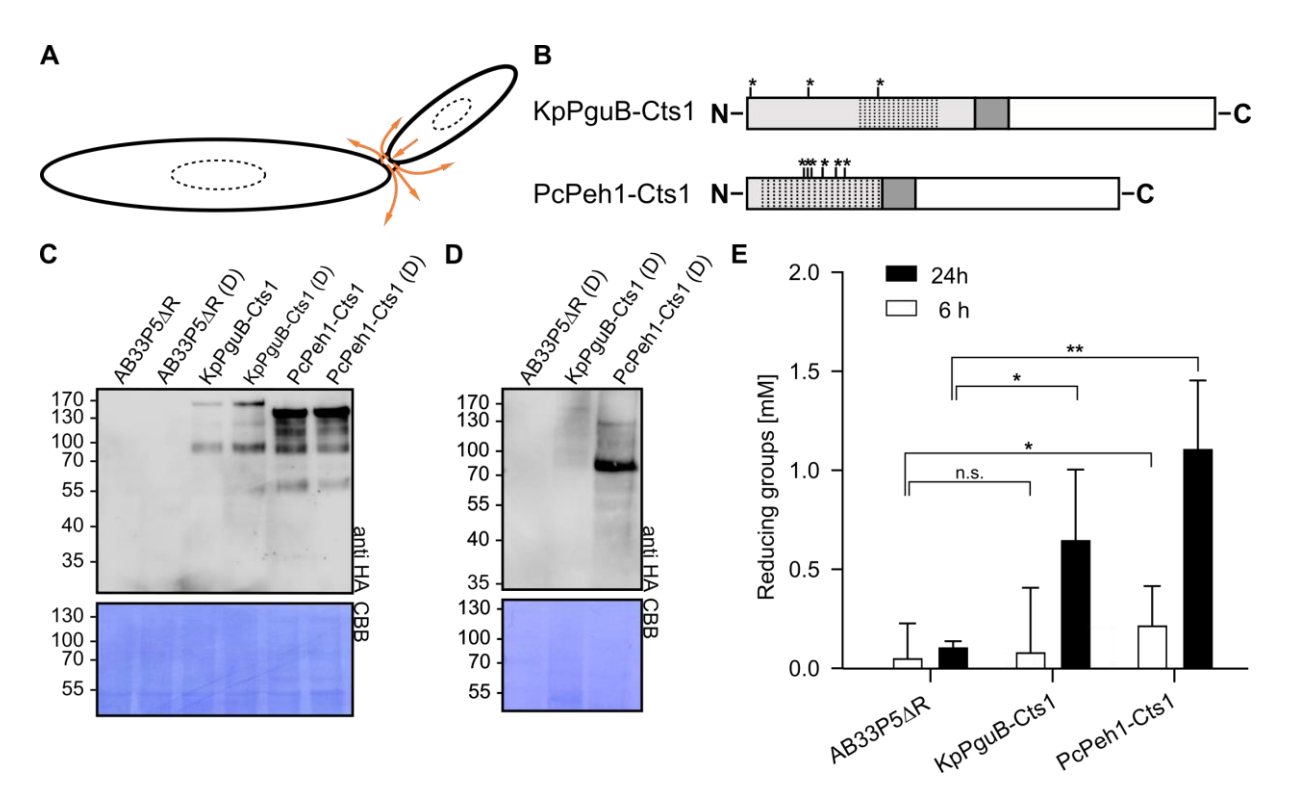


Figure 3-4: Complementation with bacterial endo- and exo-polygalacturonases. A Heterologous enzymes are secreted by lock-type unconventional secretion via the fragmentation zone of dividing yeast-like growing cells (scheme). B Representation of the two bacterial Cts1-fusion proteins used for complementation. Predicted Nglycosylation sites of endo-polygalacturonase P. carotovorum Peh1 (PcPeh1, 3 predicted sites) and exopolygalacturonase Klebsiella pneumoniae PguB (KpPguB, 6 predicted sites) are indicated by asterisks. Predicted N-terminal signal peptides were removed from the sequences to allow for Cts1-mediated unconventional secretion. Cts1 is indicated in white. An SHH-tag connects the two protein moieties (shown in dark grey). The predicted functional glucosidase hydrolase domains GH28 are indicated by dotted areas. C Expression of bacterial polygalacturonases in AB33P5ΔR (progenitor). The Western blot analysis depicts cell extracts (10 μg), which were partially deglycosylated (D). Heterologous proteins were detected using antibodies directed against the internal HA-tag. CBB, Coomassie Brilliant Blue staining of the membrane. Expected sizes of tagged proteins: KpPguB-Cts1: 134.9 kDa; PcPeh1-Cts1: 105.1 kDa. **D** Unconventional secretion of fungal polygalacturonases in AB33P5ΔR as Cts1-fusion proteins. The Western blot analysis depicts precipitated and deglycosylated culture supernatants (corresponding to 20 mL culture). Proteins were detected using antibodies directed against the internal HA-tag. CBB, Coomassie Brilliant Blue staining of the membrane. E DNS assay to detect activity of heterologous enzymes from bacterial sources. In contrast to the progenitor strain AB33P5ΔR, both engineered strains release reducing sugars from PolyGalA. The graph represents the results of three biological replicates. Error bars depict standard deviation, n.s.: p value > 0.05; *: p value < 0.05; **: p value < 0.01.

Overall, the experiments indicated that bacterial polygalacturonases could be expressed and secreted in an active state using the described unique unconventional secretion system. The

morphology of the modified strains was not impaired suggesting that the transgenes do not cause any side effects (Figure A8). Thus, the intrinsic repertoire can be complemented with bacterial enzymes. However, in comparison to the bacterial enzyme, the intrinsic endopolygalacturonase did show a higher activity suggesting that the amounts of unconventionally released bacterial enzymes might need further improvements. Limiting yields of the unconventional secretion pathway have been observed earlier and are currently addressed by different optimization steps [Terfrüchte, et al. 2018].

3.6 Complementation with conventionally secreted heterologous fungal polygalacturonases

Next, the performance of fungal polygalacturonases was investigated. Initially, the conventionally secreted fungal exo-polygalacturonase PgaX from A tubingensis (AtPgaX; accession number CAA68128.1; GH28) was tested [Kester, et al. 1996]. Therefore, an existing strain carrying a codon-optimized gene encoding an SHH-tagged version of AtPgaX under control of the P_{oma} in the *ip* locus of AB33P5ΔR was used (AB33P5ΔR/AtPgaX, Chapter 2). The corresponding enzyme was conventionally secreted via the endomembrane system using its native N-terminal signal peptide (Figure 3-5A, B). Western blot analyses of cell extracts and culture supernatants confirmed expression and secretion of the heterologous protein (Figure 3-5C, D). Specific bands were detected for AtPgaX, running significantly higher than expected for its size of 56.5 kDa (Figure 3-5C, D) [Kester, et al. 1996]. The enzyme carries eight predicted N-glycosylation sites (Figure 3-5B) for modification in the endomembrane system suggesting that the size shift could be due to posttranslational modifications. Indeed, deglycosylated protein was strongly reduced in size and ran approximately at the expected height (Figure 3-5C, D). Enzyme activity of AB33P5ΔR/AtPgaX culture supernatant was assayed by DNS assays using PolyGalA as a substrate (Figure 3-5E). Significant amounts of reducing sugars were detected when testing culture supernatants obtained from the strains expressing heterologous fungal enzymes, demonstrating that the enzyme is functionally secreted in *U. maydis*. However, only slight activity with release of about 2.5 mM reducing sugars was observed (24 h incubation; Figure 3-5E). This is in line with the previously observed low metabolic activity of this strain on PolyGalA (Chapter 2.5). The fact that released sugars

did only double with a fourfold increase of the incubation time (6 vs. 24 h) is likely due to product inhibition, as described in Chapter 2.5.

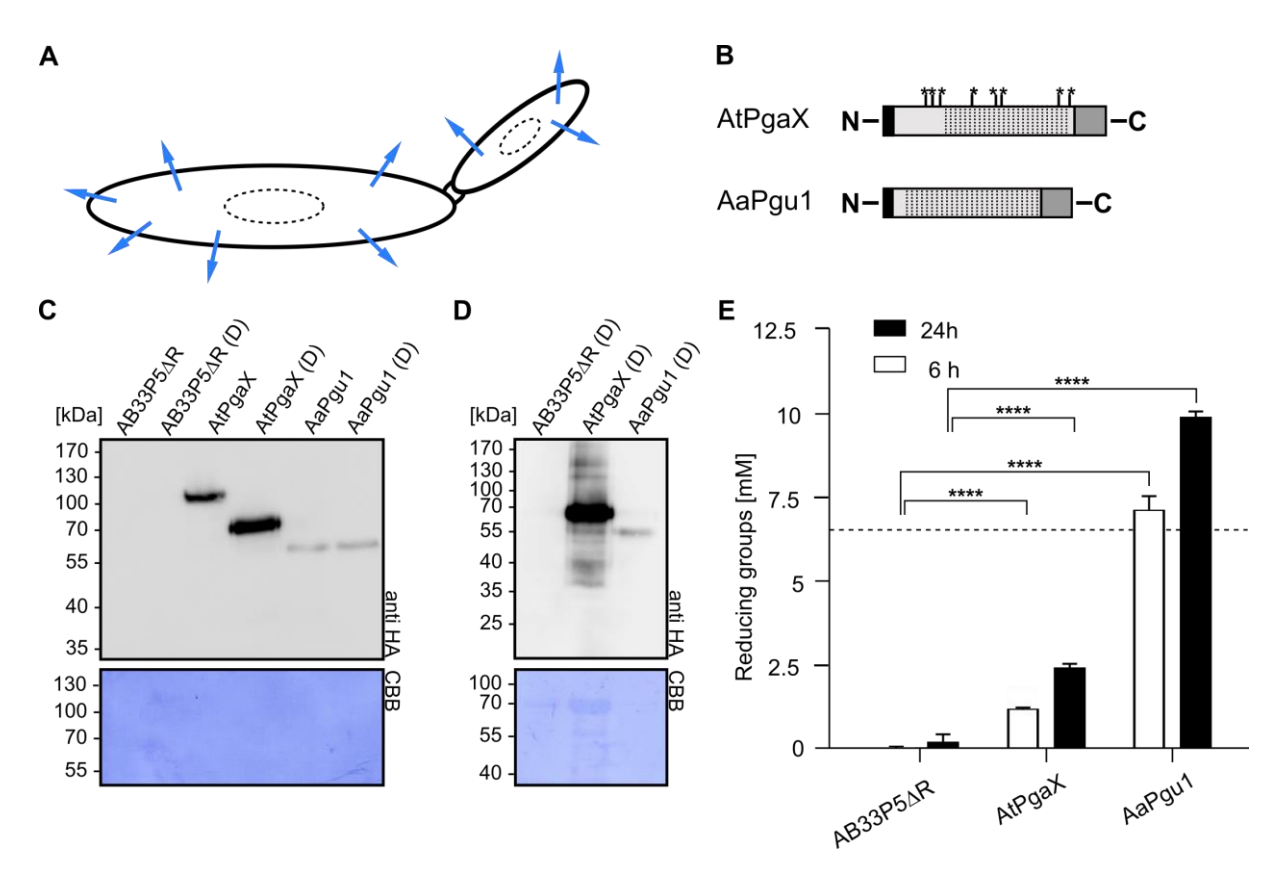


Figure 3-5: Complementation with fungal endo- and exo-polygalacturonases. A Heterologous enzymes are secreted by conventional secretion via the endomembrane system of yeast-like growing cells (scheme). **B** Representation of the two fungal proteins used for complementation. Predicted N-glycosylation sites of A. tubingensis PgaX (AtPgaX, 8 predicted sites) and A. aculeatus Pgu1 (AaPgu1, 0 predicted sites) are depicted by asterisks. Predicted N-terminal signal peptides are indicated in black. The C-terminal SHH-tag is shown in dark grey. The predicted functional glycoside hydrolase domain GH28 is indicated by dotted areas. C Expression of fungal polygalacturonases in AB33P5ΔR (progenitor strain). The Western blot analysis depicts cell extracts (10 µg), which were partially deglycosylated (D). Heterologous proteins were detected using antibodies directed against the HA-tag. CBB, Coomassie Brilliant Blue staining of the membrane. Expected sizes of tagged proteins: AtPgaX: 56.5 kDa; AaPgu1: 47.1 kDa. **D** Conventional secretion of fungal polygalacturonases in AB33P5∆R. The Western blot analysis depicts precipitated and deglycosylated culture supernatants (corresponding to 1 mL culture). Proteins were detected using antibodies directed against the HA-tag. E DNS assay to detect activity of heterologous enzymes from fungal sources on PolyGalA. In contrast to the progenitor strain AB33P5ΔR, both engineered strains were active on this polymer (release of reducing sugars). The amount of reducing groups liberated by the fungal endo-polygalacturonase AaPgu1 was higher compared to the intrinsic UmPgu1 (dashed line after 24 h). The graph represents the results of three biological replicates. Error bars depict standard deviation; ****: p value > 0.0001.

To evaluate the enzymatic power of heterologous fungal enzymes in comparison to intrinsic UmPgu1, a potent endo-polygalacturonase from *A. aculeatus* (AaPgu1, accession number

XM_020201835.1; GH28) was also tested [Abdulrachman, *et al.* 2017]. The corresponding strain was generated with a similar strategy yielding AB33P5ΔR/AaPgu1. Western blot analyses confirmed that the enzyme was produced and secreted. Consistent with the absence of *N*-glycosylation sites, it did not show a major size shift as observed for AtPgaX (Figure 3-4B-D). In DNS assays up to 10 mM reducing groups were released from PolyGalA (Figure 3-5E, 24 h incubation), confirming that the heterologous enzyme was secreted in an active state. Again, the morphology of the modified strains was not changed compared to the progenitor strain (Figure A8), indicating that the heterologous proteins do not cause any significant cellular burden or morphological aberrations.

In summary, these results suggest that the enzyme repertoire of *U. maydis* can be complemented by both bacterial and eukaryotic enzymes. Importantly, comparing the different heterologous enzymes, fungal polygalacturonases exported by conventional secretion turned out to release the highest amount of reducing sugars and are therefore likely to be the best candidates for use in PolyGalA degradation. More specifically, the strong performance of AaPgu1 suggests that it should be preferred to the intrinsic endo-polygalacturonase UmPgu1 that only released up to about 6.5 mM reducing groups (Figure 3-5E, dashed line). The AtPgaX producing strain could be exploited to supplement *U. maydis* cultures with the required exo-polygalacturonase activity.

Endo- and exo-polygalacturonases are supposed to act together on the degradation of PolyGalA to produce monomeric GalA for uptake and metabolization. Therefore, the next step towards complete PolyGalA metabolization was to combine these enzyme activities (Figure 3-6A). The generated culture supernatants of the strains AB33P5ΔR/AtPgaX and AB33P5ΔR/AaPgu1 secreting the potent fungal polygalacturonases were mixed exemplary to conduct an enzyme assay (Figure 3-6B, right bars). Since up to now all enzymes in this chapter were overexpressed in separate strains, the potential of co-fermentation of those strains was tested. This approach would allow for a flexible adaptation of strain mixtures to the respective substrate in future. For co-fermentation, the two strains were inoculated in a 1:1 ratio starting at a total optical density of 0.1. DNS assays using the culture supernatant of this co-fermentation (Figure 3-6B, left bars) revealed similar enzyme activity to the co-fermentation supernatants of axenic cultures. In both experiments, about 12 mM reducing sugars were released after 24 h (Figure 3-6B). This suggests that both enzymes work together, yielding additive amounts of reducing sugars

compared to the individual cultivations (Figure 3-5E). Thus, co-fermentations are a promising tool to analyze different combinations of hydrolytic enzymes.

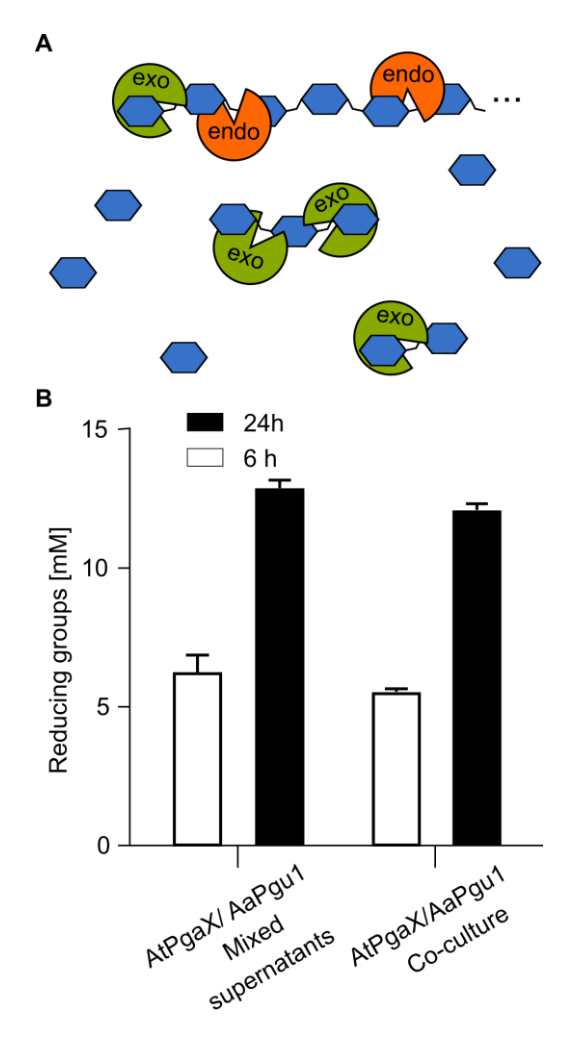


Figure 3-6: Co-fermentations of fungal endo- and exo-polygalacturonases. A Schematical representation of exo-polygalacturonases (green) and endo-polygalacturonases (orange) acting on (Poly)GalA. B Comparative DNS assays using mixed supernatants and co-cultures of strains secreting intrinsic fungal endo- and heterologous exo-polygalacturonase. Strains AB33P5 Δ R/AtPgaX and AB33P5 Δ R/AaPgu1 were used for the assay. The graph represents the results of three biological replicates. Error bars depict standard deviation. The measurements between co-fermentation and mixed supernatants showed no major differences.

3.7 Following the physiological parameters during growth on PolyGalA using RAMOS

The previously used enzyme assays clearly demonstrated that *U. maydis* could be complemented by heterologous pectinolytic enzymes. However, due to product inhibition effects and low resolution over time, these offline *in vitro* assays only allow limiting conclusions, compared to direct cultivations on PolyGalA [Kester, *et al.* 1996]. Hence,

application of the RAMOS device enabled a detailed insight into the physiology of the engineered strains. This method takes advantage of the fact that sugar consumption is stoichiometrically coupled to oxygen uptake [Antonov, et al. 2017, Antonov, et al. 2016]. In Chapter 2.5, the AtPgaX overexpressing strain was used in axenic culture to develop this technique for monitoring the behavior on PolyGalA.

The strain AB33P5ΔR/UmPgu1 overexpressing the intrinsic endo-polygalacturonase was grown on 20 g/L GalA or PolyGalA (Figure 3-7). To boost initial growth and enzyme production, all cultivations were supplemented with 4 g/L glucose as a first carbon source (Figure 3-7A). Both cultures first grew on the preferred substrate glucose, which led to a steep exponential increase of the OTR up to 11 mmol/L/h. After 7.5 h, glucose was depleted and the OTR dropped down to about 2.4 mmol/L/h. At this point, growth on the second carbon source, GalA (Figure 3-7A, blue curves) or PolyGalA (Figure 3-7A, black curve), respectively, was initiated. As described for the progenitor strain AB33P5ΔR (2.3) cells of AB33P5ΔR/UmPgu1 adapted for the growth on GalA during this phase of low metabolic activity, starting after about 10 h of cultivation time. The metabolic switch can easily be detected in the course of the RQ (Figure 3-7B): During consumption of glucose, RQ values of 1.1 are observed while during GalA consumption, the RQ increases to values of 1.4 (Figure 3-7B, blue curves). This is in line with previous RAMOS experiments and is attributed to the specific reduction levels of the substrates (Chapter 2.3). In comparison to consumption of glucose, the OTR increase during growth on GalA is less steep (Figure 3-7A, blue curves), suggesting that GalA is only slowly metabolized.

HPLC analysis confirmed that GalA was completely consumed at the end of the cultivation (data not shown). Sharp drops in the OTR and RQ indicate, that GalA was depleted after 40 h of cultivation time. As described previously, the OT during GalA metabolization can be used to estimate the residual GalA concentration (Figure 3-7C, green curves) (Chapter 2.4). This estimation yielded a GalA concentration of about 2 g/L after 40 h what deviates from the HPLC analysis. Differences in the pH value of the cultivation or the applied *U. maydis* strain could lead to a different elemental composition of the cells. The elemental composition is a key parameter for the correlation of overall consumed oxygen and consumed substrate. Therefore, the calculated residual (Poly)GalA concentration should be taken as estimation of the course of (Poly)GalA concentration but not to determine exact time points of (Poly)GalA depletion.

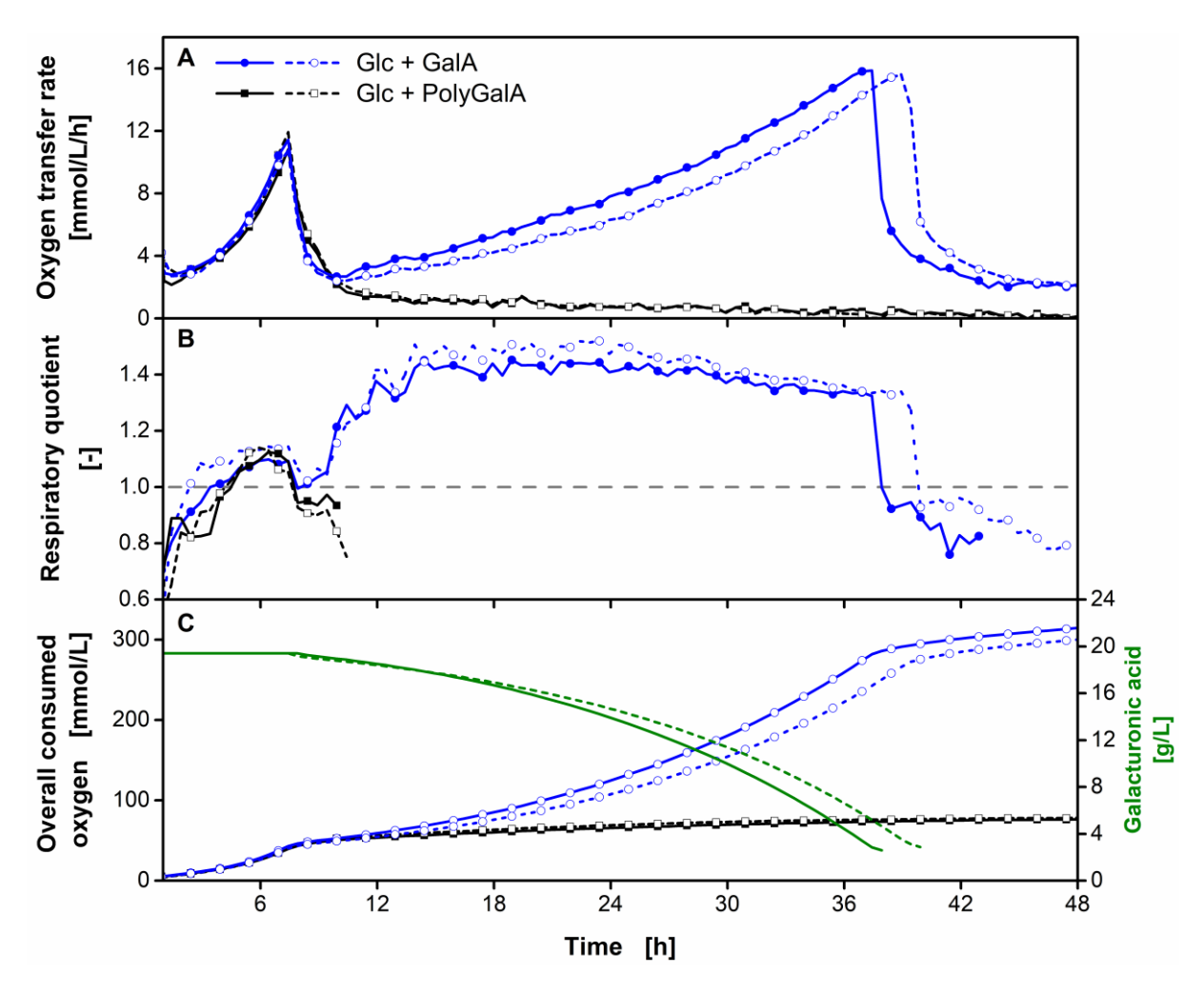


Figure 3-7: Cultivation of the UmPgu1 (endo-polygalacturonase) overexpression strain on GalA and PolyGalA. Strain AB33P5 Δ R/UmPgu1 was grown on a mixture of glucose (Glc, 4 g/L) and (Poly)GalA (20 g/L, purity 85%) as carbon sources. A Biological duplicates of OTR, represented each as line and dashed line. B Biological duplicates of RQ, represented each as line and dashed line. C, Biological duplicates of the overall consumed oxygen, represented each as line and dashed line. For the cultivation on GalA, the estimated residual GalA concentration (Chapter 2.4) is shown in green. For clarity reasons, only every third data point is shown and the RQ is only shown for OTR > 2 mmol/L/h. Culture conditions: modified Verduyn mineral medium, 0.2 M MOPS, initial pH 6.0, 250 mL flask, filling volume 20 mL, shaking frequency 300 rpm, shaking diameter 50 mm, initial OD₆₀₀ = 0.6, T = 30°C.

In contrast to the experiments on GalA, no metabolic activity could be detected for AB33P5 Δ R/UmPgu1 on PolyGalA (Figure 3-7A, black curves). This clearly indicates that the activity of only the endo-polygalacturonase enzyme is not sufficient to permit growth on the polymer. Endo-polygalacturonases typically release oligogalacturonates with a degree of polymerization of 2 to 4 which cannot transported across the cell membrane without further breakdown [Jayani, *et al.* 2005]. Hence, although the respective enzyme activity could be detected (Figure 3-3B), activation of only the intrinsic enzyme for PolyGalA degradation did

not improve growth on PolyGalA. This confirms that complementation with further heterologous enzymes, especially exo-polygalacturonases, is needed to generate monomeric GalA.

3.8 Characterizing co-fermentations using RAMOS

Figure 3-6B showed that the combination of endo- and exo-polygalacturonase activity could be beneficial for the PolyGalA degradation. Those supernatants were, however, generated using glucose as carbon source. The performance of co-fermentations on PolyGalA was evaluated using strain AB33P5ΔR/AtPgaX expressing the heterologous exo-polygalacturonase from A. tubingensis. RAMOS cultivations demonstrated the effects of adding strains producing intrinsic, fungal or bacterial endo-polygalacturonase (Figure 3-3B, Figure 3-4E and Figure 3-5E, respectively) as depicted in Figure 3-8. All cultivations were tested in biological duplicates. Figure A9 demonstrates their excellent reproducibility. Substrate conversion of AB33P5ΔR/AtPgaX in axenic culture was clearly limited (Figure 3-8A, blue). The residual PolyGalA calculated from the overall consumed oxygen during GalA consumption indicated a PolyGalA consumption of < 56%. The addition of the strain expressing intrinsic endopolygalacturonase UmPgu1 led to an increased overall substrate consumption of 85% (Figure 3-8C). The maximal OTR during GalA consumption, representing the overall enzymatic activity, was comparable to the axenic culture of the *U. maydis* strain AB33P5ΔR/AtPgaX but the PolyGalA consumption phase was elongated until 55 h of cultivation time. This indicates that the addition of endo-polygalacturonase activity led to an increased substrate accessibility for the exo-polygalacturonase enzyme. The co-fermentation with the strain expressing bacterial endo-polygalacturonase PcPeh1-Cts1 showed a slightly lower maximal OTR while the consumption phase was elongated also in comparison to the axenic culture. The overall substrate consumption of 81% was comparable to the co-fermentation with the strain expressing intrinsic endo-polygalacturonase UmPgu1. However, the PolyGalA consumption phase was elongated until 60 h of cultivation time. This long phase of low metabolic activity indicates a low enzymatic activity for PcPeh1-Cts1. These findings correlate well with the offline determined enzymatic activities for PcPeh1-Cts1 (Figure 3-4E) compared to the intrinsic UmPgu1 (Figure 3-3B).

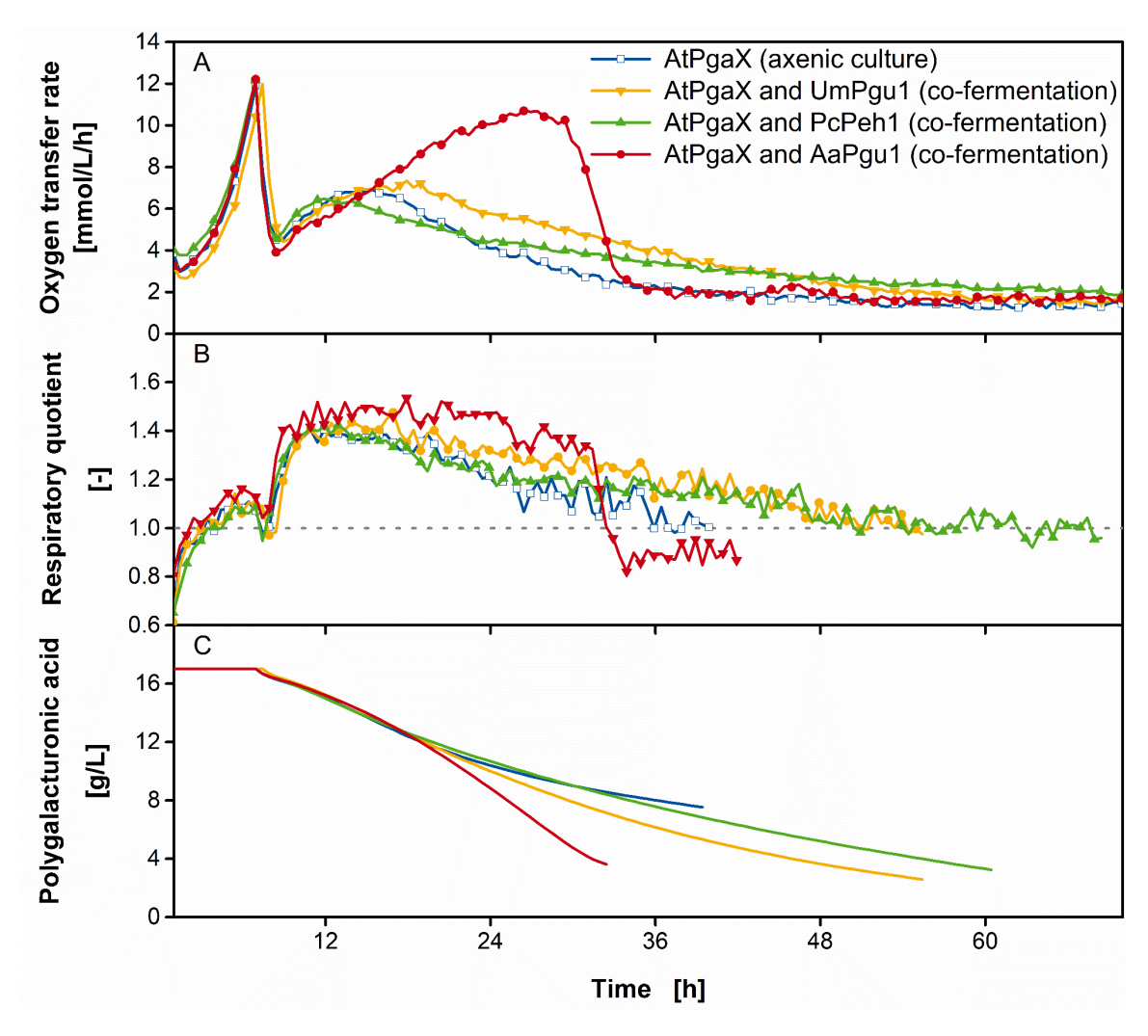


Figure 3-8: RAMOS cultivation of axenic cultures and co-fermentations on PolyGalA. The strains expressing AtPgaX (fungal exo-polygalacturonase), UmPgu1 (intrinsic endo-polygalacturonase), PcPeh1 (bacterial endo-polygalacturonase) and AaPgu1(fungal endo-polygalacturonase) were grown on a mixture of glucose (4 g/L) and PolyGalA (20 g/L, purity 85%) as carbon sources. **A** OTR. **B** RQ. **C** Residual substrate calculated from the overall consumed oxygen (Chapter 2.4). For clarity reasons, only every third data point is shown and the RQ is only shown for OTR > 2 mmol/L/h. All plots represent the mean of biological duplicates. Culture conditions: modified Verduyn mineral medium, 0.2 M MOPS, initial pH 6.0, 250 mL flask, filling volume 20 mL, shaking frequency 300 rpm, shaking diameter 50 mm, initial OD₆₀₀ = 0.6 (inoculation ratio 1:1 for co-fermentations), T = 30 °C.

Importantly, addition of the strain expressing fungal AaPgu1 did strongly increase the maximal OTR and led to the fastest consumption of PolyGalA. The overall consumed PolyGalA is with 79% comparable to the two other co-fermentations but this value was reached already after 32.5 h of cultivation time. The OTR profile mirrors precisely the growth on monomeric GalA (Figure 3-7A, red; note the different time scale on the x-axis). As already discussed for the growth on monomeric GalA, the estimated residual PolyGalA could differ for different *U. maydis* strains and cultivation conditions. Thus, in contrast to axenic cultures of

AB33P5ΔR/AtPgaX on PolyGalA, the substrate might have been consumed completely in all tested co-fermentations of the strain expressing fungal exo-polygalacturonase (AtPgaX) with strains expressing intrinsic (UmPgu1), bacterial (PcPeh1-Cts1) or fungal (AaPgu1) endo-polygalacturonase. Theses co-fermentations are a potent means to degrade the polymer PolyGalA. Among the tested variants of endo-polygalacturonase, the enzyme of fungal origin (AaPgu1) enabled the fastest metabolization of PolyGalA indicating clearly the highest enzyme activity in the culture broth. This correlates with the offline conducted enzyme assays (Figure 3-3B, Figure 3-4E and Figure 3-5E).

The influence of three enzymatic compositions was tested by varying the inoculation ratio of the most powerful strain combination. AB33P5ΔR/AtPgaX and AB33P5ΔR/AaPgu1, overexpressing fungal endo- and exo-polygalacturonase were co-fermented with a relative inoculation ratio of 5:1; 1:1 and 1:5 (Figure 3-9). A ratio of 1:1 and 1:5 (surplus of exopolygalacturonase, Figure 3-9B and C, respectively) resulted in efficient consumption of PolyGalA with complete PolyGalA hydrolysis. A 5:1 ratio (surplus of endo-polygalacturonase, Figure 3-9A) resulted in an elongated PolyGalA consumption phase. Maximal values were reached after 20.5 h of cultivation time. From that time point on, the OTR slowly decreased over a time span of 27 h indicating a limitation in monomeric GalA even in presence of PolyGalA. A basal OTR level of 2 mmol/L/h was reached after 47.5 h. Compared to this cultivation, an inoculation ratio of 1:1 (Figure 3-9B) and 1:5 (surplus of exo-polygalacturonase, Figure 3-9C) showed maximal OTRs after 28 h, respectively. In those co-fermentations, the OTR reached a basal level of 2 mmol/L/h after 36 h. The sharp drop in the OTR over a short time span (9.5 and 8 h for a ratio of 1:1 and 1:5 (surplus of exo-polygalacturonase), respectively) indicates that both, GalA and PolyGalA were depleted. At the end of the cultivation, similar OD₆₀₀ levels were reached for all co-fermentations. This indicates that the overall consumption of PolyGalA is similar with different inoculation ratios, but the time until all available PolyGalA is consumed, differs. Interestingly, offline determination of GalA in these co-fermentations revealed that in all cases, the monomer accumulated during growth on glucose (until 9 h of cultivation time), which can be attributed to the expression of hydrolytically active enzyme from the very beginning of the cultivation. Interestingly, during the first hours of growth on GalA, the hydrolysis product accumulated further for a ratio of 1:1

(Figure 3-9B, blue lines) and 1:5 (surplus of exo-polygalacturonase, Figure 3-9C, blue lines). This suggests that GalA uptake is a limiting step in the cultivation.

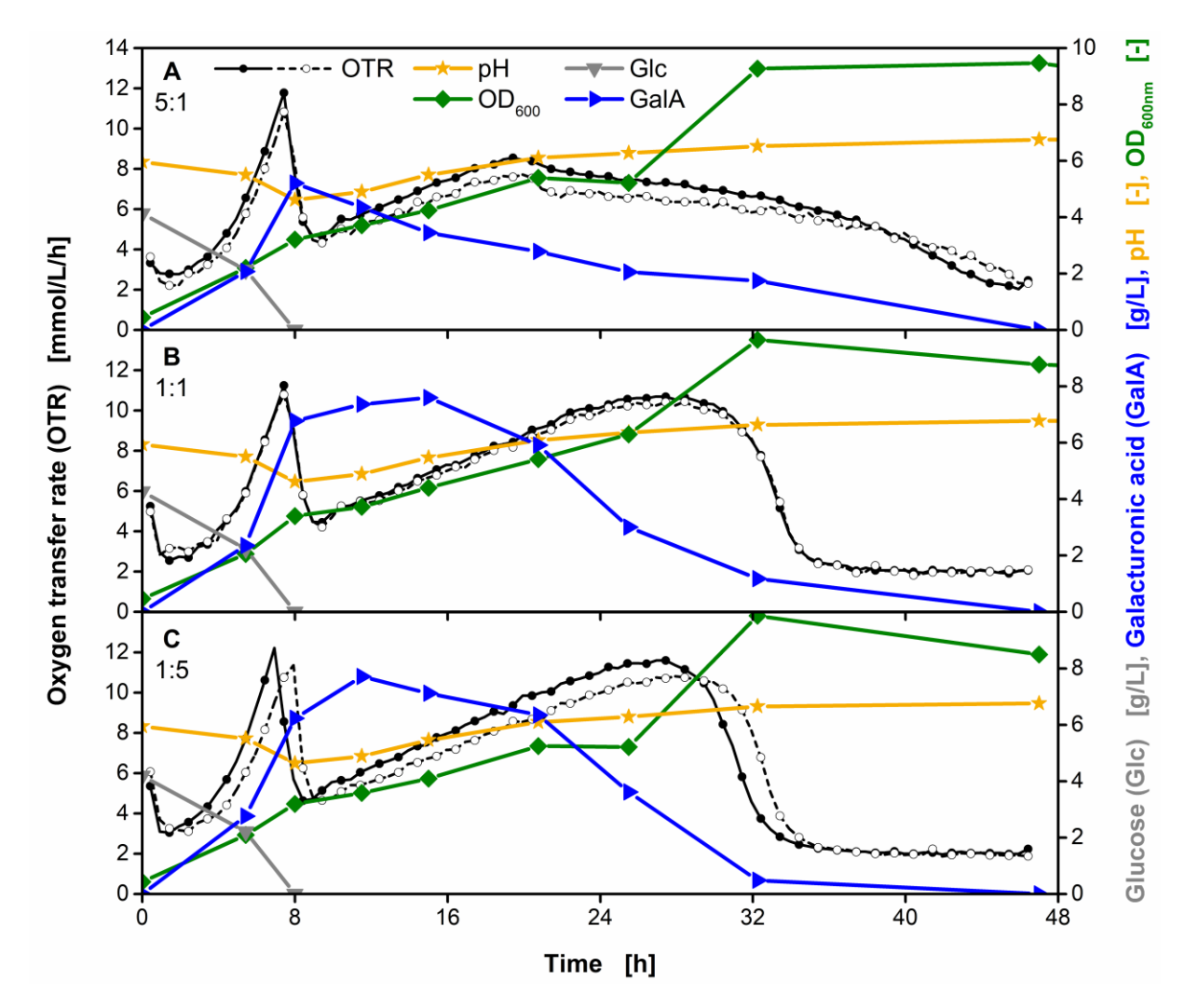


Figure 3-9: Co-fermentation of AtPgaX (fungal exo-polygalacturonase) and AaPgu1 (fungal endo-polygalacturonase) overexpression strains with different inoculation ratios on PolyGalA. The strain combination AB33P5 Δ R/AtPgaX and AB33P5 Δ R/AaPgu1 was grown in medium containing a mixture of glucose (4 g/L) and PolyGalA (20 g/L, purity 85%) as carbon sources. A Inoculation ratio 5:1 (OD₆₀₀ = 0.5 for AB33P5 Δ R/AaPgu1 and OD₆₀₀ = 0.1 for AB33P5 Δ R/AtPgaX). B Inoculation ratio 1:1 (OD₆₀₀ = 0.3 for both, AB33P5 Δ R/AtPgaX and AB33P5 Δ R/AaPgu1). C Inoculation ratio 1:5 (OD₆₀₀ = 0.1 for AB33P5 Δ R/AaPgu1 and OD₆₀₀ = 0.5 for AB33P5 Δ R/AtPgaX). Continuous and dashed black lines represent biological duplicates of RAMOS cultivations. For clarity reasons, only every third data point is shown. Culture conditions: modified Verduyn mineral medium, 0.2 M MOPS, initial pH 6.0, 250 mL flask, filling volume 20 mL, shaking frequency 300 rpm, shaking diameter 50 mm, T = 30°C.

Cultivation data of the most efficient co-fermentation with an inoculation ratio of 1:5 (initial $OD_{600} = 0.1$ for endo-polygalacturonase strain $AB33P5\Delta R/AaPgu1$ and $OD_{600} = 0.5$ for exo-

polygalacturonase strain AB33P5 Δ R/AtPgaX) was analyzed in more detail with respect to the GalA liberation rate (Figure 3-10).

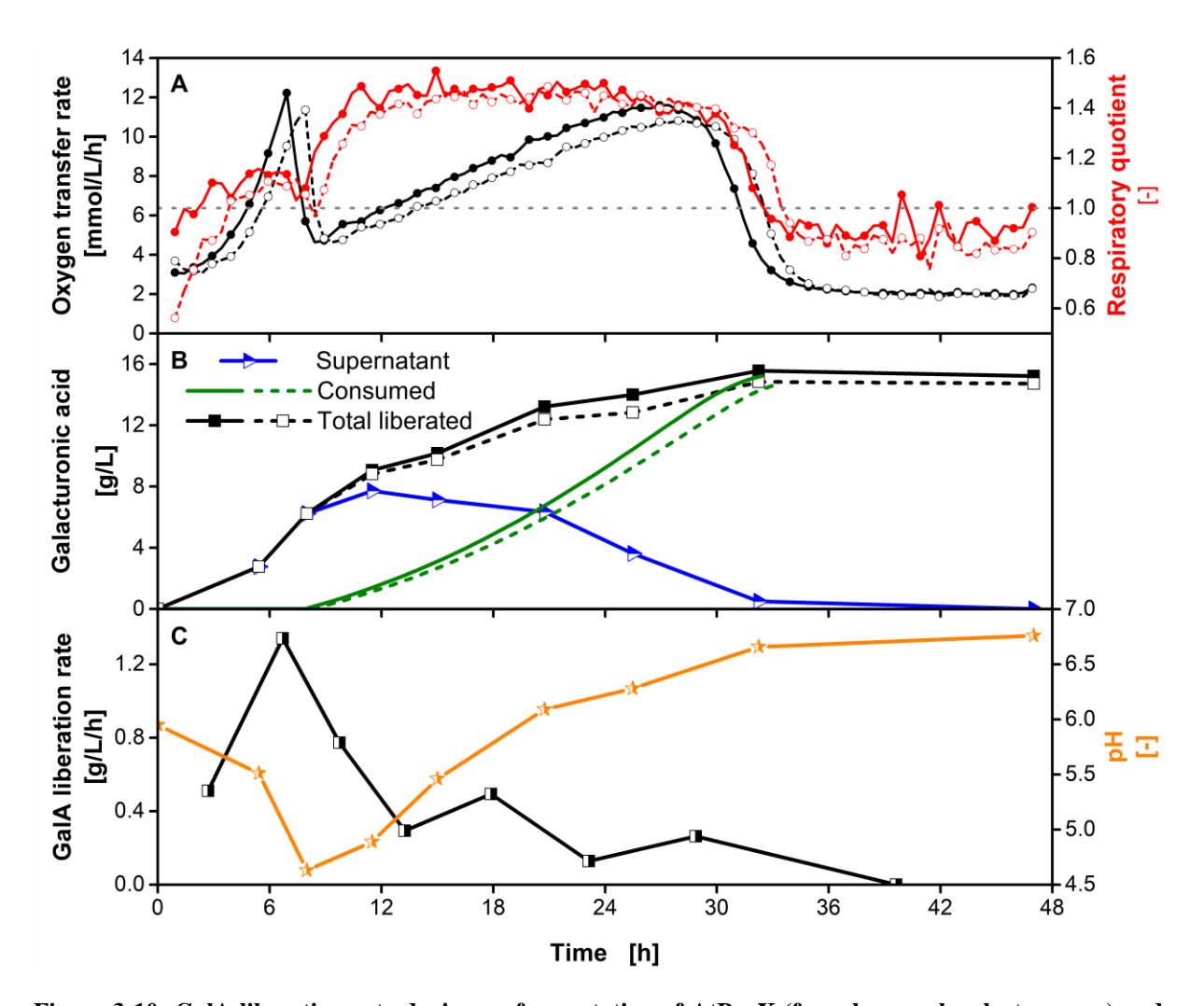


Figure 3-10: GalA liberation rate during co-fermentation of AtPgaX (fungal exo-polygalacturonase) and AaPguI (fungal endo-polygalacturonase) overexpression strains (inoculation ratio 5:1) on PolyGalA. The strains were grown on a mixture of glucose (4 g/L) and PolyGalA (20 g/L) as carbon sources. A OTR and RQ of biological duplicates (continuous and dashed lines, identical data set to Figure 3-9C) **B** Measured GalA concentration in the supernatant (GalA_{sup}) and consumed GalA (GalA_{con}), calculated from the OT as described in Chapter 2.4. Total liberated GalA (GalA_{lib}) equals the sum of both quantities (Chapter 3.2.11). **C** Calculated GalA liberation rate (mean of biological duplicates) in comparison to the offline determined pH. Culture conditions: modified Verduyn mineral medium, 0.2 M MOPS, initial pH 6.0, 250 mL flask, filling volume 20 mL, shaking frequency 300 rpm, shaking diameter 50 mm, initial OD₆₀₀ = 0.5 (AB33P5ΔR/AtPgaX) or 0.1 (AB33P5ΔR/AaPgu1), T = 30 °C.

Online measurement of the RQ (Figure 3-10A, red lines) clearly separates the glucose and GalA consumption phases. The correlation between oxygen and GalA consumption, described in Chapters 2.4, was applied to calculate the overall consumed amount of GalA over time

(GalA_{con}, Figure 3-10B, green lines). The consumption rate of total PolyGalA reached a value of 90%. Both fractions of GalA, offline measured concentration and calculated concentration of consumed GalA, were used to determine the total liberated amount of GalA during the cultivation (GalA_{lib}, Figure 3-10B, black lines, see also Chapter 3.2.11). The temporal derivative of this total liberated GalA represents the GalA liberation rate (Figure 3-10C, black line). During growth on glucose, enzymes are obviously produced efficiently, leading to an increase of the GalA liberation rate to 1.3 g/L/h. During the GalA consumption phase, the GalA liberation rate decreases to < 0.4 g/L/h. This behavior can be explained by the development of the pH value (Figure 3-10C, orange line). During growth on glucose, the pH decreases to 4.6. The expressed exo-polygalacturonase AtPgaX has a pH optimum at 4.5 [Kester, *et al.* 1996]. This value fits very well to the cultivation pH at this time point of the cultivation. As the pH increases to values up to 6.7 during consumption of GalA, the enzyme activity is likely to decrease substantially, leading to a significantly decreased liberation rate. Therefore, the course of the pH mirrors very well the course of the liberation rate.

3.9 Conclusion

In this Chapter, bioinformatics, sophisticated strain generation and online monitoring techniques were combined to establish and follow PolyGalA degradation and subsequent metabolization of its monomer GalA by *U. maydis*. This is a first and essential step towards pectin valorization. Intriguingly, it was shown that bacterial enzymes can be exported in an active state by unconventional secretion. However, yields are yet limiting.

This Chapter has also demonstrated that co-fermentations are a promising means to combine enzyme activities without tedious generation of strains carrying multiple enzymes. Inhibition by products of the enzymatic hydrolysis of biomass does not play a role in efficient one-pot consolidated bioprocesses, because the released sugars are directly fermented [Brunecky, *et al.* 2018, Carere, *et al.* 2008]. However, hydrolysis products interfere with offline DNS assays. Therefore, the online read-out of the RAMOS technique has proven to be a reliable and practical alternative to offline sampling for the characterization of cultures growing on PolyGalA. The microbial system still needs to be streamlined towards the more complex substrate pectin as well as towards higher efficiency. Next, the substrate spectrum needs to be further extended by

insertion of additional enzymes. Chapter 4 will demonstrate the potential of an extended number of pectinases in the culture broth by utilization of external enzyme cocktails during growth of the established *U. maydis* co-fermentation on pectin and sugar beet pulp.

Chapter 4

Application of online measurement tools for the investigation of microbial and enzymatic pectin degradation

4.1 Introduction

The valorization of pectin rich agricultural side streams like apple pomace or sugar beet pulp requires microorganisms that can hydrolyze the complex pectin structure consisting of numerous different sugars and types of bonds [Glass, *et al.* 2013]. In Chapter 2, the growth of *Ustilago maydis* on the main pectin monomer, galacturonic acid (GalA), was investigated in detail and a methodology was developed to estimate the residual GalA concentration in the culture broth based on the measurement of the overall consumed oxygen. Chapter 3 extended these results towards polygalacturonic acid (PolyGalA), a linear polymer representing the backbone of pectin. A co-fermentation strategy was characterized that could efficiently break down this substrate, reaching an overall substrate consumption of 90%.

Within this chapter, the growth preferences of *U. maydis* on several other pectic sugars will be evaluated. The potent co-fermentation strategy, characterized in Chapter 3, is tested on purified pectin. Since pectins differ by their origin and their degree of esterification, three different pectins were investigated: A high esterified sugar beet pectin (SP-he), a high esterified apple pectin (AP-he) and a low esterified apple pectin (AP-le). As the established co-fermentation

only yields endo- and exo-polygalacturonases, the influence of additional external enzyme cocktails (pectinase and / or cellulase) on the growth on pectin will be investigated. The method for the estimation of residual (Poly)GalA, developed in Chapter 2.4, will be applied to the cultivations on pectin to estimate the percentage of consumed pectin. As a next step, external enzymes will be supplemented during co-fermentation using sugar beet pulp as a potential industrial waste stream. Figure 4-1 gives an overview of the process parameters that are going to be investigated within this Chapter.

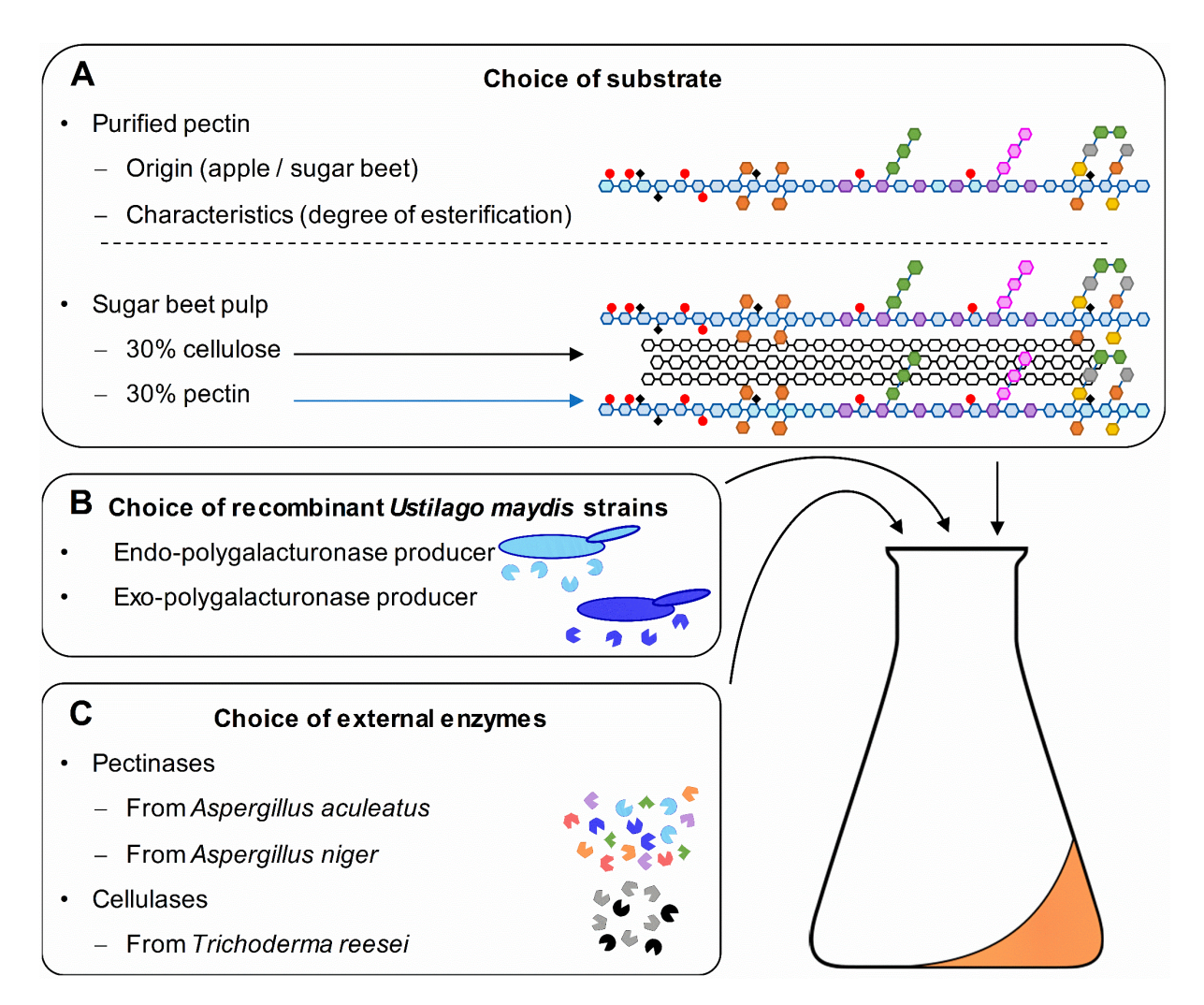


Figure 4-1: Overview of evaluated process parameters. A As substrates, purified pectin or sugar beet pulp were used. Three different kinds of pectin were tested, varying in their origin and degree of esterification. The hemicellulose content of 20-30% in sugar beet pulp is not visualized. **B** Two different recombinant *U. maydis* strains were used in axenic or co-fermentation, producing a fungal endo- or exo-polygalacturonase. **C** Depending on the substrate, two different kinds of pectinase cocktails (varying in their expression host) or cellulases were used.

4.2 Material and methods

4.2.1 Microorganisms

Within this chapter, the strains AB33P5 Δ R (no polygalacturonase expression), AB33P5 Δ R/AtPgaX (expressing an exo-polygalacturonase of fungal origin) and AB33P5 Δ R/AaPgu1 (expressing an endo-polygalacturonase of fungal origin) were cultivated. An extensive description of those strains is given in Chapter 3.2.1.

4.2.2 Pectin and sugar beet pulp composition

The pectins AU202 (high esterified apple pectin, AP-he), RU301 (high esterified sugar beet pectin, SP-he) and AU910 (low esterified apple pectin, AP-le) were kindly provided by Herbstreith & Fox (Neuenbürg, Germany). Sugar beet pulp, ground to a particle size of < 100 µm was kindly provided by Pfeifer & Langen (Cologne, Germany). Table 4-1 gives an overview on the composition and characteristics (degree of esterification, percentage of non-esterified GalA in the total substrate), based on information provided by the manufacturer and obtained from literature.

Table 4-1: Composition and characteristics of pectin and sugar beet pulp.

	SP-he	AP-he	AP-le	Sugar beet pulp
Arabinose	10.0% ¹	1.0%²	1.0%²	20.9%³
Galactose	5.9% ¹	2.6%2	2.6%2	5.1% ³
Glucose	0.4%1	$3.6\%^2$ $3.6\%^2$		21.1% ³
Mannose	0.1% ¹	0.0%2	0.0%2	1.1% ³
Rhamnose	2.3%1	2.2%2	2.2%2	2.4% ³
Xylose	0.2%1	1.4%²	1.4%²	1.7%³
Galacturonic acid	67% ⁴	78% ⁴	72% ⁴	21.1% ³
Other components	14.1%	11.2%	17.2%	26.6%
Degree of esterification	54% ⁴	68% ⁴	4.8% ⁴	64% ⁴

	SP-he	AP-he	AP-le	Sugar beet pulp
Degree of non-esterified	30.1%	25.0%	68.5%	7.6%
GalA in total substrate ⁵				

¹ [Rombouts and Thibault 1986]

4.2.3 Cultivation media, external enzymes and cultivation conditions

All cultivations were performed in minimal Verduyn medium at the same conditions as described in Chapter 2.2.2 but with an initial pH of 6.0. Pectins (SP-he, AP-he, AP-le) were dissolved in hot water at a concentration of 40 g/L and the pH was adjusted to 6.0 with 10 M NaOH before autoclaving. 400 mg sugar beet pulp were suspended directly in each individual RAMOS flask in 10 mL of water before autoclaving (final filling volume: $V_L = 20$ mL)

For cultivations with external enzymes, pectinase from *A. aculeatus* (p-Aa, product number P26111, Sigma-Aldrich, now Merck, Darmstadt, Germany), pectinase from *A. niger* (p-An, product number 17389, Sigma-Aldrich) or cellulase from *T. reesei* (c-Tr, product number C2730, Sigma-Aldrich) were used. All cocktails were used at the concentration recommended by the manufacturer. The inoculated cultivation medium was supplemented with the stated amount of enzyme cocktails at the beginning of cultivation.

4.2.4 Cultivation with online monitoring in the RAMOS or µRAMOS device

Cultivations in 250 mL shake flasks in the RAMOS device were performed as described in Chapter 2.2.3.

Measurement of the OTR in each individual well of a 48-well round well plate (MTP-R48-B, m2p labs GmbH, Baesweiler, Germany) covered with a sterile barrier (900371-T, HJ-Bioanalytik GmbH, Erkelenz, Germany) was conducted in an in-house built µRAMOS device

² [Zaleska, et al. 2000]

³ [Micard, et al. 1996]

⁴ Manufacturers information

⁵ Calculated from GalA content and degree of esterification

[Flitsch, et al. 2016]. The culture was grown in minimal Verduyn media as described in chapter 2.2.2 and inoculated to an OD_{600} of 0.1 from a preculture grown overnight. The cultivation was performed with a filling volume of 0.8 mL per well, a shaking diameter of 3 mm and a shaking frequency of 1000 rpm. The cultivation was conducted at 30°C.

4.3 Simultaneous cultivation on multiple different pectic sugars

A high overall metabolization rate for co-fermentations on PolyGalA was described in Chapter 3 with a consumption of total substrate of up to 90%. Figure 4-2 demonstrates that both strains of the envisaged co-culture show an identical OTR profile, when growing axenic on GalA. Thus, it can be assumed that one strain does not overgrow the other one and both strains are still present and able to produce active endo- and exo-polygalacturonase until the end of the fermentation. This intrinsic ability of *U. maydis* to consume GalA is advantageous when compared to other model organisms like *S. cerevisiae*. The latter lacks metabolic pathway for GalA metabolization. First attempts were made to implement a bacterial pathway from *Lactococcus lactis* in *S. cerevisiae*, but the set of required enzymes is incomplete until yet [Huisjes, *et al.* 2012].

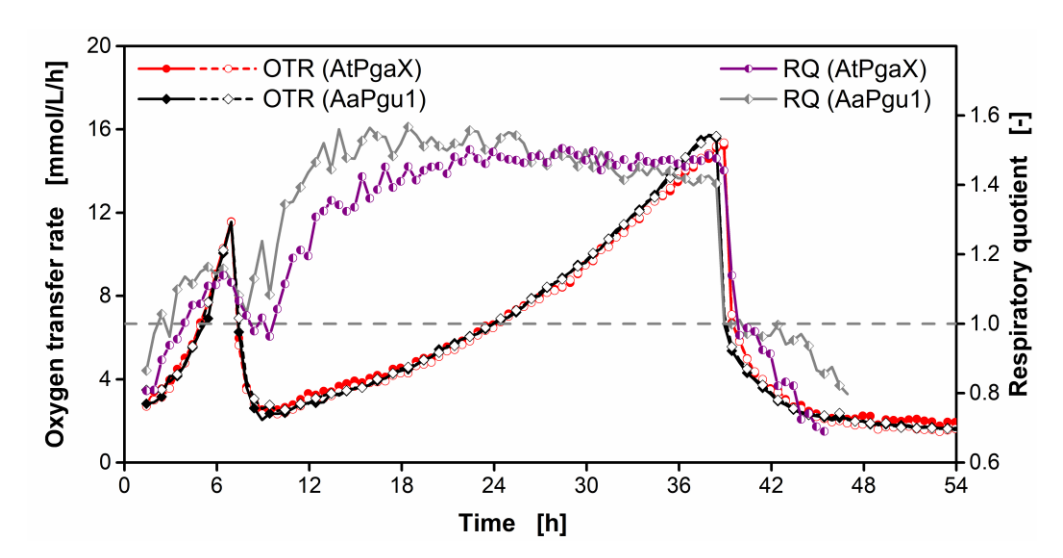


Figure 4-2: Axenic cultivation of *U. maydis* AB33P5 \triangle /AtPgaX and AB33P5 \triangle /AaPgu1 on GalA. The strains were grown on a mixture of glucose (4 g/L) and GalA (20 g/L) as carbon sources. OTR of biological duplicates (red and black curves) and mean of biological duplicates of RQ (purple and grey curve). For clarity reasons, the RQ is only shown for OTR > 2 mmol/L/h. Culture conditions: modified Verduyn medium, 0.2 M MOPS, pH 6.0, 250 mL flask, filling volume 20 mL, shaking frequency 300 rpm, shaking diameter 50 mm, initial OD₆₀₀ = 0.6, temperature 30 °CThe high metabolization rate of PolyGalA by the co-fermentation strategy

(Chapter 3.8) shifts the focus of interest towards more complex substrates such as pectin or sugar beet pulp. The pectic substrates investigated so far (GalA or PolyGalA) contained only non-esterified GalA as sugar unit. The first generation of feedstocks for industrial biotechnology focused on fermentations with a single carbon source like glucose. With the utilization of complex waste streams to reduce substrate cost and to increase sustainability of the process, the sequential or parallel consumption of various different carbon sources by a single organism became more and more important [van Maris, et al. 2006]. The complete utilization of biomass-derived pectin as carbon source requires a high number of different metabolic pathways. As listed in Table 4-1, pectin contains, besides GalA, other sugars including galactose, xylose, rhamnose, arabinose and mannose. Additionally, when investigating the growth on sugar beet pulp, cellulose may be hydrolysed, releasing glucose. A cultivation in the μRAMOS device verified that the *U. maydis* strain AB33P5Δ, precursor of the applied co-fermentation strains, was able to grow on xylose, GalA, rhamnose and arabinose (Figure A 10A). Galactose as major component of pectin is known to show toxic effects on U. maydis wildtype strains [Schuler, et al. 2018]. Indeed, a cultivation with 20 g/L glucose and 20 g/L galactose showed a sharp drop to 0 mmol/L/h after depletion of glucose and lower concentrations of galactose did not result in its metabolization (Figure A 10B, red curves). Due to the potential toxic effect of galactose, it was not investigated further as carbon source for U. maydis cultivations.

The potential of the co-fermentation developed in Chapter 3 (*U. maydis* AB33P5ΔR/AtPgaX and AB33P5ΔR/AaPgu1 with an inoculation ratio of 5:1) to metabolize the main pectic sugars was investigated by online monitoring of cultures supplemented with different fractions of six different carbon sources. The reference medium contained 5 g/L of glucose, mannose, xylose, GalA, rhamnose and arabinose each. For different cultivations, the concentration of one of the included sugars was increased to 10 g/L, while the other sugars remained at a concentration of 5 g/L. The profiles of the OTR over time are shown in Figure 4-3.

Glucose is consumed first as it is the most favourable carbon source (Figure 4-3A). The shoulder at 10 h of cultivation time and 15 mmol/L/h is increased to 27 mmol/L/h (blue arrow) compared to the reference cultivation. Figure 4-3B and C demonstrate that xylose and mannose are consumed after glucose, indicated by an increase in the respective peaks. The OTR peak after 14 h is increased in both cases compared to the reference cultivation. However, between

xylose and mannose, no clear substrate preference can be detected. Next, GalA is consumed (Figure 4-3D), as the consumption phase between 16 and 22 h is elongated until 26 h of cultivation time and the maximum OTR at the end of this consumption phase is increased from 21 to 23 mmol/L/h compared to the reference cultivation.

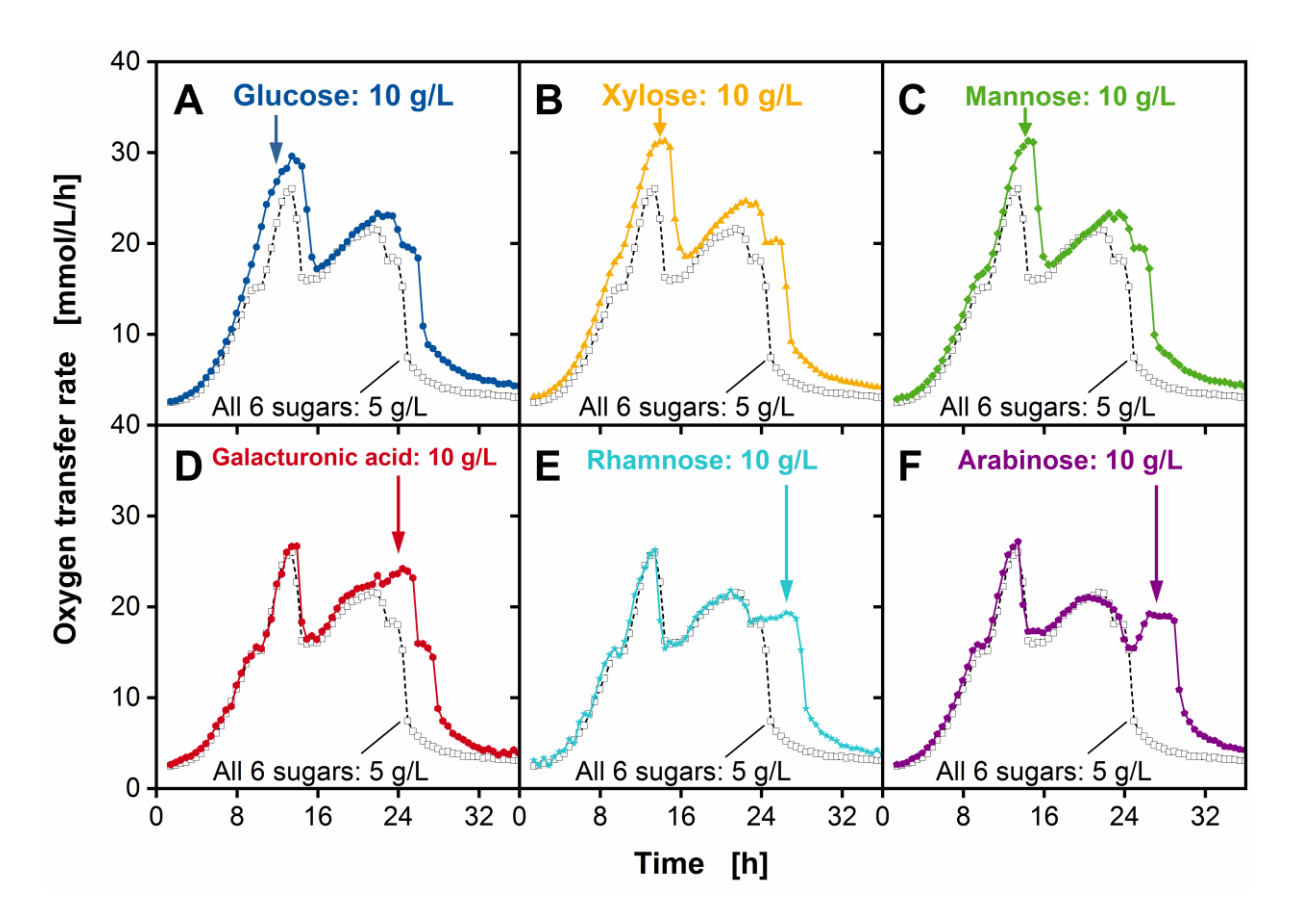


Figure 4-3: Substrate preference of an *U. maydis* co-fermentation for different pectic sugars. The strain combination AB33P5 Δ R/AtPgaX (overexpressing a fungal exo-polygalacturonase) and AB33P5 Δ R/AaPgu1 (overexpressing a fungal endo-polygalacturonase) was grown in medium containing 5 g/L of each, glucose, xylose, mannose, GalA, rhamnose and arabinose (black, dashed line in A-F). In parallel, the concentration of single sugars was increased to 10 g/L, while the others remained at 5 g/L. Corresponding growth profiles are shown for **A** 10 g/L glucose (blue line), **B** 10 g/L xylose (yellow line), **C** 10 g/L mannose (green line), **D** 10 g/L GalA (red line), **E** 10 g/L rhamnose (turquoise line) and **F** 10 g/L arabinose (purple line), respectively. Arrows indicate differences between the respective cultivation and the reference. Culture conditions: modified Verduyn medium, 0.1 M MOPS, 0.1 M MES, pH 6.0, 250 mL flask, filling volume 20 mL, shaking frequency 300 rpm, shaking diameter 50 mm, initial OD₆₀₀(AB33P5 Δ R/AtPgaX) = 0.5, initial OD₆₀₀(AB33P5 Δ R/AaPgu1) = 0.1, temperature 30 °C

After GalA, rhamnose is consumed (Figure 4-3E). Here, no significant increase in the OTR can be detected, but the consumption phase between 23 and 24 h of cultivation time is elongated until 27 h compared to the reference cultivation. The constant OTR level during rhamnose consumption indicates a low biomass formation. As last of the tested substrates, arabinose is

consumed (Figure 4-3F). Here, a novel peak appears after 26 h that was not visible in the reference cultivation. Thus, arabinose is the least preferred substrate. It can be concluded that all sugars potentially present in sugar beet pulp can be consumed by the described co-culture of *U. maydis*.

Other microorganisms were also evaluated for their potential to grow on pectic sugars. Two genetically modified strains of the genus *Erwinia* were able to grow and form products on GalA, PolyGalA and citrus pectin but at a significantly lower growth rate compared to growth on glucose [Grohmann, *et al.* 1998]. Moreover, the product spectrum changed with the carbon source. During growth on glucose, mostly ethanol was formed while during growth on GalA, the main product switched to acetate. These observations demonstrate that a change of the carbon source could influence the entire metabolic network in the cell [Grohmann, *et al.* 1998]. Cultivating *U. maydis* on GalA, PolyGalA or pectin could thus lead to a different product spectrum compared to the cultivation on glucose. In future, novel screenings should be performed to identify versatile products when cultivating *U. maydis* on GalA, PolyGalA or pectin.

When multiple different sugars are present simultaneously, carbon catabolite repression plays a major role in their sequential consumption. This phenomenon has already been studied in Escherichia coli, yeasts and filamentous fungi [Moses and Prevost 1966, Ronne 1995]. In most cases, the presence of glucose as preferred substrate represses the expression of enzymes involved in the metabolization of different carbon sources. This way, no energy is lost for the maintenance of less efficient metabolic pathways. Figure 4-3 demonstrated the ability of U. maydis to consume six different sugars that are present in plant-derived biomass. A. niger was tested for the ability to metabolize the same set of sugars during batch fermentations on each of the sugars separately but also in mixtures [Lameiras, et al. 2018]. In that study, the kinetics of substrate uptake and consumption were investigated in detail. Similar to the observation in Figure 4-3B and C (xylose and mannose), no clear preference could be defined for A. niger between glucose, xylose and mannose. This was explained by their competition in substrate uptake. As the transmembrane transport system was limiting for these sugars, no preference for intracellular metabolization was measured [Lameiras, et al. 2018]. Glucose, xylose and mannose were not affected by carbon catabolite repression. Contrary, GalA, rhamnose and arabinose consumption was repressed by the presence of the other sugars

[Lameiras, et al. 2018]. The observed sequence of consumption by *U. maydis* (Figure 4-3) reflect similar kinetics to *A. niger*. Thus, the underlying mechanisms of transport limitation during consumption of glucose, xylose and mannose on one hand and carbon catabolite repression for GalA, rhamnose and arabinose seem to be the same for *U. maydis*.

4.4 Estimation of correlation factors for oxygen consumption and consumption of complex pectic substrates

U. maydis can metabolize all six sugars that were tested within Chapter 4.3. This makes *U. maydis* a favorable organism for the microbial degradation of complex substrates such as pectin or sugar beet pulp. In Chapter 2, a method for the online determination of residual PolyGalA based on the overall consumed oxygen was introduced. This methodology has to be extended to be applicable for the determination of consumed substrate for cultivation on pectin or sugar beet pulp.

The key calibration factor $\frac{v_0}{v_s}$ describes the molar linkeage of oxygen consumption to substrate consumption, as stated in Chapter 2.4. This factor for PolyGalA as substrate can be applied for the estimation of the residual substrate concentration during co-fermentation of AB33P5 Δ R/AtPgaX and AB33P5 Δ R/AaPgu1 on pectin (Figure 4-3). The strains produce exoand endo-polygalacturonases that release GalA as only hydrolysis product. Both enzymes can act only on non-esterified GalA residues. Therefore, the consumed substrate, even when total pectin is used as carbon source, can only be the fraction of non-esterified (Poly)GalA residues. Table 4-1 shows the fraction of non-esterified GalA residues in the tested pectins. To have a distinct definition of the PolyGalA consumption phase, the start of PolyGalA consumption was defined by the RQ drop after glucose depletion. The end of PolyGalA consumption was defined by a second drop in the RQ below 1, following the RQ plateau at 1.2 to 1.4 during (Poly)GalA consumption. This way, the PolyGalA consumption phase can be defined, even if the course of the OTR is not explicit.

When external enzymes were added to the cultivation, it was estimated that all pectin components are released as fermentable sugars. A mixed correlation factor (mCF) was

calculated for pectin, based on the methodology described in Chapter 4.3. For each cultivation shown in Figure 4-3, the consumption phase of the sugar applied at 10 g/L was defined based on the OTR for the main and the reference cultivation, respectively. The integral of the OTR during the consumption phase of a specific sugar describes the respective overall consumed oxygen (OT_S). Based on the OT_S of the main (OT_S^2) and the reference cultivation (OT_S^1) and the applied concentrations of $\beta_S^2 = 10 \ g/L$ for the main and $\beta_S^1 = 5 \ g/L$ for the reference cultivation, CF was calculated, according to Equation (10).

$$CF = \frac{OT_S^2 - OT_S^1}{\beta_S^2 - \beta_S^1}$$
 (10)

CF: correlation factor $\left[^{mmol_{O_2}}\!/_{g_S}\right]$

 OT_S : overall consumed oxygen during consumption of substrate S [mmol/L]

 β_s : mass concentration of substrate S [g/L]

Thus, the CF describes the amount of oxygen required for consumption of 1 g of the respective substrate. CF values calculated for all six tested sugars are listed in Table 4-2.

Table 4-2: Experimentally determined correlation factors (CFs) for oxygen and sugar consumption.

Sugar	Sum formula	$CF\left[^{mmol_{O_2}}/g_{S} ight]$	
Glucose	C ₆ H ₁₂ O ₆	15.6	
Xylose	$C_5H_{10}O_5$	13.2	
Mannose	$C_6H_{12}O_6$	14.7	
Galacturonic acid	C ₆ H ₁₀ O ₇	15.8	
Rhamnose	$C_6H_{12}O_5$	14.2	
Arabinose	$C_5H_{10}O_5$	10.8	
Polygalacturonic acid*	[C ₆ H ₈ O ₆] _n	15.2	

^{*} CF for PolyGalA was obtained more precisely in Chapter 2.4. The value is given here as comparison.

The relative composition of the six tested sugars in pectins and sugar beet pulp (Table 4-1) was used to calculate their respective normalized mass fraction w* and the mCF as described by

Equation (11). This mCF enabled the rough estimation of consumed pectin or sugar beet pulp, based on the OT during its consumption phase. The resulted mCFs are listed in Table 4-3.

$$mCF = \sum_{i=0}^{n} CF_i \cdot w_i^* \tag{11}$$

mCF: mixed correlation factor $\left[{^{mmol}_{O_2}}/{g_S}\right]$

 CF_i : correlation factor of component i ${mmol_{O_2}/g_S}$

 w_i^* : normalized mass fraction of component i [%(w/w)]

Table 4-3: Experimentally determined mCFs for oxygen and pectin / sugar beet pulp consumption.

Substrate	Normalized mass fractions for tested sugars w [*] [%(w/w)]					mCF $\left[rac{mmol_{O_2}}{g_{S}} ight]$	
	Glu-	Xy-	Man-	Galacturonic	Rham-	Arabi-	
	cose	lose	nose	acid	nose	nose	
Pectin SP-he	0.6	0.2	0.2	83.8	2.8	12.5	15.1
Pectin AP-he	4.2	1.6	0.0	90.5	2.6	1.2	15.7
Pectin AP-le	4.5	1.7	0.0	89.8	2.7	1.2	15.6
Sugar beet pulp	30.9	2.5	1.6	30.9	3.5	30.6	14.2

4.5 Growth on pectin

4.5.1 Influence of pectin characteristics

Within this chapter, three different pectins were evaluated: SP-he, AP-he and AP-le. Figure 4-4 shows a cultivation of the co-culture established in Chapter 3 on a mixture of glucose (4 g/L) and each of the three pectins (20 g/L). SP-he and AP-he show an identical glucose peak after 8 h of cultivation time (Figure 4-4A, green and yellow curves), followed by a (Poly)GalA

consumption phase of different length. GalA consumption is proven by the increase in the RQ between 10 and 14 h for SP-he and between 10 and 19 h for AP-he (Figure 4-4B, green and yellow curves). AP-le shows an elongated lag-phase and a lower OTR maximum after 10 h of cultivation (Figure 4-4A, blue curves). Between 10 and 15 h, the OTR stays constant at a plateau of 5 mmol/L/h. Compared to the other cultivations, this phase can be attributed to GalA consumption. However, the RQ does not increase during this phase (Figure 4-4B, blue curve). After longer cultivation times of 20 h, the OTR of AP-le starts to increase again, showing a low metabolic activity until 40 h. As the RQ increases already after 15 h to values of 1.2 to 1.4, this phase can be attributed to GalA consumption. During preparation of the culture medium for the AP-le cultivation, the pectin solution was gelling much stronger than the other two pectins. This might have had an influence on the growth behavior of *U. maydis*. Glucose and other medium components might have diffused into or out of the cross-linked area of AP-le pectin. If those nutrients are not constantly available, slow releasing of medium components from the crosslinked pectin could explain both, the elongated lag-phase and the constant OTR between 10 and 15 h. Similar OTR profiles were generated by slow-releasing polymer matrices embedding glucose crystals in a small-scale fed-batch system [Keil, et al. 2019].

Figure 4-4C shows the course of the estimated residual pectic substrate, calculated from the OT applying the CF for PolyGalA that was determined in Chapter 2.4 (Table 4-2). The choice of the right CF is essential for the correct estimation of residual substrate. In this case, the applied *U. maydis* co-culture provides endo- and exo-polygalacturonase activity. Even when the culture was grown on pectin or more complex substrates, those enzymes can only hydrolyze non-esterified GalA residues, why the cells are exposed to the same monomers, GalA only, as during cultivation on PolyGalA.

None of the cultivations shown in Figure 4-4C reached a complete substrate consumption. The cultivation on SP-he consumed 2.5 g/L (12%) of the total substrate, the cultivation on AP-he 4.7 g/L (24%) and the cultivation on AP-le 6.1 g/L (30%). The consumption with respect to the total substrate can be seen in Figure 4-4D (open bars). These low consumption rates can be explained by the composition of the applied pectins. GalA represents only 67 - 78% of all pectic sugars (Table 4-1). The produced endo- and exo-polygalacturonases can only hydrolyze the non-esterified fraction of those GalA residues, leading to a much lower degree of theoretically available GalA (25 – 68.5%, Table 4-1) compared to PolyGalA (where the corresponding value

would be 100%). The fraction of this theoretically available substrate is visualized in Figure 4-4D (diagonally hatched bars).

Cultivations on AP-le showed the highest overall substrate consumption. This could be explained by the low degree of esterification, leading to more non-esterified GalA that could be hydrolyzed by the endo- and exo-polygalacturonases. Figure 4-4D (horizontally hatched bars) shows the substrate consumption with respect to the theoretically available substrate (in this case non-esterified GalA residues). Here, the cultivation on AP-he showed the highest value. 95% of the non-esterified GalA was consumed, indicating that the PolyGalA regions in this type of pectin were well accessible for endo- and exo-polygalacturonases.

Two reference cultivations show the growth of AB33P5 Δ R/AtPgaX and AB33P5 Δ R/AaPgu1 in axenic culture on SP-he (Figure A 11) and AP-he (Figure A 12, black and grey curves). In both cases, only a weak metabolization of GalA can be detected. This demonstrates the beneficial effect of *U. maydis* co-fermentations for the hydrolysis and metabolization of pectins.

Certain anaerobic digestive bacteria like *Lachnospira multiparus* or *Faecalibacterium prausnitzii* have been demonstrated to produce pectinolytic enzymes enabling their growth on pectin [Dušková and Marounek 2001, Lopez-Siles, *et al.* 2012]. Other organisms are only rarely tested for their ability to grow on pectin as this substrate is only low abundant in nature and challenging to degrade enzymatically.

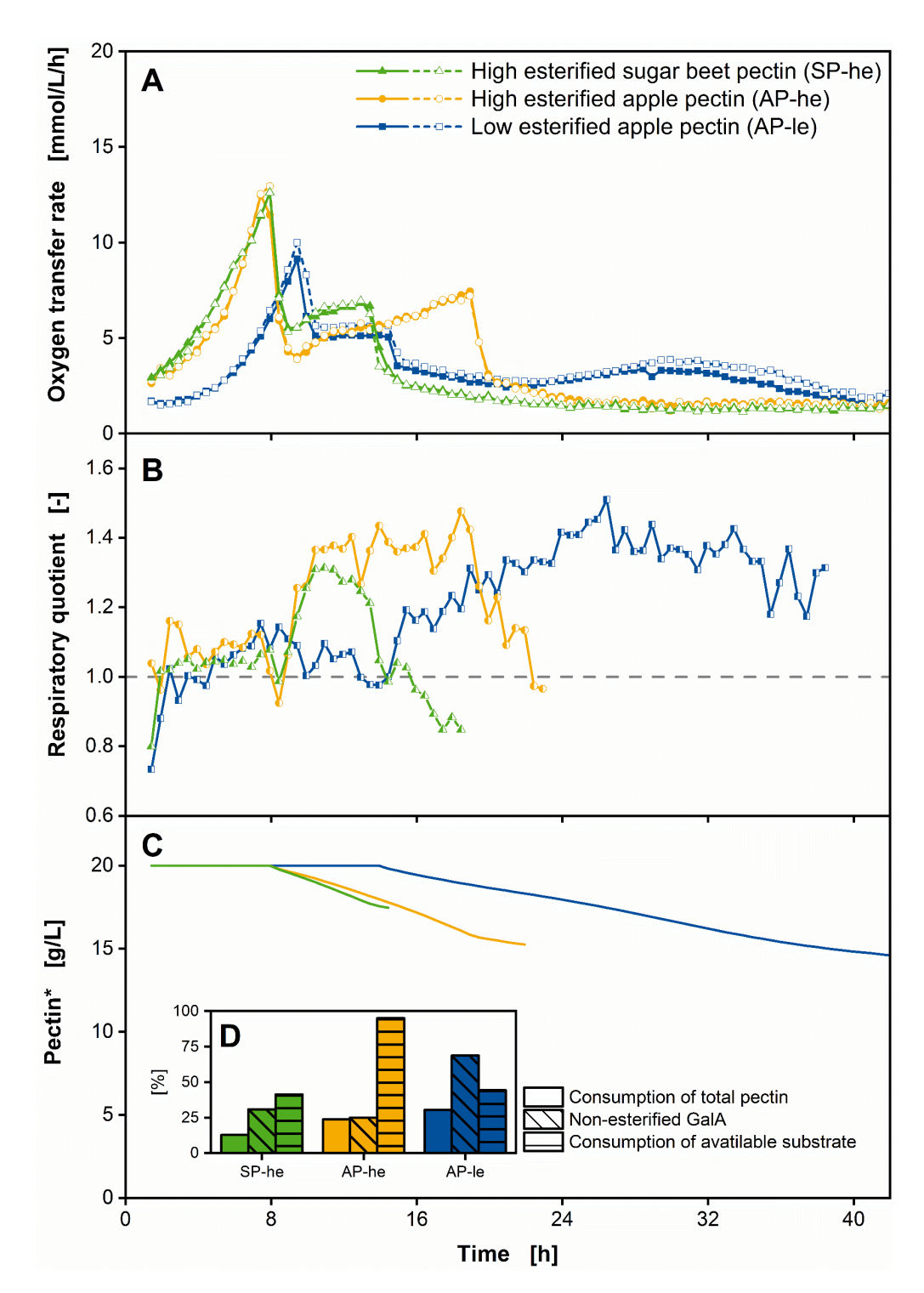


Figure 4-4: Comparison of *U. maydis* **co-fermentation growth on different pectins.** The strain combination AB33P5 Δ R/AtPgaX (exo-polygalacturonase) and AB33P5 Δ R/AaPgu1 (endo-polygalacturonase) was grown on a mixture of glucose (4 g/L) and pectin (20 g/L) as carbon sources. Three different types of pectin were tested: high esterified sugar beet pectin (SP-he, green curves), high esterified apple pectin (AP-he, yellow curves) and low esterified apple pectin (AP-le, red curves). **A** OTR of biological duplicates, represented each as line and dashed line. **B** Mean of biological duplicates of RQ. For clarity reasons, the RQ is only shown for OTR > 2 mmol/L/h. **C** Mean of biological duplicates of residual pectin calculated from the overall consumed oxygen as described in Chapter 3.2.9. End of pectin consumption was defined by the RQ drop below 1. **D** Consumption analysis of the

evaluated pectins. Percentage of consumed from total pectin (open bars), fraction of theoretically available from total pectin (diagonally hatched bars) and percentage of consumed from theoretically available pectin (horizontally hatched bars). Culture conditions: modified Verduyn medium, 0.2 M MOPS, pH 6.0, 250 mL flask, filling volume 20 mL, shaking frequency 300 rpm, shaking diameter 50 mm, initial $OD_{600}(AB33P5\Delta R/AtPgaX) = 0.5$, initial $OD_{600}(AB33P5\Delta R/AtPgaX) = 0.1$, temperature 30 °C

4.5.2 Influence of external enzyme additions

Reaching higher total substrate metabolization for the tested pectins requires the additional use of external enzymes increasing the overall pectinolytic activity. Within this chapter, three different commercial enzyme cocktails were tested: pectinases from *A. niger* (p-An), pectinases from *A. aculeatus* (p-Aa) and cellulases from *T. reesei* (c-Tr). Two essential enzymes for a higher metabolization rate of homogalacturonan are pectin-methylesterase and acetylesterase. Those enzymes can remove methyl or acetyl groups from the polygalacturonic acid backbone, making it accessible for endo- and exo-polygalacturonases. Other enzymes hydrolyze the side chains containing other sugars like rhamnose, arabinose or xylose. The external enzyme cocktails were expected to provide a wide variety of pectinases, leading in theory to a complete hydrolysis of the pectin. The entire provided pectin should thus be hydrolyzed to monomeric sugars that are available for microbial consumption.

The OTR of cultures with or without addition of external enzymes growing on SP-he is shown in Figure 4-5A. Addition of c-Tr to the cultivation medium slightly increased the OTR during GalA consumption (Figure 4-5A, yellow curves) in comparison to the culture without external enzymes (Figure 4-5A, green curves). However, addition of c-Tr resulted in no increased total substrate consumption (Figure 4-5D, yellow and green open bars). In both cultivations, 13% of the total substrate were consumed. This is in line with the used substrate, as cellulases are not expected to have hydrolytic activity towards pectin. Therefore, the theoretically available substrate (Figure 4-5D, yellow and green diagonally hatched bars) equals the percentage of the non-esterified GalA. The applied CF for the calculation of residual pectin (Figure 4-5C, green and yellow curves) was the same as for PolyGalA (Table 4-2).

Addition of pectinase p-An resulted in a remarkable increase in the metabolic activity (Figure 4-5A, blue curves). After glucose consumption, an even higher OTR maximum of 18 mmol/L/h was reached after 16 h during consumption of GalA. The elongated GalA consumption phase

(Figure 4-5B, blue curve) correlates with the high estimated total substrate consumption of 47% (Figure 4-5C and D, blue curve / bars).

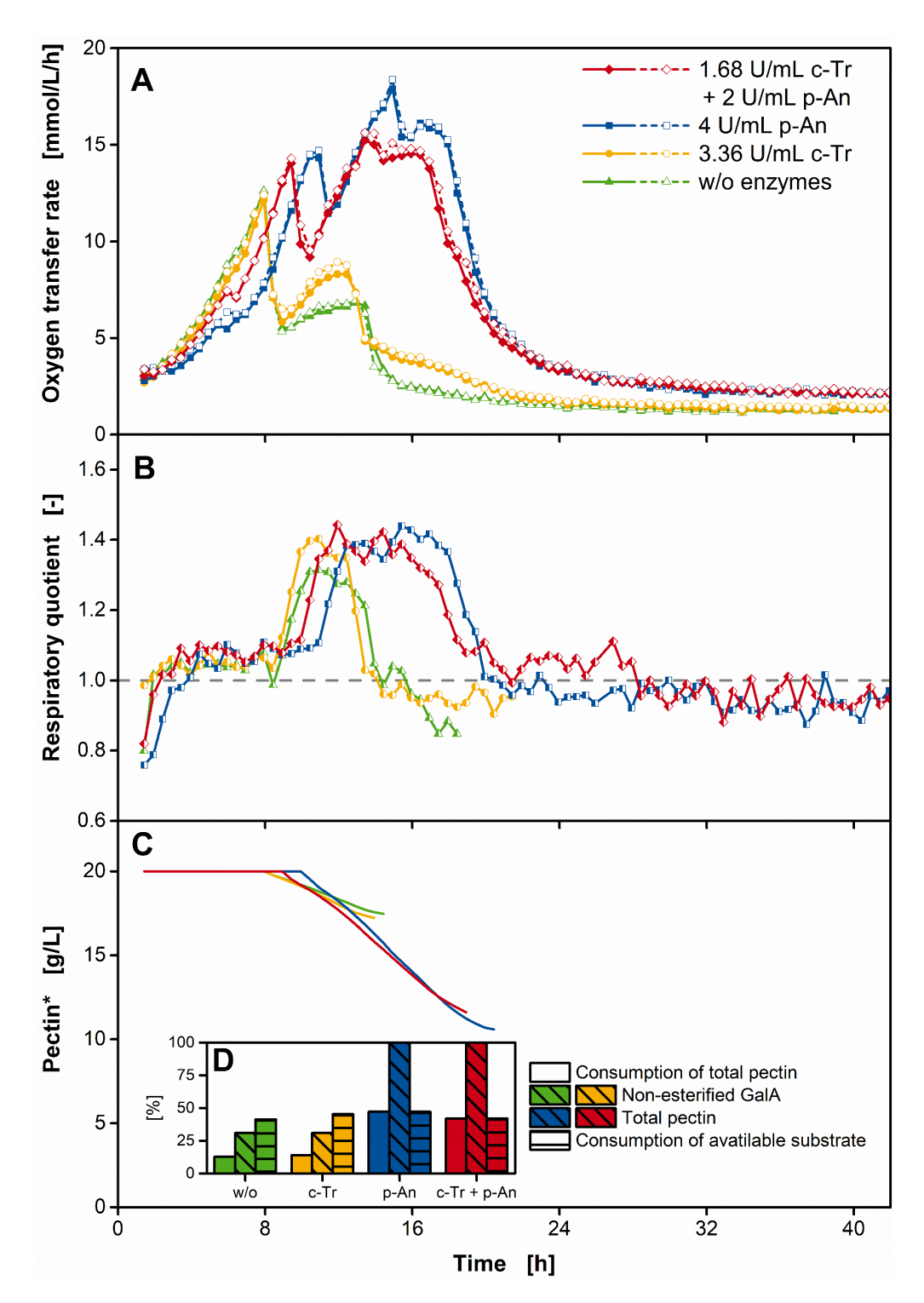


Figure 4-5: Influence of external enzymes on U. may dis co-fermentation on sugar beet pectin SP-he. The strain combination AB33P5 Δ R/AtPgaX (exo-polygalacturonase) and AB33P5 Δ R/AaPgu1 (endo-polygalacturonase) was grown on a mixture of glucose (4 g/L) and high esterified sugar beet pectin (SP-he, 20 g/L)

as carbon sources. The inoculated medium was supplemented with 4 U/mL pectinase from *A. niger* (p-An, blue curves), 3.36 U/mL cellulase from *T. reesei* (c-Tr, yellow curves) or 1.68 U/mL c-Tr and 2 U/mL p-An (red curves). A reference cultivation without addition of external enzymes is shown in green. A OTR of biological duplicates, represented each as line and dashed line. **B** Mean of biological duplicates of RQ. For clarity reasons, the RQ is only shown for OTR > 2 mmol/L/h. **C** Mean of biological duplicates of residual pectin calculated from the overall consumed oxygen as described in Chapter 4.4. End of pectin consumption was defined by the RQ drop below 1. **D** Consumption analysis of the evaluated pectins. Percentage of consumed from total pectin (open bars), fraction of theoretically available from total pectin (diagonally hatched bars, composition is indicated for each colour in the figure legend) and percentage of consumed from theoretically available pectin (horizontally hatched bars). Culture conditions: modified Verduyn medium, 0.2 M MOPS, pH 6.0, 250 mL flask, filling volume 20 mL, shaking frequency 300 rpm, shaking diameter 50 mm, initial OD₆₀₀(AB33P5 Δ R/AtPgaX) = 0.5, initial OD₆₀₀(AB33P5 Δ R/AaPgu1) = 0.1, temperature 30 °C

The pectinase cocktail p-An thus enabled the metabolization of almost half of the provided pectin substrate. The mCF for the estimation of residual pectin is given in Table 4-3. Halving the enzymatic activity of both external enzymes, c-Tr and p-An, resulted in the OTR profile shown in Figure 4-5A (red curves). The OTR profile looks similar but slightly lower compared to the culture with only p-An. The total substrate consumption (42%) is only slightly reduced compared to the culture with only p-An (Figure 4-5D, red open bar). The differences could be explained by the amount of enzyme used. In the culture with both, p-An and c-Tr, the amount of each individual enzyme was only half as high as in the culture with p-An or c-Tr alone. The addition of c-Tr alone (Figure 4-5, yellow curves) demonstrated that cellulases are not necessary for the hydrolysis of pectins. However, the addition of 4 U/mL of p-An to the cultivation showed similar results to the addition of 2 U/mL of p-An. This suggests that the enzyme concentration was not the hydrolysis-limiting factor during the cultivation. For both cultivations with p-An, the theoretically available amount of substrate equals the total pectin (Figure 4-5D, blue and red diagonally hatched bars). Addition of p-An has been demonstrated to influence the metabolization rate of SP-he substantially.

Addition of pectinase from *A. aculeatus* (p-Aa) during axenic or co-cultivation of AB33P5ΔR/AtPgaX and AB33P5ΔR/AaPgu1 on AP-he resulted in the metabolic activity shown in Figure 4-6. While the co-fermentation without addition of p-Aa resulted in a low metabolic activity that can be attributed to GalA consumption (Figure 4-6A, yellow curves), addition of p-Aa increased the OTR during pectin metabolization significantly (Figure 4-6A, green curves). Compared to the co-fermentation, axenic cultivations of AB33P5ΔR/AtPgaX (Figure 4-6A, grey curve), AB33P5ΔR/AaPgu1 (Figure 4-6A, black curve) and their progenitor strain AB33P5ΔR (Figure 4-6A, blue curves) supplemented with p-Aa showed only a slightly

reduced OTR level. Figure 4-6B defines, as before, the GalA or pectin consumption phase, leading to the course of residual pectin shown in Figure 4-6C.

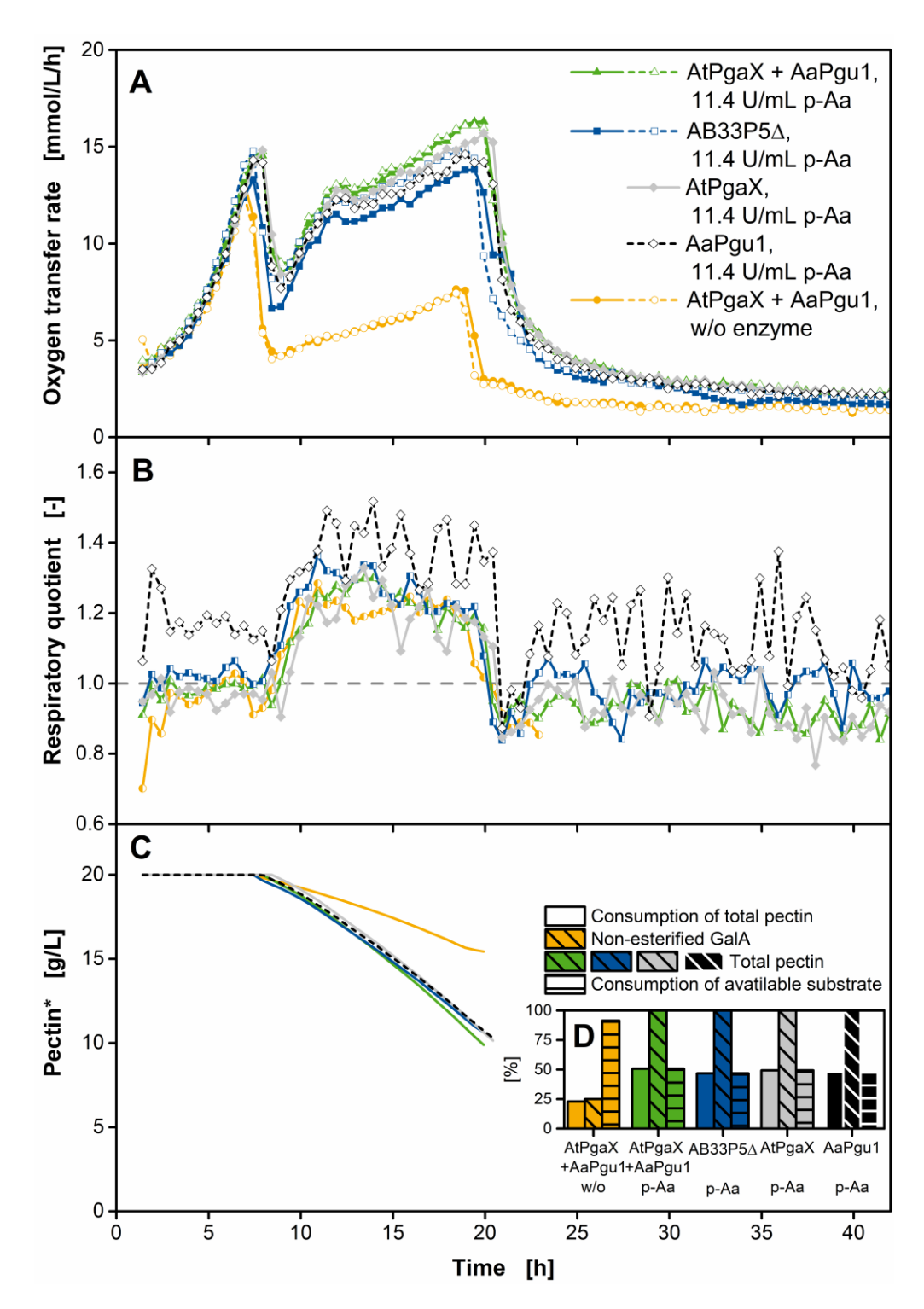


Figure 4-6: Influence of external pectinase on *U. maydis* axenic and co-fermentation on high esterified apple pectin AP-he. The strains AB33P5 Δ R/AtPgaX (exo-polygalacturonase) and AB33P5 Δ R/AaPgu1 (endo-polygalacturonase) were grown in axenic or co-fermentation as well as their progenitor strain AB33P5 Δ R on a

mixture of glucose (4 g/L) and high esterified apple pectin (AP-he, 20 g/L) as carbon sources. The inoculated medium was supplemented with 11.4 U/mL pectinase from *A. aculeatus* (p-Aa). Axenic cultures are shown for AB33P5 Δ R/AtPgaX (grey curve), AB33P5 Δ R/AaPgu1 (black curves) *and* AB33P5 Δ R (blue curves). Cofermentation of AB33P5 Δ R/AtPgaX and AB33P5 Δ R/AaPgu1 are shown with (yellow curves) or without (green curves) addition of p-Aa. **A** OTR of biological duplicates (green, blue and yellow curves) or the RQ. For clarity reasons, the RQ is only shown for OTR > 2 mmol/L/h. **C** Mean of biological duplicates (green, blue and yellow curves) of residual pectin calculated from the overall consumed oxygen as described in Chapter 4.4. End of pectin consumption was defined by the RQ drop below 1. **D** Consumption analysis of the evaluated pectins. Percentage of consumed from total pectin (open bars), fraction of theoretically available from total pectin (diagonally hatched bars, composition is indicated for each colour in the figure legend) and percentage of consumed from theoretically available pectin (horizontally hatched bars). Culture conditions: modified Verduyn medium, 0.2 M MOPS, pH 6.0, 250 mL flask, filling volume 20 mL, shaking frequency 300 rpm, shaking diameter 50 mm, initial OD₆₀₀ = 0.6 (ratio 5:1 for AB33P5 Δ R/AtPgaX : AB33P5 Δ R/AaPgu1 co-fermentation), temperature 30 °C

As discussed above for the cultivations with p-An, the theoretically available substrate equals the total pectin. This is represented in Figure 4-6D (diagonally hatched bars). The mCF for the estimation of residual pectin is given in Table 4-3. Production of endo- and exopolygalacturonases by the cultivated *U. maydis* strains has, in this case, only a minor effect on the consumption of total pectin (Figure 4-6D, open bars). While AB33P5ΔR consumed 48% of the total pectin, the co-fermentation consumed 52%. Those values are comparable to the consumption of SP-he, shown in Figure 4-5D (blue bars). These results indicate that the main pectinolytic activity was provided by the added p-Aa cocktail. The endo- and exopolygalacturonase activity produced by the overexpression strains were detectable but had only a low influence on the overall hydrolysis of AP-he.

Addition of cellulases showed no beneficial effect on the growth of the progenitor strain AB33P5 Δ R on AP-he (Figure A 12, green and yellow curves). This is in line with the previous observation during cultivation on SP-he (Figure 4-5, yellow curves) and supports the assumption, that cellulases show no hydrolytic activity towards pectin.

Enzymes were used previously for the hydrolysis of plant biomass to generate fermentable sugars. Rodrigues, *et al.* [2015] used the commercial enzyme cocktails Celluclast and Cellic CTec2 to hydrolyse wheat straw for ethanol fermentation with *S. cerevisiae*. With those enzyme cocktails, hydrolysis yields of 52 to 81% (Celluclast) and up to 98% (CTec2) were achieved [Rodrigues, *et al.* 2015]. The hydrolysis yields of pectin reported in this chapter are lower with about 50%. The main difference between these two systems can be found in the polymer

structure of the substrate. Wheat straw mainly consists of cellulose, a linear glucose polymer that is easily degradable enzymatically. The complex nature of pectin with numerous different sugar linkages and side chains makes a complete hydrolysis much more difficult. Therefore, it is not surprising that the total hydrolysis yields are lower on pectin, compared to cellulose.

4.6 Growth on sugar beet pulp

The addition of pectinases increased the total substrate consumption of the established cofermentation on SP-he from 13 to 47% (Figure 4-5D, open bars) and on AP-he from 23 to 52% (Figure 4-6D, open bars). The next step towards valorization of industrial waste streams is the utilization of sugar beet pulp, a high-abundant waste stream of the sugar refinery process. Usually, pretreatment of sugar beet pulp for fermentations comprises a single autoclaving step and no further treatments [Edwards and Doran-Peterson 2012]. To test the influence of different autoclaving procedures, sugar beet pulp was autoclaved directly in the RAMOS flask dry or suspended in a liquid film. The flasks were filled with medium and inoculated with the established co-culture of AB33P5ΔR/AtPgaX and AB33P5ΔR/AaPgu1 without addition of external enzymes. All cultivations resulted in no significant metabolization (Figure A 13). However, sugar beet pulp that was autoclaved in water led to a slightly increased OT during glucose consumption. Probably, the cellulosic network was weakened during autoclaving in liquid and small amounts of glucose were released from the cellulose fraction of sugar beet pulp. A weakened structure should be beneficial for hydrolysis as the pectin fraction becomes better reachable for enzymes. Therefore, sugar beet pulp for cultivations with external enzymes (Figure 4-7) was treated the same way. Figure 4-7A shows the OTR profile for co-fermentations of AB33P5ΔR/AtPgaX and AB33P5ΔR/AaPgu1 with addition of p-Aa and / or c-Tr. Addition of c-Tr (yellow curves) leads to a second, smaller peak between 10 and 16 h of cultivation time. As the RQ is not increasing in that period (Figure 4-7B, yellow curve), no GalA is consumed. Instead glucose that was released from the cellulose fraction was most probably metabolized. The addition of p-Aa (Figure 4-7A, blue curves) leads to a stepwise declining OTR profile. The RQ does not increase clearly (Figure 4-7B, blue curve) preventing a clear statement about the consumed substrates.

A combination of c-Tr and p-Aa (Figure 4-7A, red curves) resulted in a similar profile to the cultivation with only p-Aa. Again, the RQ remains low (Figure 4-7B, red curve), compared to the cultivations on pectin (Figure 4-5B and Figure 4-6B). In Chapters 2, 3 and 4.5, the pectin or (Poly)GalA consumption phases were defined by the RQ. Contrary, during growth on sugar beet pulp, the RQ does not clearly indicate the start or end of the phase of sugar beet pulp consumption. Here, the phase of sugar beet pulp metabolization was estimated to begin after the glucose peak and the correlated drop in the RQ after about 7.5 Figure 4-7B). The end of sugar beet pulp consumption was defined by the drop of the OTR below 2 mmol/L/h. With those assumptions and the mCF listed in Table 4-3, the residual sugar beet pulp concentration during the cultivation was estimated (Figure 4-7C). The calculation of the total substrate consumption is presented in Figure 4-7D. The reference culture without addition of external enzymes showed no metabolization of sugar beet pulp (green asterisks). This is not surprising, as the theoretically available substrate (in this case equal to the non-esterified GalA) represents only 8% of the total substrate (Figure 4-7D, green, diagonally hatched bar). The consumption of total substrate was significantly increased for addition of c-Tr (26%), p-An (50%) or both enzymes (55%). The theoretically available amount of substrate differs among all cultivations. In case of p-Aa addition, the pectin fraction (30% of total substrate, Figure 4-7D, blue, diagonally hatched bar) should be accessible. With addition of c-Tr, the cellulose fraction of 30% in total sugar beet pulp could be hydrolysed. Additionally, endo- and exopolygalacturonase produced by the co-culture could, in theory, liberate 8% (fraction of nonesterified GalA in total sugar beet pulp, Table 4-1). This results in a fraction of available substrate of 38% (Figure 4-7D, yellow, diagonally hatched bar). With addition of both enzymes, 30% of each, pectin and cellulose, are theoretically accessible, leading to 60% of available substrate in total sugar beet pulp (Figure 4-7D, red, diagonally hatched bar). Relating the consumed substrate to the theoretically available substrate resulted in a value of 170% for the cultivation with p-Aa. This indicates that the used pectinase cocktail shows additional activities towards other fractions of sugar beet pulp. Whether those fractions are cellulose and / or hemicellulose remains unclear.

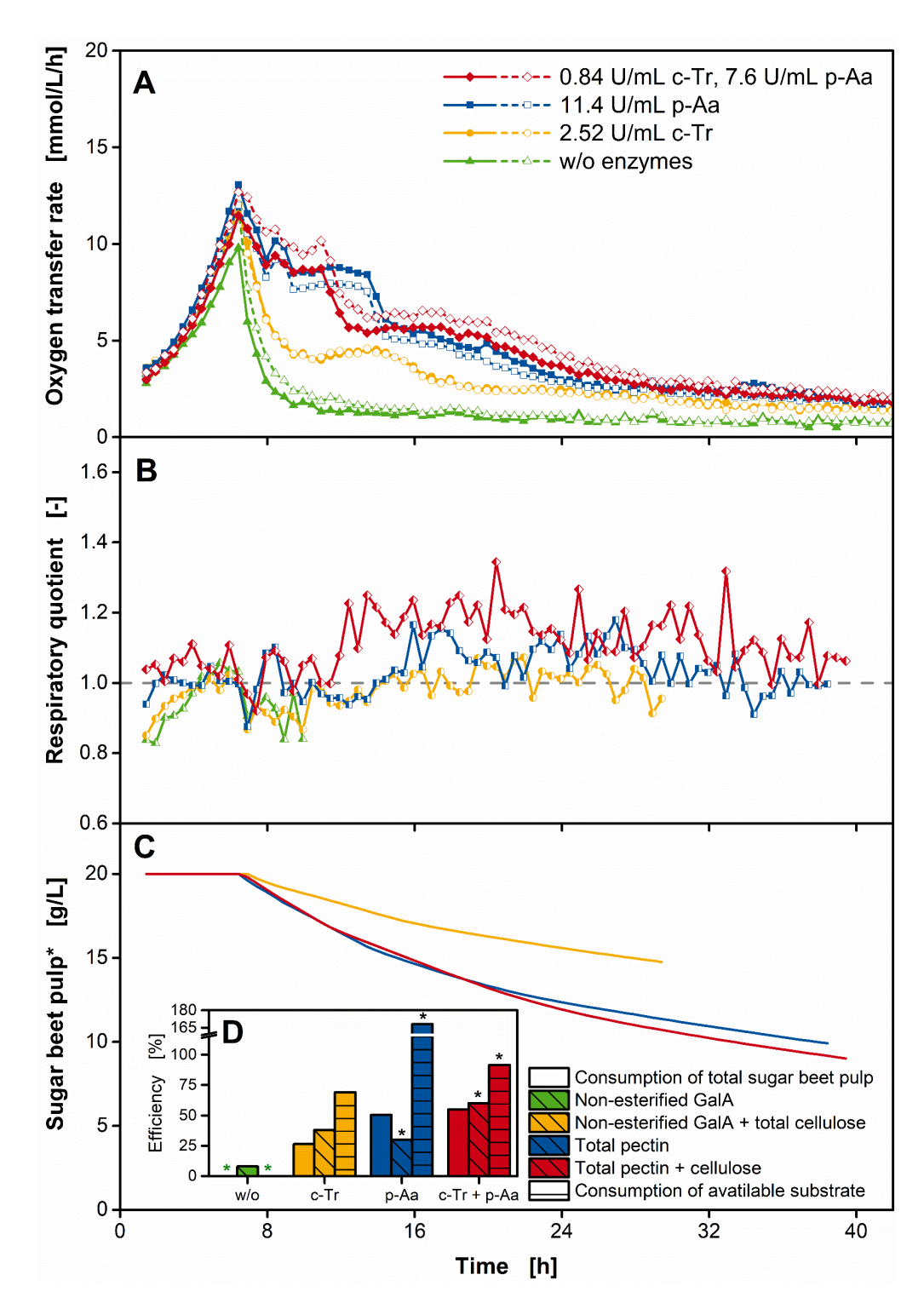


Figure 4-7: Influence of external enzymes on U. may dis co-fermentation on sugar beet pulp. The strain combination AB33P5 Δ /AtPgaX (overexpressing a fungal exo-polygalacturonase) and AB33P5 Δ /AaPgu1 (overexpressing a fungal endo-polygalacturonase) was grown on a mixture of glucose (4 g/L) and sugar beet pulp (20 g/L) as carbon sources. The inoculated medium was supplemented with 11.4 U/mL pectinase from A. aculeatus (p-Aa, blue curves), 2.52 U/mL cellulase from T. reesei (c-Tr, yellow curves) or 0.84 U/mL c-Tr and 7.6 U/mL p-Aa (red curves). A reference cultivation without addition of external enzymes is shown in green. A OTR of biological duplicates, represented each as line and dashed line. B Mean of biological duplicates of the RQ. For clarity reasons, the RQ is only shown for OTR > 2 mmol/L/h. C Mean of biological duplicates of residual sugar

beet pulp, calculated from the overall consumed oxygen as described in Chapter 4.4. End of sugar beet pulp consumption was defined by the OTR drop below 2 mmol/L/h. **D** Consumption analysis of the evaluated pectins. Percentage of consumed from total pectin (open bars), fraction of theoretically available from total pectin (diagonally hatched bars, composition is indicated for each colour in the figure legend) and percentage of consumed from theoretically available pectin (horizontally hatched bars). Green asterisks indicate no detectable consumption of sugar beet pulp. Black asterisks indicate potential cross-reactivity of the applied enzymes that could increase the percentage of theoretical available substrate. Culture conditions: modified Verduyn medium, 0.2 M MOPS, pH 6.0, 250 mL flask, filling volume 20 mL, shaking frequency 300 rpm, shaking diameter 50 mm, initial $OD_{600}(AB33P5\Delta/AtPgaX) = 0.5$, initial $OD_{600}(AB33P5\Delta/AaPgu1) = 0.1$, temperature 30 °C

Beside sugar beet pulp, citrus processing waste is also rich in pectin. This substrate has been used to produce ethanol with genetically modified *S. cerevisiae* strains [Widmer, *et al.* 2010]. Growth of *S. cerevisiae* can be inhibited by accumulation of limonene. To prevent this inhibition, the substrate was pretreated harshly at 160°C and steam purging to break down the limonene [Widmer, *et al.* 2010]. Utilization of sugar beet pulp does not require such harsh pretreatment as no inhibitory effects are known. The standard autoclaving procedure is sufficient in this case [Edwards and Doran-Peterson 2012].

In the past years, some efforts have already been made to establish a consolidated bioprocess based on sugar beet pulp. These processes comprise linked CAZyme production, sugar beet pulp hydrolysis and product formation. Grohmann, et al. [1998] used Erwinia sp. to convert pectin-rich materials into ethanol. Hydrolysis was achieved by external pectinase cocktails in that case. In a similar process, a genetically modified E. coli strain was supplemented with pectinases, cellulases and hemicellulases to enable the production of ethanol from sugar beet pulp [Rorick, et al. 2011]. These examples represent non-consolidated bioprocesses, as the enzymes were not produced in place. The current production hosts of CAZymes like T. reesei or A. niger lack a high-value product and a suited method for their use in bioreactors [Glass, et al. 2013, Klement, et al. 2012, Lara-Marquez, et al. 2011, Papagianni, et al. 1998]. U. maydis has the potential to overcome these limitations by providing both requirements, CAZyme production and product formation. However, great efforts have to be made in future research.

4.7 Conclusion

In this chapter, it was shown that *U. maydis* can grow on six of the most abundant sugars present in pectin. Those sugars were consumed one after the other with a clear order of preference. Together with literature data for the composition of pectin and sugar beet pulp and the obtained metabolic data, mCFs for the estimation of residual pectin or sugar beet pulp were calculated. Co-fermentations of *U. maydis* strains producing endo- and exo-polygalacturonase on three different pectins showed only limited metabolic activity. The addition of external cellulases showed no significant effect while addition of pectinase cocktails increased the metabolization rate significantly. The calculated mCFs helped to estimate the consumption of total substrate for those cultivations, reaching values of up to 52%.

Co-fermentations of *U. maydis* on sugar beet pulp showed no metabolic activity. The addition of external pectinase and / or cellulase induced a significant metabolic activity, indicating that the substrate was consumed partially. Cellulase addition accounted for saccharification of the cellulose fraction, leading to an increase in the total sugar beet pulp metabolization to 26%. Pectinase addition or a combined addition of cellulase an pectinase resulted in a total substrate consumption of up to 55%.

Reaching higher metabolization rates for *U. maydis* co-fermentations without addition of external enzymes thus requires strains that can produce additional enzymes, such as pectin-methylesterase or acetylesterase, which are essential for the de-esterification of the homogalacturonan backbone of pectin. Degradation of pectin is a key step towards the utilization of sugar beet pulp as an abundant and low-cost substrate for microbial fermentations of high-value products.

Chapter 5

Summary and outlook

The present thesis provides a reliable method to online estimate the residual substrate concentration during microbial fermentations in small-scale. This method is based on the measurement of the metabolic activity and a fixed stoichiometric ratio of substrate consumption, oxygen consumption and biomass formation. Especially in fermentations of carbon sources that are challenging to quantify via offline methods, the presented online estimation model can be useful. This is the case for complex substrates like sugar beet pulp, which are used within biorefinery processes.

In Chapter 2, growth of *U. maydis* on galacturonic acid (GalA), the main pectin sugar unit, was characterized. The RAMOS device enabled a detailed analysis of the correlation between GalA and oxygen consumption. Varying the GalA concentration in the medium revealed a fixed stoichiometric ratio to the overall consumed oxygen (OT). With this data, a calculation model was developed that enabled the determination of residual GalA concentration at each time point of the cultivation without offline sampling. This model was applied to analyze the growth of an *U. maydis* strain expressing an exo-polygalacturonase from *Aspergillus tubingensis*. This strain was grown on polygalacturonic acid (PolyGalA), the main backbone in pectin. Beside determination of the residual PolyGalA concentration in the culture broth, respiration monitoring assisted in determination of the enzyme activity of the expressed enzyme during cultivation. The enzyme activity obtained from respiration data was compared to enzyme activities obtained from offline measurements. The activities determined from respiration

monitoring were shown to be less prone to product inhibition as the hydrolysis product GalA accumulates during offline assays. In contrast, GalA is consumed constantly during microbial fermentations, why the novel measurement principle was shown to be advantageous over offline methods.

In Chapter 3, the enzyme repertoire of *U. maydis* for PolyGalA degradation was further extended. A bioinformatic survey supported the need for heterologous CAZymes in order to make *U. maydis* capable of degrading complex polymers like pectin. Various endo- and exopolygalacturonases of intrinsic, fungal and bacterial origin were overexpressed and secreted. An intrinsic endo-polygalacturonase was activated by promoter exchange. Bacterial endo- and exo-polygalacturonases were successfully secreted using a lock-type unconventional secretion system that prevents posttranslational modifications. Those modifications might potentially reduce the enzyme activity. Finally, fungal endo- and exo-polygalacturonases from Aspergillus sp. were expressed in U. maydis and secreted via the conventional pathway. All secreted enzymes were tested for their activity via offline DNS assays. Bacterial enzymes provided only minor enzymatic activities compared to enzymes of fungal origin. However, the unconventional secretion system might constitute an additional valuable tool to improve biomass degradation in the future. Following strain generation, endo- and exopolygalacturonase producing strains were cultivated in co-fermentation on PolyGalA in the RAMOS device. Endo-polygalacturonase producing strains showed no metabolic activity when cultivated in axenic culture on PolyGalA. The enzyme releases only shorter GalA oligomers that cannot be taken up or consumed by *U. maydis*. However, in co-culture with strains expressing exo-polygalacturonase, the endo-polygalacturonase activity became visible in the respiration profile. This approach enabled the comparison of endo-polygalacturonases from different origin. Fungal enzymes from Aspergillus tubingensis demonstrated the fastest GalA liberation making this system favorable for future applications. But also intrinsic and bacterial enzymes increased the overall PolyGalA consumption compared to axenic cultures. Afterwards, the ratio of endo- and exo-polygalacturonase was varied by different inoculation ratios of the production strains. A $5 \times$ surplus of exo-polygalacturonase activity has been demonstrated to lead to a fast consumption of PolyGalA. Co-cultures inoculated with this ratio showed an OTR profile similar to growth on monomeric GalA. The GalA concentration in the culture supernatant increased during glucose consumption and at the beginning of PolyGalA

consumption. The GalA liberation rate was determined from the measured concentration of GalA in the culture supernatant and the consumed amount of GalA, calculated from the OT. This rate depends strongly on the pH. That is consistent with the pH-dependent activity of the exo-polygalacturonase releasing GalA monomers.

In Chapter 4, the substrate complexity for growth of the established *U. maydis* co-culture was further increased. Three different pectins and sugar beet pulp were given as carbon source with or without addition of external enzymes. Those substrates entail numerous different sugars to the culture broth that could all serve as carbon sources. The capability of *U. maydis* to metabolize and preference among six different sugars (glucose, xylose, mannose, GalA, rhamnose, arabinose) was proven by supplementation of the culture medium with all sugars simultaneously. The respiration activity during consumption of each sugar led to the rough estimation of experimental correlation factors (CFs) between oxygen and substrate consumption. These factors were processed to mixed correlation factors (mCFs) for the estimation of residual substrate during cultivations on pectin or sugar beet pulp.

The characteristics of high-esterified sugar beet pectin (SP-he), high-esterified apple pectin (AP-he) and low-esterified apple pectin (AP-le) influenced the overall pectin consumption of co-fermentations. With the highest degree of non-esterified GalA residues, AP-le reached the highest value of total pectin consumption. Taking into account that in theory only non-esterified GalA residues can be hydrolyzed, AP-he showed the highest consumption of available substrate. However, only 24% of the total substrate was hydrolyzed and consumed. Afterwards, the cultures were supplemented with external pectinases and cellulases. This quantifies the potential of future *U. maydis* strains or co-fermentations harboring multiple different enzymatic activities. Whereas cellulases had no significant effect on the metabolization of pectin, external pectinases significantly increased the totally consumed substrate to about 50%. Finally, the cofermentation was grown on sugar beet pulp, supplemented with external enzymes. A total substrate conversion of about 55% was reached for the addition of pectinase and cellulase cocktails. These findings are a solid foundation for establishing an efficient consolidated bioprocess for sugar beet pulp degradation and subsequent production of glycolipids or organic acids in future. U. maydis has the potential to compete with current workhorses in the field of consolidated bioprocessing.

Promoting *U. maydis* in this field of applications still comprises two challenges to be mastered: The metabolization rate of sugar beet pulp without addition of external enzymes and the formation of a value-added product. Higher metabolization rates for *U. maydis* cofermentations without addition of external enzymes require strains that can produce additional enzymes, such as pectin-methylesterase or acetylesterase. These enzymes are essential for the de-esterification of the pectin backbone homogalacturonan. Degradation of pectin is a key challenge towards the utilization of sugar beet pulp as an abundant and low-cost substrate for microbial fermentations of high-value products. Even though many secondary metabolites can be produced in *U. maydis*, e.g., organic acids or glycolipids, the GalA metabolism needs to be streamlined further towards those products. So far, none of the value-added products was produced from GalA as carbon source. This is a major prerequisite and remains a second key challenge for the establishment of a consolidated bioprocess based on the fermentation of pectin-rich biomass waste streams by *U. maydis* in future.

Bibliography i

Bibliography

- Abbott DW and Boraston AB (2007): The Structural Basis for Exopolygalacturonase Activity in a Family 28 Glycoside Hydrolase. Journal of Molecular Biology 368(5), 1215-22.
- Abdulrachman D, Thongkred P, Kocharin K, Nakpathom M, Somboon B, Narumol N, Champreda V, Eurwilaichitr L, Suwanto A, Nimchua T and Chantasingh D (2017): Heterologous expression of *Aspergillus aculeatus* endo-polygalacturonase in *Pichia pastoris* by high cell density fermentation and its application in textile scouring. BMC Biotechnol 17(1), 15.
- AFMB. (2018). "Carbohydrate Active Enzymes database." Retrieved 25 June 2018, from http://www.cazy.org/.
- Alcantara J, Mondala A, Hughey L and Shields S (2017): Direct succinic acid production from minimally pretreated biomass using sequential solid-state and slurry fermentation with mixed fungal cultures. Fermentation 3(3), 30.
- Amore A, Amoresano A, Birolo L, Henrissat B, Leo G, Palmese A and Faraco V (2012): A family GH51 alpha-L-arabinofuranosidase from *Pleurotus ostreatus*: identification, recombinant expression and characterization. Appl Microbiol Biotechnol 94(4), 995-1006.
- Anderlei T and Büchs J (2001): Device for sterile online measurement of the oxygen transfer rate in shaking flasks. Biochem Eng J 7(2), 157-62.
- Anderlei T, Zang W, Papaspyrou M and Büchs J (2004): Online respiration activity measurement (OTR, CTR, RQ) in shake flasks. Biochem Eng J 17(3), 187-94.
- Anders N, Humann H, Langhans B and Spieß AC (2015): Simultaneous determination of acidsoluble biomass-derived compounds using high performance anion exchange

ii Bibliography

chromatography coupled with pulsed amperometric detection. Anal Methods 7(18), 7866-73.

- Andrić P, Meyer AS, Jensen PA and Dam-Johansen K (2010): Reactor design for minimizing product inhibition during enzymatic lignocellulose hydrolysis: II. Quantification of inhibition and suitability of membrane reactors. Biotechnol Adv 28(3), 407-25.
- Antonov E, Schlembach I, Regestein L, Rosenbaum MA and Büchs J (2017): Process relevant screening of cellulolytic organisms for consolidated bioprocessing. Biotechnol Biofuels 10, 106.
- Antonov E, Wirth S, Gerlach T, Schlembach I, Rosenbaum MA, Regestein L and Büchs J (2016): Efficient evaluation of cellulose digestibility by *Trichoderma reesei* Rut-C30 cultures in online monitored shake flasks. Microb Cell Fact 15(1), 164.
- Aschenbroich J, Hussnaetter KP, Stoffels P, Langner T, Zander S, Sandrock B, Bolker M, Feldbrügge M and Schipper K (2018): The germinal centre kinase Don3 is crucial for unconventional secretion of chitinase Cts1 in *Ustilago maydis*. Biochim Biophys Acta Proteins Proteom.
- Bader J, Mast-Gerlach E, Popović MK, Bajpai R and Stahl U (2010): Relevance of microbial coculture fermentations in biotechnology. J Appl Microbiol 109(2), 371-87.
- Banuett F and Herskowitz I (1994): Morphological Transitions in the Life Cycle of Ustilago maydis and Their Genetic Control by the a and b Loci. Exp Mycol 18(3), 247-66.
- Bélafi-Bakó K, Eszterle M, Kiss K, Nemestóthy N and Gubicza L (2007): Hydrolysis of pectin by *Aspergillus niger* polygalacturonase in a membrane bioreactor. J Food Eng 78(2), 438-42.
- BeMiller JN (2001). Complex Polysaccharides. Glycoscience: Chemistry and Chemical Biology. Fraser-Reid, BO, Tatsata, K and Thiem, J. Heidelberg, Springer. 1865-82.

Bibliography

Benz JP, Protzko RJ, Andrich JM, Bauer S, Dueber JE and Somerville CR (2014): Identification and characterization of a galacturonic acid transporter from *Neurospora crassa* and its application for *Saccharomyces cerevisiae* fermentation processes. Biotechnol Biofuels 7(1), 20.

- Biz A, Sugai-Guerios MH, Kuivanen J, Maaheimo H, Krieger N, Mitchell DA and Richard P (2016): The introduction of the fungal D-galacturonate pathway enables the consumption of D-galacturonic acid by *Saccharomyces cerevisiae*. Microb Cell Fact 15(1), 144.
- Blake JD and Richards GN (1968): Problems of lactonisation in the analysis of uronic acids. Carbohydr Res 8(3), 275-81.
- Bölker M, Basse CW and Schirawski J (2008): *Ustilago maydis* secondary metabolism—From genomics to biochemistry. Fungal Genet Biol 45, Supplement 1, S88-S93.
- Bosch K, Frantzeskakis L, Vranes M, Kämper J, Schipper K and Gohre V (2016): Genetic manipulation of the plant pathogen *Ustilago maydis* to study fungal biology and plant microbe interactions. J Vis Exp (115), e54522.
- Brachmann A, König J, Julius C and Feldbrügge M (2004): A reverse genetic approach for generating gene replacement mutants in *Ustilago maydis*. Molecular genetics and genomics: MGG 272(2), 216-26.
- Brachmann A, Weinzierl G, Kämper J and Kahmann R (2001): Identification of genes in the bW/bE regulatory cascade in *Ustilago maydis*. Mol Microbiol 42(4), 1047-63.
- Branco RHR, Serafim LS and Xavier AMRB (2018): Second Generation Bioethanol Production: On the Use of Pulp and Paper Industry Wastes as Feedstock. Fermentation 5(1), 4.
- Brefort T, Doehlemann G, Mendoza-Mendoza A, Reissmann S, Djamei A and Kahmann R (2009): *Ustilago maydis* as a pathogen. Annu Rev Phytopathol 47, 423-45.

iv Bibliography

Brunecky R, Chung D, Sarai NS, Hengge N, Russell JF, Young J, Mittal A, Pason P, Vander Wall T, Michener W, Shollenberger T, Westpheling J, Himmel ME and Bomble YJ (2018): High activity CAZyme cassette for improving biomass degradation in thermophiles. Biotechnol Biofuels 11(1), 22.

- Caffall KH and Mohnen D (2009): The structure, function, and biosynthesis of plant cell wall pectic polysaccharides. Carbohydr Res 344(14), 1879-900.
- Cano-Canchola C, Acevedo L, Ponce-Noyola P, Flores-Martinez A, Flores-Carreon A and Leal-Morales CA (2000): Induction of lytic enzymes by the interaction of *Ustilago maydis* with *Zea mays* tissues. Fungal Genet Biol 29(3), 145-51.
- Carere RC, Sparling R, Cicek N and Levin BD (2008): Third generation biofuels via direct cellulose fermentation. Int J Mol Sci 9(7).
- Carpita NC (1996): Structure and biogenesis of the cell wall of grasses. Annu Rev Plant Physiol Plant Mol Biol 47(1), 445-76.
- CAZypedia Consortium (2018): Ten years of CAZypedia: a living encyclopedia of carbohydrate-active enzymes. Glycobiology 28(1), 3-8.
- CBS. (2019). "SignalP-5.0 Server." Retrieved 2019/02/10, from http://www.cbs.dtu.dk/services/SignalP/.
- Christensen ML and Eriksen NT (2002): Growth and proton exchange in recombinant *Escherichia coli* BL21. Enzyme Microb Technol 31(4), 566-74.
- Couturier M, Navarro D, Olive C, Chevret D, Haon M, Favel A, Lesage-Meessen L, Henrissat B, Coutinho PM and Berrin JG (2012): Post-genomic analyses of fungal lignocellulosic biomass degradation reveal the unexpected potential of the plant pathogen *Ustilago maydis*. BMC Genom 13, 57.

Bibliography

Cragg SM, Beckham GT, Bruce NC, Bugg TDH, Distel DL, Dupree P, Etxabe AG, Goodell BS, Jellison J, McGeehan JE, McQueen-Mason SJ, Schnorr K, Walton PH, Watts JEM and Zimmer M (2015): Lignocellulose degradation mechanisms across the tree of life. Curr Opin Chem Biol 29, 108-19.

- Daas PJH, Meyer-Hansen K, Schols HA, De Ruiter GA and Voragen AGJ (1999): Investigation of the non-esterified galacturonic acid distribution in pectin with endopolygalacturonase. Carbohydr Res 318(1), 135-45.
- de Vries RP (2003): Regulation of *Aspergillus* genes encoding plant cell wall polysaccharide-degrading enzymes; relevance for industrial production. Appl Microbiol Biotechnol 61(1), 10-20.
- Dimou E and Nickel W (2018): Unconventional mechanisms of eukaryotic protein secretion. Curr Biol 28(8), R406-R10.
- Djamei A and Kahmann R (2012): *Ustilago maydis*: dissecting the molecular interface between pathogen and plant. PLoS Pathog 8(11), e1002955.
- Doehlemann G, Wahl R, Vranes M, de Vries RP, Kämper J and Kahmann R (2008): Establishment of compatibility in the *Ustilago maydis*/maize pathosystem. J Plant Physiol 165(1), 29-40.
- Doran JB, Cripe J, Sutton M and Foster B (2000): Fermentations of pectin-rich biomass with recombinant bacteria to produce fuel ethanol. Appl Biochem Biotechnol 84-86, 141-52.
- Dušková D and Marounek M (2001): Fermentation of pectin and glucose, and activity of pectin-degrading enzymes in the rumen bacterium *Lachnospira multiparus*. Lett Appl Microbiol 33(2), 159-63.
- Edwards M and Doran-Peterson J (2012): Pectin-rich biomass as feedstock for fuel ethanol production. Appl Microbiol Biotechnol 95(3), 565-75.

vi Bibliography

Emaga TH, Rabetafika N, Blecker CS and Paquot M (2012): Kinetics of the hydrolysis of polysaccharide galacturonic acid and neutral sugars chains from flaxseed mucilage. Biotechnol Agron Soc 16(2), 139-47.

- EMBL-EBI. (2019). "Clustal Omega." Retrieved 2019/02/10, from https://www.ebi.ac.uk/Tools/msa/clustalo/.
- Federici L, Caprari C, Mattei B, Savino C, Di Matteo A, De Lorenzo G, Cervone F and Tsernoglou D (2001): Structural requirements of endopolygalacturonase for the interaction with PGIP (polygalacturonase-inhibiting protein). Proc Natl Acad Sci USA 98(23), 13425-30.
- Feedimpex EFM. (2019). "ED&F Man Feedimpex." Retrieved 2019/02/10, from http://www.feedimpex.com/usage-sugar-beet-pellets
- Feldbrügge M, Kellner R and Schipper K (2013): The biotechnological use and potential of plant pathogenic smut fungi. Appl Microbiol Biotechnol 97(8), 3253-65.
- Flitsch D, Krabbe S, Ladner T, Beckers M, Schilling J, Mahr S, Conrath U, Schomburg WK and Büchs J (2016): Respiration activity monitoring system for any individual well of a 48-well microtiter plate. J Biol Eng 10(1), 14.
- Flor-Parra I, Vranes M, Kämper J and Pérez-Martín J (2006): Biz1, a zinc finger protein required for plant invasion by *Ustilago maydis*, regulates the levels of a mitotic cyclin. Plant Cell 18(9), 2369-87.
- Garna H, Mabon N, Wathelet B and Paquot M (2004): New method for a two-step hydrolysis and chromatographic analysis of pectin neutral sugar chains. J Agric Food Chem 52(15), 4652-9.
- Garrido E, Voß U, Müller P, Castillo-Lluva S, Kahmann R and Pérez-Martín J (2004): The induction of sexual development and virulence in the smut fungus *Ustilago maydis* depends on Crk1, a novel MAPK protein. Genes Dev 18(24), 3117-30.

Bibliography vii

Geiser E, Reindl M, Blank LM, Feldbrügge M, Wierckx N and Schipper K (2016): Activating intrinsic carbohydrate-active enzymes of the smut fungus *Ustilago maydis* for the degradation of plant cell wall components. Appl Environ Microbiol 82(17), 5174-85.

- Geiser E, Wiebach V, Wierckx N and Blank LM (2014): Prospecting the biodiversity of the fungal family Ustilaginaceae for the production of value-added chemicals. Fungal Biol Biotechnol 1(1), 1-10.
- Glass NL, Schmoll M, Cate JH and Coradetti S (2013): Plant cell wall deconstruction by ascomycete fungi. Annu Rev Microbiol 67, 477-98.
- Glauche F, Glazyrina J, Cruz Bournazou MN, Kiesewetter G, Cuda F, Goelling D, Raab A, Lang C and Neubauer P (2017): Detection of growth rate-dependent product formation in miniaturized parallel fed-batch cultivations. Eng Life Sci 17(11), 1215-20.
- Green MR and Sambrook J (2012): Molecular cloning: A laboratory manual. Fourth edition. Cold Spring Harbor Laboratory Press, 2028.
- Grohmann K, Manthey J, Cameron R and Buslig B (1998): Fermentation of galacturonic acid and pectin-rich materials to ethanol by genetically modified strains of *Erwinia*. Biotechnol Lett 20(2), 195-200.
- Gupta R, Jung E and Brunak S. (2004). "Prediction of N-glycosylation sites in human proteins." Retrieved 2019/02/10, from http://www.cbs.dtu.dk/services/NetNGlyc/.
- Haag C, Klein T and Feldbrügge M (in press): Functional *in vivo* analysis of ESCRT components using model fungi. Methods in Mol Biol In: The ESCRT Complex: Methods and Protocols, eds Emmanuel Culetto and Renaud Legouis, Springer Science & Buisness Media New York.
- Hartmann HA, Krüger J, Lottspeich F and Kahmann R (1999): Environmental signals controlling sexual development of the corn smut fungus *Ustilago maydis* through the transcriptional regulator Prf1. Plant Cell 11(7), 1293-306.

viii Bibliography

Hewald S, Linne U, Scherer M, Marahiel MA, Kämper J and Bölker M (2006): Identification of a gene cluster for biosynthesis of mannosylerythritol lipids in the basidiomycetous fungus *Ustilago maydis*. Appl Environ Microbiol 72(8), 5469-77.

- Holliday R (1974). *Ustilago maydis*. Bacteria, Bacteriophages, and Fungi. King, RC. Springer US. 575-95.
- Huisjes EH, Luttik MA, Almering MJ, Bisschops MM, Dang DH, Kleerebezem M, Siezen R, van Maris AJ and Pronk JT (2012): Toward pectin fermentation by *Saccharomyces cerevisiae*: Expression of the first two steps of a bacterial pathway for D-galacturonate metabolism. J Biotechnol 162(2-3), 303-10.
- IBIS. (2019). "PEDANT Institute of Bioinformatics and Systems Biology." Retrieved 2019/02/10, from http://pedant.gsf.de/pedant3htmlview/pedant3view?Method=analysis&Db=p3_t237631_Us_t_maydi_v2GB.
- Ibrahim E, Jones KD, Taylor KE, Hosseney EN, Mills PL and Escudero JM (2017): Molecular and biochemical characterization of recombinant cel12B, cel8C, and peh28 overexpressed in *Escherichia coli* and their potential in biofuel production. Biotechnol Biofuels 10, 52.
- Jäger G, Wulfhorst H, Zeithammel EU, Elinidou E, Spiess AC and Büchs J (2011): Screening of cellulases for biofuel production: Online monitoring of the enzymatic hydrolysis of insoluble cellulose using high-throughput scattered light detection. Biotechnol J 6(1), 74-85.
- Jayani RS, Saxena S and Gupta R (2005): Microbial pectinolytic enzymes: A review. Process Biochem 40(9), 2931-44.
- Joanna B, Michal B, Piotr D, Agnieszka W, Dorota K and Izabela W (2018). Chapter 13 Sugar Beet Pulp as a Source of Valuable Biotechnological Products. Advances in Biotechnology for Food Industry. Holban, AM and Grumezescu, AM. Academic Press. 359-92.

Bibliography

Kahmann R, Romeis T, Bölker M and Kämper J (1995): Control of mating and development in *Ustilago maydis*. Curr Opin Genet Dev 5(5), 559-64.

- Kamm B and Kamm M (2004): Principles of biorefineries. Appl Microbiol Biotechnol 64(2), 137-45.
- Kämper J, Kahmann R, Bölker M, Ma L-J, Brefort T, Saville BJ, Banuett F, Kronstad JW, Gold SE, Müller O, Perlin MH, Wösten HAB, de Vries R, Ruiz-Herrera J, *et al.* (2006): Insights from the genome of the biotrophic fungal plant pathogen *Ustilago maydis*. Nature 444, 97.
- Keil T, Dittrich B, Lattermann C, Habicher T and Büchs J (2019): Polymer-based controlled-release fed-batch microtiter plate diminishing the gap between early process development and production conditions. J Biol Eng 13(1), 18.
- Kent LM, Loo TS, Melton LD, Mercadante D, Williams MA and Jameson GB (2016): Structure and properties of a non-processive, salt-requiring, and acidophilic pectin methylesterase from *Aspergillus niger* provide insights into the key determinants of processivity control. J Biol Chem 291(3), 1289-306.
- Kester HC, Kusters-van Someren MA, Müller Y and Visser J (1996): Primary structure and characterization of an exopolygalacturonase from *Aspergillus tubingensis*. Eur J Biochem 240(3), 738-46.
- Khachatryan V, Sirunyan AM, Tumasyan A, Adam W, Bergauer T, Dragicevic M, Erö J, Friedl M, Frühwirth R, Ghete VM, Hartl C, Hörmann N, Hrubec J, Jeitler M, *et al.* (2015): Search for decays of stopped long-lived particles produced in proton-proton collisions at Sqrt(s) = 8 TeV. Eur Phys J C Part Fields 75(4), 151.
- Khrunyk Y, Münch K, Schipper K, Lupas AN and Kahmann R (2010): The use of FLP-mediated recombination for the functional analysis of an effector gene family in the biotrophic smut fungus *Ustilago maydis*. New Phytol 187(4), 957-68.

x Bibliography

Klement T, Milker S, Jager G, Grande PM, Dominguez de Maria P and Büchs J (2012): Biomass pretreatment affects *Ustilago maydis* in producing itaconic acid. Microb Cell Fact 11, 43.

- Koepke J, Kaffarnik F, Haag C, Zarnack K, Luscombe NM, König J, Ule J, Kellner R, Begerow D and Feldbrügge M (2011): The RNA-binding protein Rrm4 is essential for efficient secretion of endochitinase Cts1. Mol Cell Proteomics 10(12), M111 011213.
- Krall SM and McFeeters RF (1998): Pectin hydrolysis: Effect of temperature, degree of methylation, pH, and calcium on hydrolysis rates. J Agric Food Chem 46(4), 1311-5.
- Kreyenschulte D, Heyman B, Eggert A, Maßmann T, Kalvelage C, Kossack R, Regestein L, Jupke A and Büchs J (2018): In situ reactive extraction of itaconic acid during fermentation of *Aspergillus terreus*. Biochem Eng J 135, 133-41.
- Kumar R, Singh S and Singh OV (2008): Bioconversion of lignocellulosic biomass: biochemical and molecular perspectives. J Ind Microbiol Biotechnol 35(5), 377-91.
- Laemmli UK (1970): Cleavage of structural proteins during the assembly of the head of bacteriophage T4. Nature 227(5259), 680-5.
- Lameiras F, Ras C, ten Pierick A, Heijnen JJ and van Gulik WM (2018): Stoichiometry and kinetics of single and mixed substrate uptake in *Aspergillus niger*. Bioprocess Biosyst Eng 41(2), 157-70.
- Lampugnani ER, Khan GA, Somssich M and Persson S (2018): Building a plant cell wall at a glance. J Cell Sci 131(2), jcs207373.
- Lara-Marquez A, Zavala-Paramo MG, Lopez-Romero E and Camacho HC (2011): Biotechnological potential of pectinolytic complexes of fungi. Biotechnol Lett 33(5), 859-68.

Bibliography xi

Levigne S, Ralet M-C and Thibault J-F (2002): Characterisation of pectins extracted from fresh sugar beet under different conditions using an experimental design. Carbohydr Polym 49(2), 145-53.

- Lombard V, Golaconda Ramulu H, Drula E, Coutinho PM and Henrissat B (2014): The carbohydrate-active enzymes database (CAZy) in 2013. Nucleic Acids Res 42(Database issue), D490-D5.
- Lopez-Siles M, Khan TM, Duncan SH, Harmsen HJM, Garcia-Gil LJ and Flint HJ (2012): Cultured representatives of two major phylogroups of human colonic *Faecalibacterium* prausnitzii can utilize pectin, uronic acids, and host-derived substrates for growth. Appl Environ Microbiol 78(2), 420-8.
- Loubradou G, Brachmann A, Feldbrügge M and Kahmann R (2001): A homologue of the transcriptional repressor Ssn6p antagonizes cAMP signalling in *Ustilago maydis*. Mol Microbiol 40(3), 719-30.
- Maassen N, Panakova M, Wierckx N, Geiser E, Zimmermann M, Bölker M, Klinner U and Blank LM (2014): Influence of carbon and nitrogen concentration on itaconic acid production by the smut fungus *Ustilago maydis*. Eng Life Sci 14(2), 129-34.
- Martens-Uzunova ES and Schaap PJ (2008): An evolutionary conserved d-galacturonic acid metabolic pathway operates across filamentous fungi capable of pectin degradation. Fungal Genet Biol 45(11), 1449-57.
- Martens-Uzunova ES and Schaap PJ (2009): Assessment of the pectin degrading enzyme network of *Aspergillus niger* by functional genomics. Fungal Genet Biol 46 Suppl 1, S170-S9.
- Martinez D, Berka RM, Henrissat B, Saloheimo M, Arvas M, Baker SE, Chapman J, Chertkov O, Coutinho PM, Cullen D, Danchin EG, Grigoriev IV, Harris P, Jackson M, *et al.* (2008): Genome sequencing and analysis of the biomass-degrading fungus *Trichoderma reesei* (syn. *Hypocrea jecorina*). Nat Biotechnol 26(5), 553-60.

xii Bibliography

May CD (1990): Industrial pectins: Sources, production and applications. Carbohydr Polym 12(1), 79-99.

- Micard V, Renard CMGC and Thibault JF (1996): Enzymatic saccharification of sugar-beet pulp. Enzyme Microb Technol 19(3), 162-70.
- Miller GL (1959): Use of dinitrosalicylic acid reagent for determination of reducing sugar. Anal Chem 31(3), 426-8.
- Mohnen D (2008): Pectin structure and biosynthesis. Curr Opin Plant Biol 11(3), 266-77.
- Moses V and Prevost C (1966): Catabolite repression of β-galactosidase synthesis in *Escherichia coli*. Biochem J 100(2), 336-53.
- Mueller O, Kahmann R, Aguilar G, Trejo-Aguilar B, Wu A and de Vries RP (2008): The secretome of the maize pathogen *Ustilago maydis*. Fungal Genet Biol 45 Suppl 1, S63-70.
- Mühlmann M, Kunze M, Ribeiro J, Geinitz B, Lehmann C, Schwaneberg U, Commandeur U and Büchs J (2017): Cellulolytic RoboLector towards an automated high-throughput screening platform for recombinant cellulase expression. J Biol Eng 11(1), 1.
- NCBI. (2019). "Standard Protein BLAST." Retrieved 2019/02/10, from https://blast.ncbi.nlm.nih.gov/Blast.cgi?PAGE=Proteins&PROGRAM=blastp&BLAST_P ROGRAMS=blastp&PAGETYPE=BlastSearch&DATABASE=refseq_protein&DESCRIPTIONS=100.
- Nielsen H (2017): Predicting secretory proteins with SignalP. Methods in molecular biology 1611, 59-73.
- Nishi HH and Elin RJ (1985): Three turbidimetric methods for determining total protein compared. Clinical chemistry 31(8), 1377-80.

Bibliography xiii

Nurizzo D, Turkenburg JP, Charnock SJ, Roberts SM, Dodson EJ, McKie VA, Taylor EJ, Gilbert HJ and Davies GJ (2002): *Cellvibrio japonicus* alpha-L-arabinanase 43A has a novel five-blade beta-propeller fold. Nat Struct Biol 9(9), 665-8.

- Oberoi HS, Vadlani PV, Madl RL, Saida L and Abeykoon JP (2010): Ethanol Production from Orange Peels: Two-Stage Hydrolysis and Fermentation Studies Using Optimized Parameters through Experimental Design. J Agric Food Chem 58(6), 3422-9.
- Olson DG, McBride JE, Joe Shaw A and Lynd LR (2012): Recent progress in consolidated bioprocessing. Curr Opin Biotechnol 23(3), 396-405.
- Ortiz GE, Ponce-Mora MC, Noseda DG, Cazabat G, Saravalli C, Lopez MC, Gil GP, Blasco M and Alberto EO (2017): Pectinase production by *Aspergillus giganteus* in solid-state fermentation: optimization, scale-up, biochemical characterization and its application in olive-oil extraction. J Ind Microbiol Biotechnol 44(2), 197-211.
- Papagianni M, Mattey M and Kristiansen B (1998): Citric acid production and morphology of *Aspergillus niger* as functions of the mixing intensity in a stirred tank and a tubular loop bioreactor. Biochem Eng J 2(3), 197-205.
- Paulino BN, Pessôa MG, Molina G, Kaupert Neto AA, Oliveira JVC, Mano MCR and Pastore GM (2017): Biotechnological production of value-added compounds by ustilaginomycetous yeasts. Appl Microbiol Biotechnol 101(21), 7789-809.
- Pedrolli DB, Monteiro AC, Gomes E and Carmona EC (2009): Pectin and pectinases: production, characterization and industrial application of microbial pectinolytic enzymes. Open Biotechnol J 3, 9-18.
- Philip P, Kern D, Goldmanns J, Seiler F, Schulte A, Habicher T and Büchs J (2018): Parallel substrate supply and pH stabilization for optimal screening of *E. coli* with the membrane-based fed-batch shake flask. Microb Cell Fact 17, 69.

xiv Bibliography

Rafiq S, Kaul R, Sofi SA, Bashir N, Nazir F and Ahmad Nayik G (2016): Citrus peel as a source of functional ingredient: A review. J Saudi Soc Agric Sci 02(05), 794-800.

- Reindl M, Hänsch S, Weidtkamp-Peters S and Schipper K (2019): A potential lock-type mechanism for unconventional secretion in fungi. Int J Mol Sci 20(3), 460.
- Rinaldi R, Engel P, Büchs J, Spiess AC and Schuth F (2010): An integrated catalytic approach to fermentable sugars from cellulose. ChemSusChem 3(10), 1151-3.
- Rivas B, Torrado A, Torre P, Converti A and Dominguez JM (2008): Submerged citric acid fermentation on orange peel autohydrolysate. J Agric Food Chem 56(7), 2380-7.
- Robert X and Gouet P (2014): Deciphering key features in protein structures with the new ENDscript server. Nucleic Acids Res 42(Web Server issue), W320-4.
- Rodrigues AC, Haven MØ, Lindedam J, Felby C and Gama M (2015): Celluclast and Cellic® CTec2: Saccharification/fermentation of wheat straw, solid–liquid partition and potential of enzyme recycling by alkaline washing. Enzyme Microb Technol 79-80, 70-7.
- Rombouts FM and Thibault J-F (1986): Feruloylated pectic substances from sugar-beet pulp. Carbohydr Res 154(1), 177-87.
- Ronne H (1995): Glucose repression in fungi. TIG 11(1), 12-7.
- Rorick R, Nahar N and Pryor SW (2011): Ethanol production from sugar beet pulp using *Escherichia coli* KO11 and *Saccharomyces cerevisiae*. Biol Eng Trans 3(4), 199-209.
- Salmerón-Santiago KG, Pardo JP, Flores-Herrera O, Mendoza-Hernández G, Miranda-Arango M and Guerra-Sánchez G (2011): Response to osmotic stress and temperature of the fungus *Ustilago maydis*. Arch Microbiol 193(10), 701.
- Sarkari P, Reindl M, Stock J, Müller O, Kahmann R, Feldbrügge M and Schipper K (2014): Improved expression of single-chain antibodies in *Ustilago maydis*. J Biotechnol 191, 165-75.

Bibliography xv

Schipper K and Doehlemann G (2012). Compatibility in biotrophic plant–fungal interactions: *Ustilago maydis* and friends. Signaling and Communication in Plant Symbiosis. Perotto, S and Baluška, F. Berlin, Heidelberg, Springer Berlin Heidelberg. 213-38.

- Schuler D, Höll C, Grün N, Ulrich J, Dillner B, Klebl F, Ammon A, Voll LM and Kämper J (2018): Galactose metabolism and toxicity in *Ustilago maydis*. Fungal Genet Biol 114, 42-52.
- Schuster M, Schweizer G, Reissmann S and Kahmann R (2016): Genome editing in *Ustilago maydis* using the CRISPR-Cas system. Fungal Genet Biol 89, 3-9.
- Senechal F, Wattier C, Rusterucci C and Pelloux J (2014): Homogalacturonan-modifying enzymes: structure, expression, and roles in plants. J Exp Bot 65(18), 5125-60.
- Sievers F, Wilm A, Dineen D, Gibson TJ, Karplus K, Li W, Lopez R, McWilliam H, Remmert M, Soding J, Thompson JD and Higgins DG (2011): Fast, scalable generation of high-quality protein multiple sequence alignments using Clustal Omega. Mol Syst Biol 7, 539.
- Siguier B, Haon M, Nahoum V, Marcellin M, Burlet-Schiltz O, Coutinho PM, Henrissat B, Mourey L, O'Donohue MJ, Berrin JG, Tranier S and Dumon C (2014): First structural insights into alpha-L-arabinofuranosidases from the two GH62 glycoside hydrolase subfamilies. J Biol Chem 289(8), 5261-73.
- Singh N, Mathur AS, Tuli DK, Gupta RP, Barrow CJ and Puri M (2017): Cellulosic ethanol production via consolidated bioprocessing by a novel thermophilic anaerobic bacterium isolated from a Himalayan hot spring. Biotechnol Biofuels 10(1), 73.
- Spiro MD, Kates KA, Koller AL, O'Neill MA, Albersheim P and Darvill AG (1993): Purification and characterization of biologically active 1,4-linked α-d-oligogalacturonides after partial digestion of polygalacturonic acid with endopolygalacturonase. Carbohydr Res 247, 9-20.

xvi Bibliography

Stock J, Sarkari P, Kreibich S, Brefort T, Feldbrügge M and Schipper K (2012): Applying unconventional secretion of the endochitinase Cts1 to export heterologous proteins in *Ustilago maydis*. J Biotechnol 161(2), 80-91.

- Stock J, Terfrüchte M and Schipper K (2016). A reporter system to study unconventional secretion of proteins avoiding N-glycosylation in *Ustilago maydis*. Unconventional Protein Secretion: Methods and Protocols. Pompa, A and De Marchis, F. New York, NY, Springer New York. 149-60.
- Terfrüchte M, Joehnk B, Fajardo-Somera R, Braus GH, Riquelme M, Schipper K and Feldbrügge M (2014): Establishing a versatile Golden Gate cloning system for genetic engineering in fungi. Fungal Genet Biol 62, 1-10.
- Terfrüchte M, Reindl M, Jankowski S, Sarkari P, Feldbrügge M and Schipper K (2017): Applying unconventional secretion in *Ustilago maydis* for the export of functional nanobodies. Int J Mol Sci 18(5).
- Terfrüchte M, Wewetzer S, Sarkari P, Stollewerk D, Franz-Wachtel M, Macek B, Schlepütz T, Feldbrügge M, Büchs J and Schipper K (2018): Tackling destructive proteolysis of unconventionally secreted heterologous proteins in *Ustilago maydis*. J Biotechnol 284, 37-51.
- Teugjas H and Väljamäe P (2013): Product inhibition of cellulases studied with 14C-labeled cellulose substrates. Biotechnol Biofuels 6(1), 104.
- Trindade LV, Desagiacomo C, de Moraes Polizeli MdLT, de Lima Damasio AR, Lima AMF, Gomes E and Bonilla-Rodriguez GO (2016): Biochemical characterization, thermal stability, and partial sequence of a novel exo-polygalacturonase from the thermophilic fungus *Rhizomucor pusillus* A13.36 obtained by submerged cultivation. Biomed Res Int 2016, 10.
- Valverde ME, Paredes-López O, Pataky JK, Guevara-Lara F and Pineda TS (1995): Huitlacoche (*Ustilago maydis*) as a food source biology, composition, and production. Crit Rev Food Sci Nutr 35(3), 191-229.

Bibliography xvii

van Maris AJA, Abbott DA, Bellissimi E, van den Brink J, Kuyper M, Luttik MAH, Wisselink HW, Scheffers WA, van Dijken JP and Pronk JT (2006): Alcoholic fermentation of carbon sources in biomass hydrolysates by *Saccharomyces cerevisiae*: current status. Antonie Leeuwenhoek 90(4), 391-418.

- Verduyn C, Postma E, Scheffers WA and Van Dijken JP (1992): Effect of benzoic acid on metabolic fluxes in yeasts: a continuous-culture study on the regulation of respiration and alcoholic fermentation. Yeast 8(7), 501-17.
- Voll A, Klement T, Gerhards G, Büchs J and Marquardt W (2012): Metabolic modelling of itaconic acid fermentation with *Ustilago maydis*. Chem Eng Trans 27, 367-72.
- Vollmeister E, Schipper K, Baumann S, Haag C, Pohlmann T, Stock J and Feldbrugge M (2012): Fungal development of the plant pathogen *Ustilago maydis*. FEMS Microbiol Rev 36(1), 59-77.
- Widmer W, Zhou W and Grohmann K (2010): Pretreatment effects on orange processing waste for making ethanol by simultaneous saccharification and fermentation. Bioresour Technol 101(14), 5242-9.
- Willats WGT, Knox JP and Mikkelsen JD (2006): Pectin: new insights into an old polymer are starting to gel. Trends Food Sci Technol 17(3), 97-104.
- Xu SX, Qin X, Liu B, Zhang DQ, Zhang W, Wu K and Zhang YH (2015): An acidic pectin lyase from *Aspergillus niger* with favourable efficiency in fruit juice clarification. Lett Appl Microbiol 60(2), 181-7.
- Yadav S, Yadav PK, Yadav D and Yadav KDS (2009): Pectin lyase: A review. Process Biochem 44(1), 1-10.
- Yuan P, Meng K, Wang Y, Luo H, Shi P, Huang H, Bai Y, Yang P and Yao B (2012): A protease-resistant exo-polygalacturonase from *Klebsiella sp.* Y1 with good activity and stability over a wide pH range in the digestive tract. Bioresour Technol 123, 171-6.

xviii Bibliography

Zaleska H, Ring SG and Tomasik P (2000): Apple pectin complexes with whey protein isolate. Food Hydrocoll 14(4), 377-82.

- Zambanini T, Hartmann SK, Schmitz LM, Büttner L, Hosseinpour Tehrani H, Geiser E, Beudels M, Venc D, Wandrey G, Büchs J, Schwarzländer M, Blank LM and Wierckx N (2017): Promoters from the itaconate cluster of *Ustilago maydis* are induced by nitrogen depletion. Fungal Biol Biotechnol 4(1), 11.
- Zarnack K, Maurer S, Kaffarnik F, Ladendorf O, Brachmann A, Kämper J and Feldbrügge M (2006): Tetracycline-regulated gene expression in the pathogen *Ustilago maydis*. Fungal Genet Biol 43(11), 727-38.
- Zhang J, Zhang G, Wang W, Wang W and Wei D (2018): Enhanced cellulase production in *Trichoderma reesei* RUT C30 via constitution of minimal transcriptional activators. Microb Cell Fact 17(1), 75.
- Zhang Z, Dong J, Zhang D, Wang J, Qin X, Liu B, Xu X, Zhang W and Zhang Y (2018): Expression and characterization of a pectin methylesterase from *Aspergillus niger* ZJ5 and its application in fruit processing. J Biosci Bioeng 126(6), 690-6.
- Zhou L, Obhof T, Schneider K, Feldbrügge M, Nienhaus GU and Kämper J (2018): Cytoplasmic transport machinery of the SPF27 homologue Num1 in *Ustilago maydis*. Sci Rep 8(1), 3611.

Appendix xix

Appendix

Appendices for Chapter 2

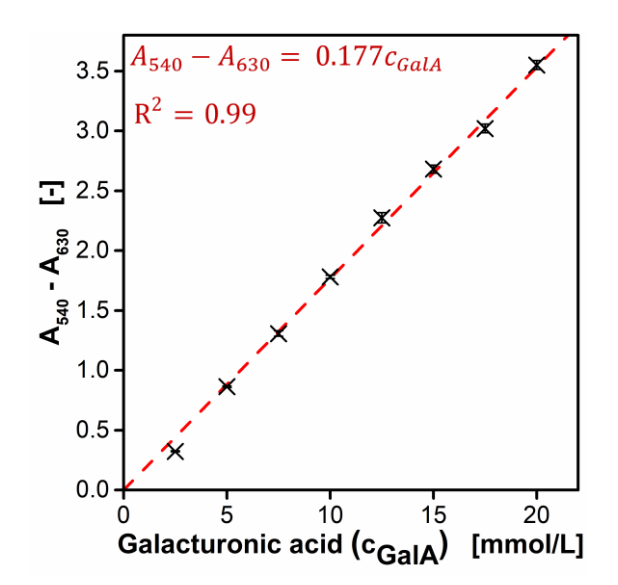


Figure A1: Exemplary calibration curve for offline DNS assay on reducing groups. Samples of 2.5 to 20 mM GalA were incubated with DNS reagent as described in Chapter 2.2.4.6. Absorption at 540 and 630 nm was measured in triplicates in a microtiter plate using a plate reader. Error bars represent standard deviation of technical triplicates. The calibration factor and coefficient of determination are specified in the plot.

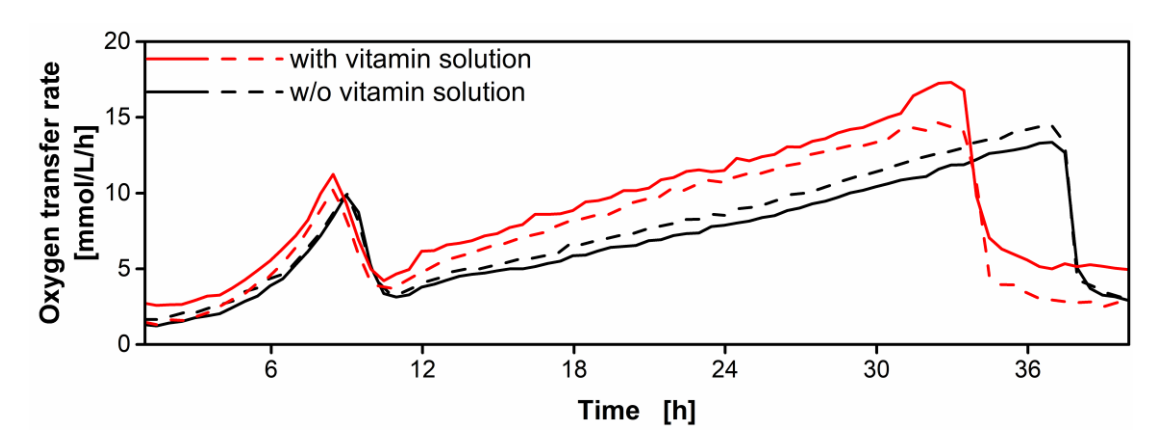


Figure A2: Comparison of U. maydis AB33P5 Δ R cultivation in modified Verduyn medium with and without vitamin supplementation. The strain was grown on glucose (4 g/L) and GalA (20 g/L) as carbon sources. Biological duplicates of OTR, represented each as line and dashed line. Culture conditions: modified Verduyn medium, 0.1 M MOPS, pH 6.5, 250 mL flask, filling volume 20 mL, shaking frequency 300 rpm, shaking diameter 50 mm, initial OD₆₀₀ = 0.2, T = 30 °C.

xx Appendix

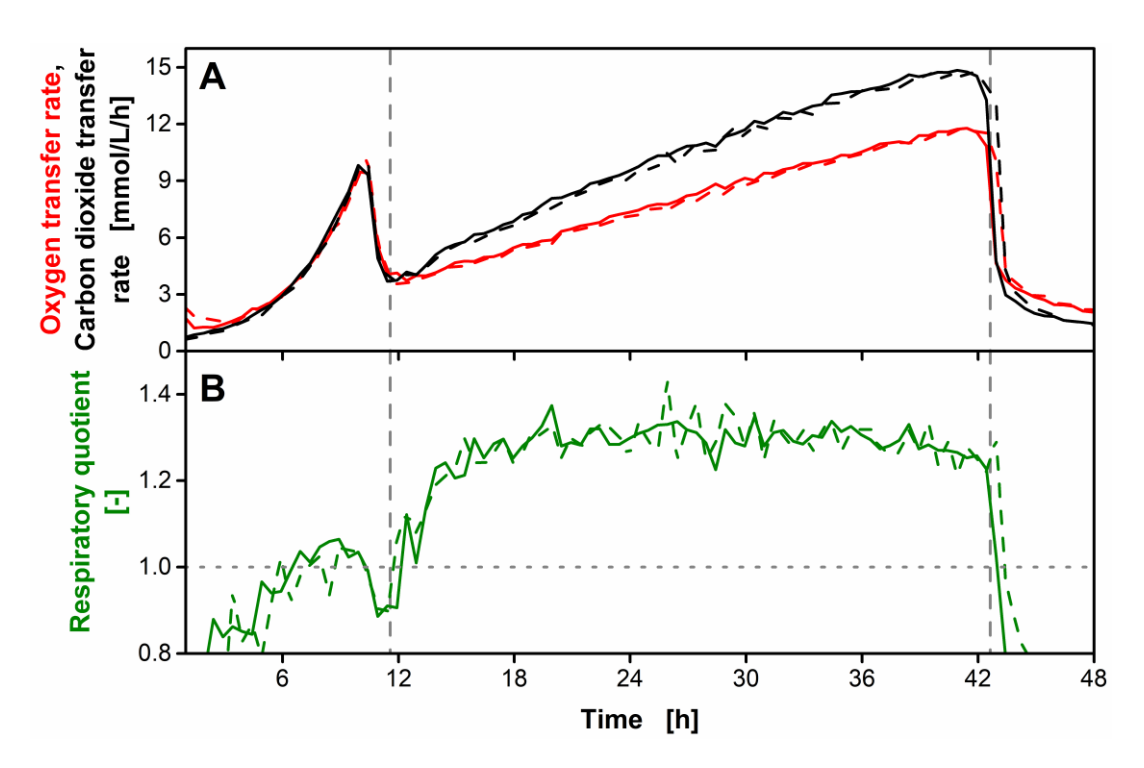


Figure A3: RQ during the cultivation of *U. maydis* AB33P5ΔR on GalA (same cultivation as shown in Figure 2-1). The strain was grown on glucose (4 g/L) and GalA (20 g/L) as carbon sources. Vertical dashed lines indicate depletion times for glucose (11.5 h) and GalA (43 h). A Biological duplicates of OTR and CTR, represented each as line and dashed line. B Biological duplicates of the RQ, represented each as line and dashed line. Horizontal dotted line represents RQ = 1. Culture conditions: modified Verduyn medium, 0.2 M MOPS, pH 6.5, 250 mL flask, filling volume 20 mL, shaking frequency 300 rpm, shaking diameter 50 mm, initial OD₆₀₀ = 0.2, T = 30 °C.

Appendix xxi

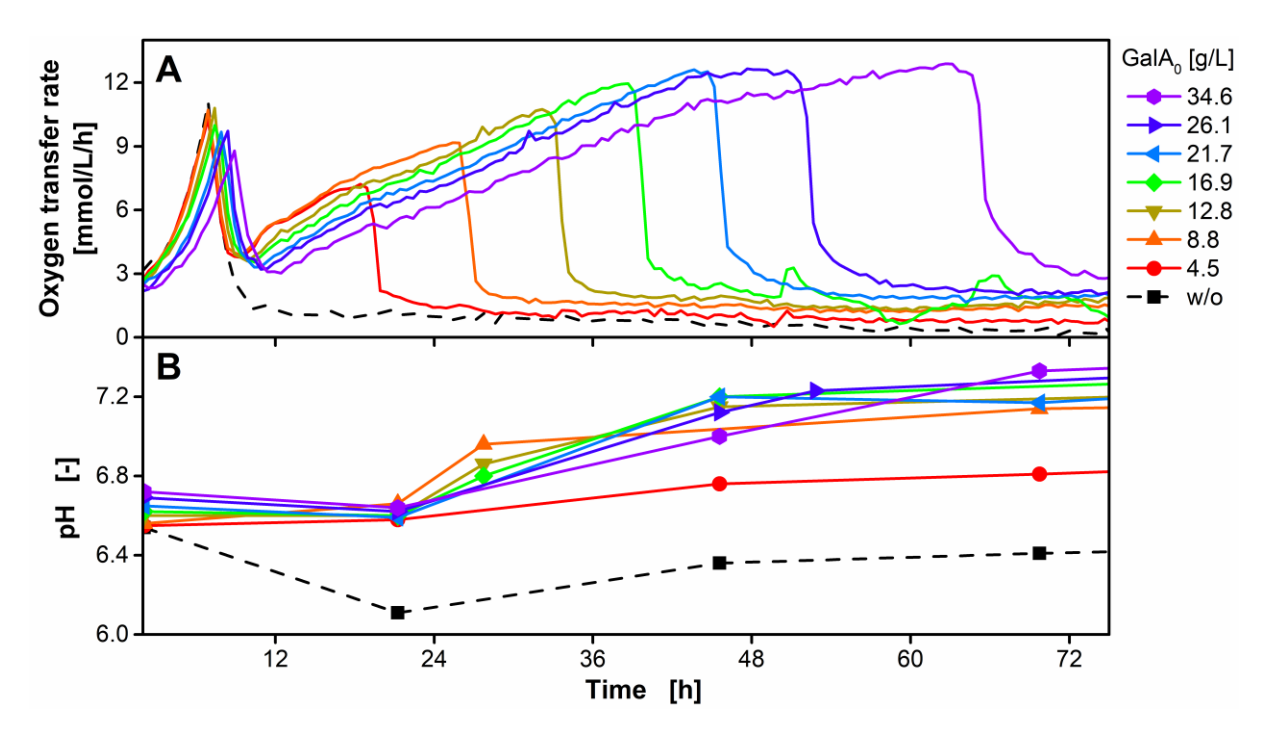


Figure A4: Development of the pH value during the cultivation of U. maydis AB33P5ΔR/AtPgaX on GalA (same cultivation as shown in Figure 2-2). The medium was supplemented with glucose (4 g/L) and varying amounts of GalA (GalA₀) and buffer. 0, 4.5, 8.8, 12.8, 16.9, 21.7, 26.1 and 34.6 g/L GalA medium was supplemented with 0.1, 0.1, 0.1, 0.15, 0.2, 0.25, 0.3 and 0.4 M MOPS respectively. A OTR. B pH value determined from shake flasks cultured in parallel. Culture conditions: modified Verduyn medium, initial pH 6.5, 250 mL flask, filling volume 20 mL, shaking frequency 300 rpm, shaking diameter 50 mm, initial OD₆₀₀ = 0.65, T = 30 °C.

xxii Appendix

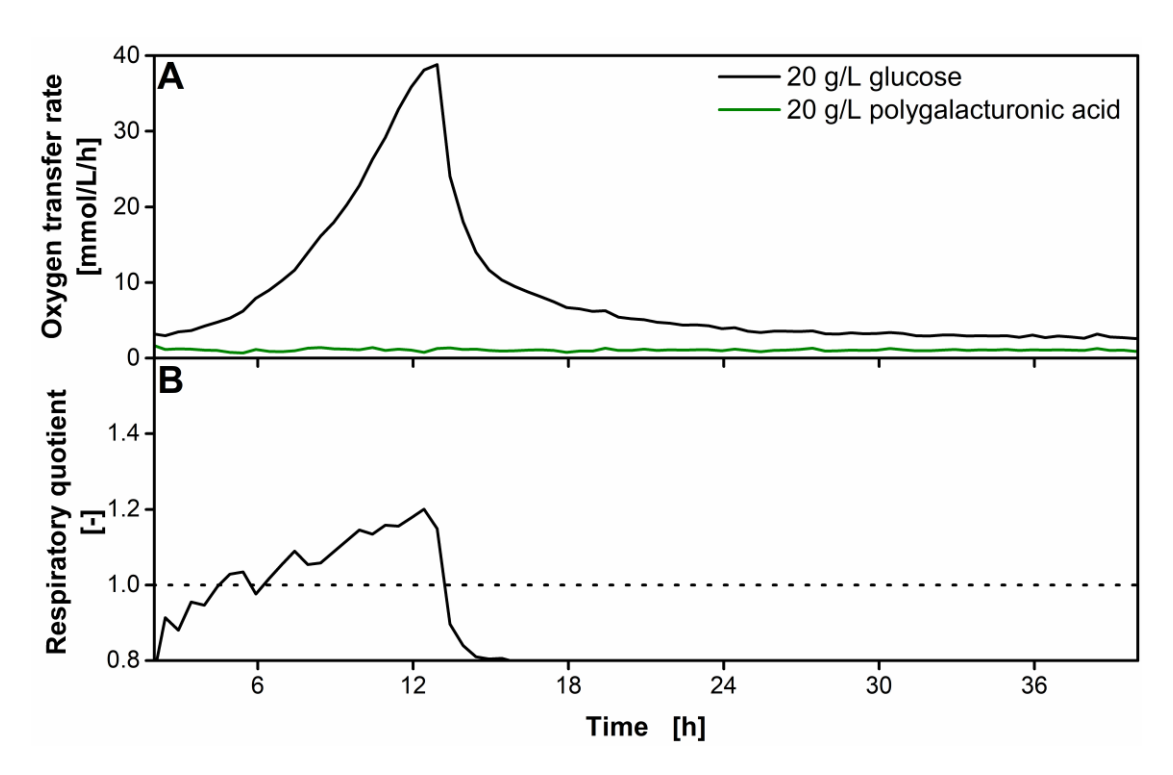


Figure A5: Control cultivation of *U. maydis* **AB33P5**Δ**R**/**AtPgaX on glucose and PolyGalA.** The strain was grown on 20 g/L glucose or 20 g/L PolyGalA as single carbon source. **A** OTR. **B** RQ. The dotted horizontal line represents RQ = 1. For clarity reasons, the RQ is only shown for OTR > 2 mmol/L/h. Culture conditions: modified Verduyn medium, 0.1 M MOPS and 0.1 M MES, initial pH 6.0, 250 mL flask, filling volume 15 mL, shaking frequency 300 rpm, shaking diameter 50 mm, initial OD₆₀₀ = 0.6, temperature 30 °C.

Appendix xxiii

Appendices for Chapter 3

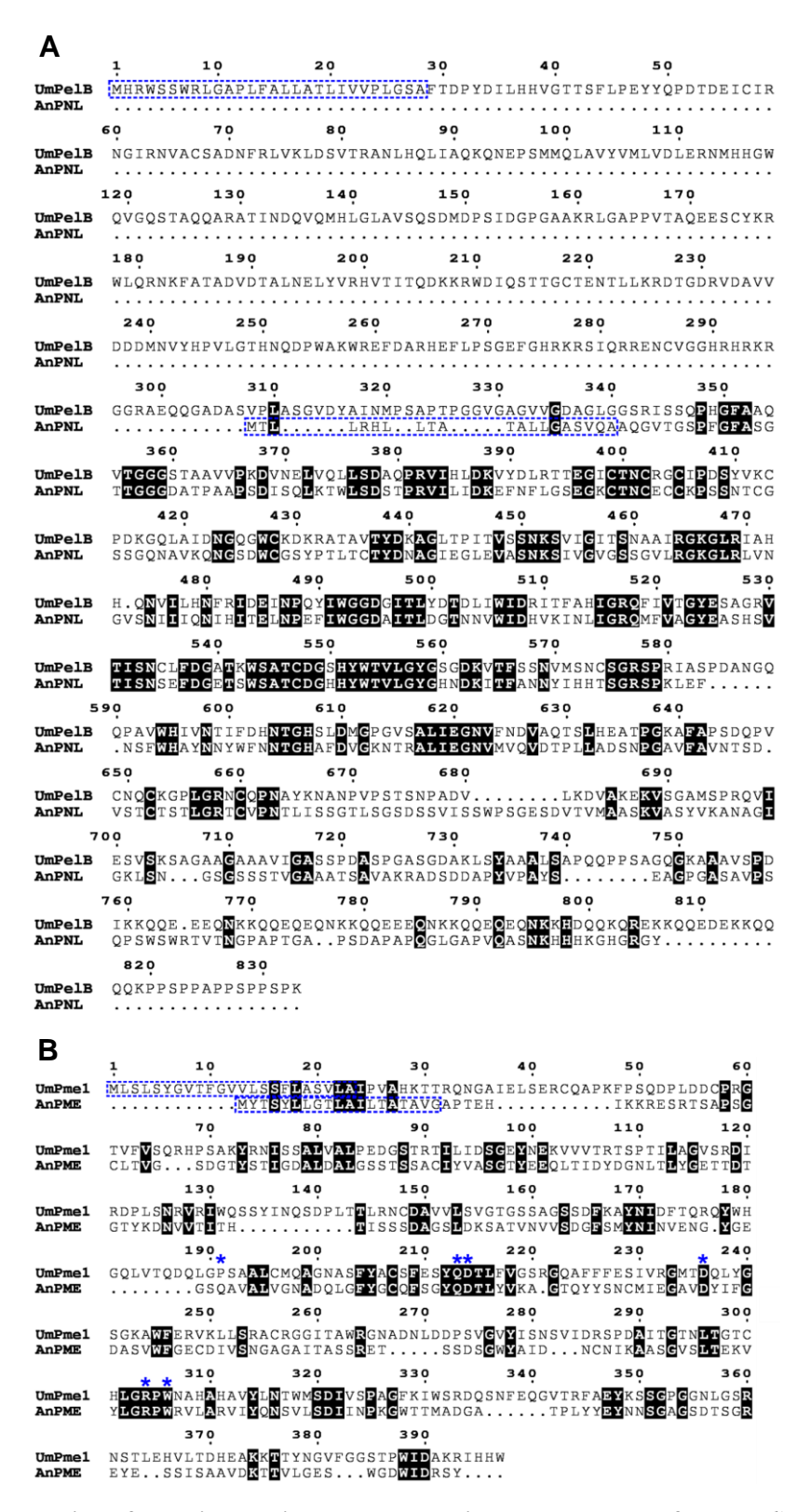


Figure A6: Conservation of putative pectin lyase and pectin methylesterase of *U. maydis*. A Amino acid alignment showing the homology between the well-characterized acidic pectin lyase PNL-ZJ5A (AnPNL;

xxiv Appendix

accession number <u>KM588308.1</u>) from *A. niger* and UmPelB (UMAG_04708; accession number <u>KIS66646.1</u>). Identical amino acids are depicted with a black background. The *U. maydis* protein carries a large N-terminal elongation of about 350 amino acids which is not present in the characterized homolog. **B** Amino acid alignment showing the homology between the well-characterized acidic pectin methyl esterase PME-ZJ5A (AnPME; accession number <u>MG397069.1</u>) from *A. niger* and UmPmel (UMAG_12233; accession number <u>KIS68427.1</u>). Identical amino acids are depicted with a black background. Asterisks depict active residues of AnPME which are largely conserved in UmPmel [Kent, *et al.* 2016]. The predicted N-terminal signal peptides are indicated by the blue dashed boxes.

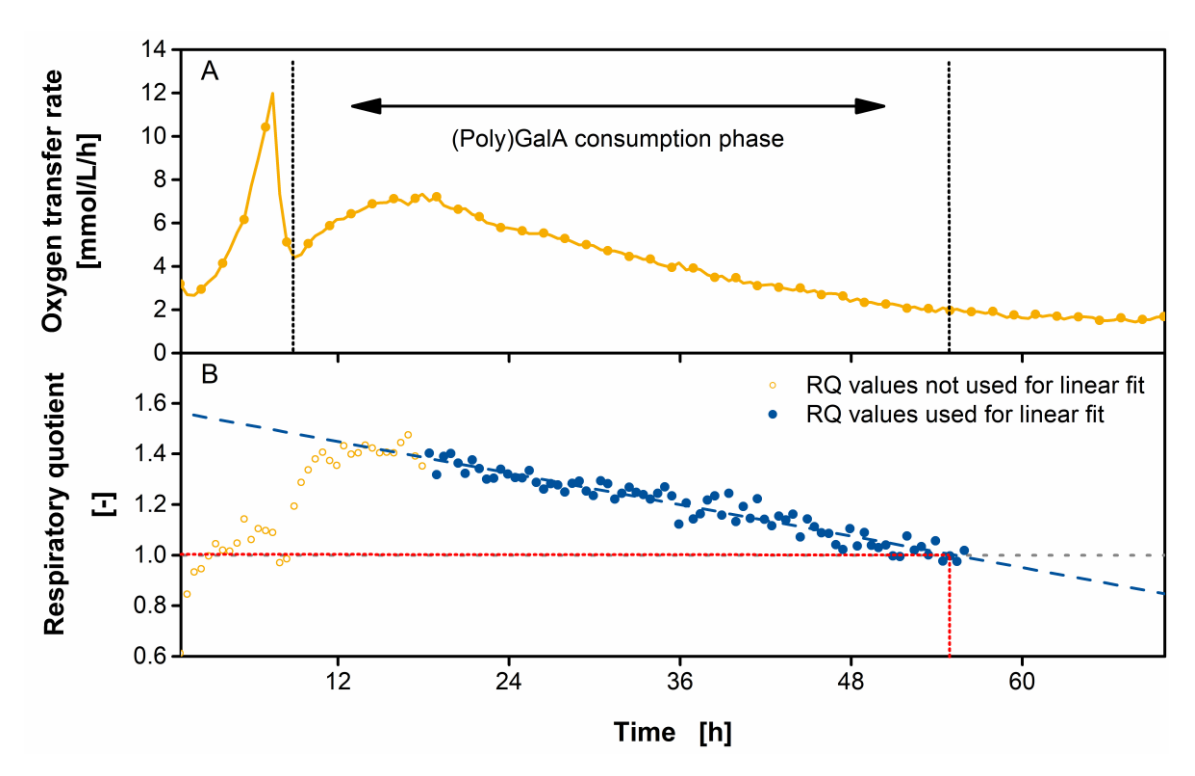


Figure A7: Exemplary definition of (Poly)GalA consumption phase during co-fermentation of *U. maydis* on PolyGalA. Strains AB33P5ΔR/AtPgaX (expressing fungal exo-polygalacturonase) and AB33P5ΔR/UmPgu1 (expressing intrinsic endo-polygalacturonase) were grown on glucose (4 g/L) and PolyGalA (20 g/L, purity 85%) as carbon sources. A OTR. Vertical, dashed lines represent the (Poly)GalA consumption phase. For clarity reasons, only every third data point of the mean of biological duplicates is shown. B RQ. For clarity reasons, every data point of the mean of biological duplicates is shown. Starting with decreasing OTR values, RQ values were linearly fitted (blue dots). End of the (Poly)GalA consumption phase was defined as the time point, where the linear fit of the RQ reaches a value of 1.0 (here after 36 h of cultivation time). Culture conditions: modified Verduyn mineral medium, 0.2 M MOPS, initial pH 6.0, 250 mL flask, filling volume 20 mL, shaking frequency 300 rpm, shaking diameter 50 mm, initial OD₆₀₀ = 0.6 (inoculation ratio 1:1), T = 30 °C.

Appendix xxv

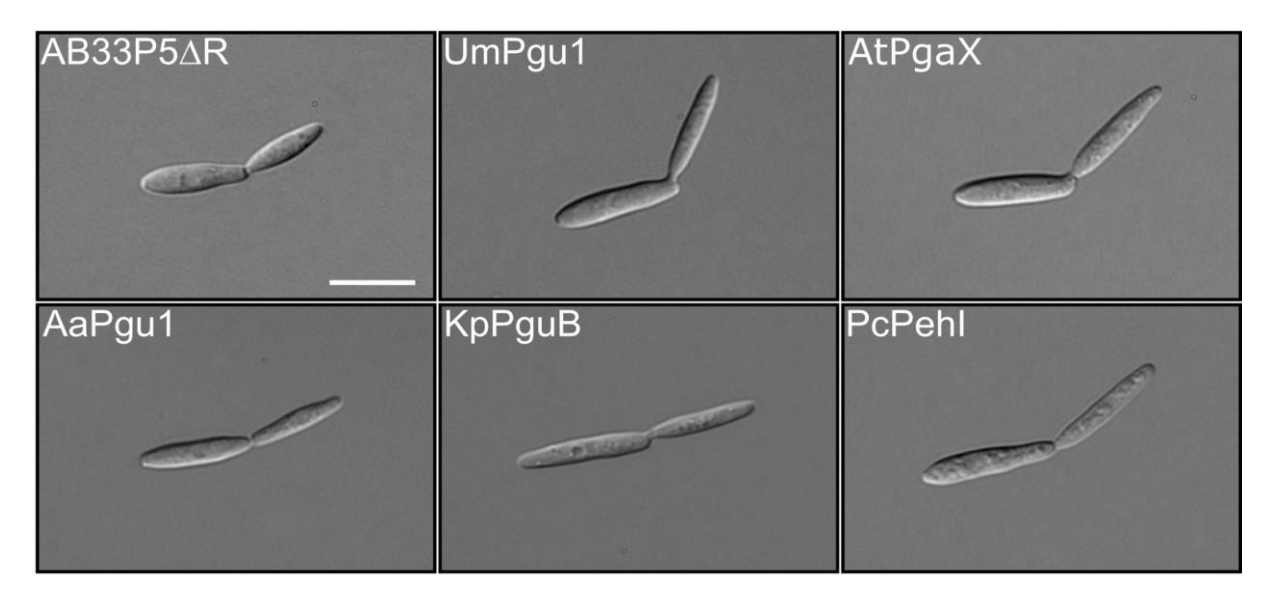


Figure A8: The morphology of strains overexpressing pectinases is not disturbed. Micrographs show representative yeast-like growing cells of indicated AB33P5 Δ R derivatives in the final stage of budding. Size bar, 20 μ m.

xxvi Appendix

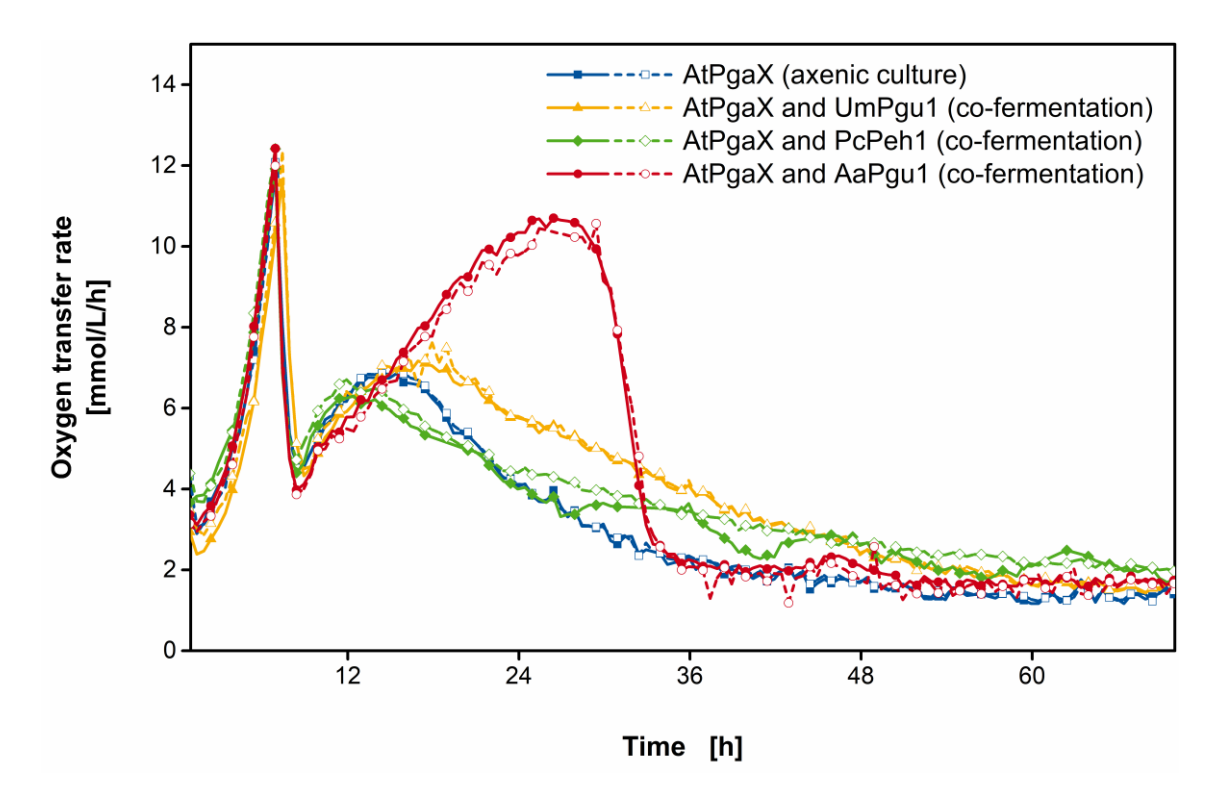


Figure A9: Biological duplicates of axenic culture and co-fermentations on PolyGalA. The strains expressing AtPgaX (fungal exo-polygalacturonase), UmPgu1 (intrinsic endo-polygalacturonase), PcPeh1 (bacterial endo-polygalacturonase) and AaPgu1(fungal endo-polygalacturonase) were grown on a mixture of glucose (4 g/L) and PolyGalA (20 g/L, purity 85%) as carbon sources. OTR over time of biological duplicates, represented each as line and dashed line. Culture conditions: modified Verduyn mineral medium, 0.2 M MOPS, initial pH 6.0, 250 mL flask, filling volume 20 mL, shaking frequency 300 rpm, shaking diameter 50 mm, initial OD600 = 0.6 (inoculation ratio 1:1 for co-fermentations), T = 30 °C.

Table A1: Validation of complete glucose consumption. The glucose concentrations were determined by DNS assays in culture supernatants used for polygalacturonase assays after 24 h incubation in modified Verduyn medium with 1 g/L initial glucose (Glc) supplementation (compare to 2.7). A negative control lacking glucose supplementation (w/o Glc) was analysed in parallel.

Sample	Reducing groups [mM]	Standard deviation [mM]
Culture supernatant AB33P5∆R	0.592	0.039
Culture supernatant AB33P5∆R/UmPgu1	0.561	0.029
Culture supernatant AB33P5∆R/AtPgaX	0.585	0.047
Verduyn w/o Glc	0.555	0.017
Verduyn (with 10 g/L Glc)	68.172	0.012

Appendix xxvii

Table A2: Intrinsic repertoire for pectin degradation.

Gene ID¹	Protein ²	Predicted function / prediced major substrate (potential CaZy family)	Characterized homolog (% identity)	Signal peptide prediction (SignalP4.	Remarks
umag_02510; accession number KIS69158.1	Pgu1	endo- polygalacturonase/H G (GH28/PL6)	Fusarium moniliforme Pga [Federici, et al. 2001]; accession number Q07181.1 (overall identity 46%/identity w/o N- terminal signal peptide 45%) (Fig. 2)	present	
umag_04708; accession number KIS66646.1	Pel1	related to pectin lyase B precursor/HG (PL6)	A. niger acidic pectin lyase PNL-ZJ5A (overall identity 22%; 40.2% identity in 387 amino acid C-terminal overlap) (Fig. S2) [Xu, et al. 2015]; accession number KM588308.1	present	Pectin or pectate lyase possible; contains elongated N- terminus (about 340 aa) compared to Ascomycete homologs, potential misannotation
umag_12233; accession number KIS68427.1	Pme1	Putative pectinesterase/pectin methylesterase/HG (CE8)	pectin methylesterase PME- ZJ5A from <i>A. niger</i> (overall identity 24%; 28% identity in 397 amino acid overlap) (Fig. S2) [Kent, <i>et al.</i> 2016, <i>Z Zhang, et al.</i> 2018]; accession number MG397069.1	present	Active site residues largely conserved [Kent, et al. 2016]

xxviii Appendix

Gene ID ¹	Protein ²	Predicted function / prediced major substrate (potential CaZy family)	Characterized homolog (% identity)	Signal peptide prediction (SignalP4.	Remarks
umag_01829; accession number KIS70669.1	Afu1	α-L- arabinofuranosidase/ RGI and II, XG (GH51)	Pleurotus ostreatus PoAbf (overall identity 28%/identity w/o N-terminal signal peptide 27%) [Amore, et al. 2012]; accession number CCC33068.1	present	
umag_00837; accession number KIS70909.1	Afu2	α-L- arabinofuranosidase/ RGI and II, XG (GH51)	Pleurotus ostreatus PoAbf (overall identity 32%/identity w/o N-terminal signal peptide 32%) [Amore, et al. 2012]; accession number CCC33068.1	present	
umag_04309; accession number KIS67202.1	Afu3 [formerly published as UmAbf62 A]	α-L- arabinofuranosidase/ RGI and II, XG (GH62_2)	N/A ⁴	present	Activity confirmed and characterized by Siguier et al., 2014 [Siguier, et al. 2014]
umag_03416; accession number KIS68317.1	Afu4	α-1,5-arabinanase/ RGI and II (GH43)	Cellvibrio japonicus Arb43A (overall identity 17%/identity w/o N-terminal signal peptide 18%) [Nurizzo, et al. 2002]; accession number WP_012486466	present	

Appendix xxix

Gene ID ¹	Protein ²	Predicted function / prediced major substrate (potential CaZy family)	Characterized homolog (% identity)	Signal peptide prediction (SignalP4. 1) ³	Remarks
umag_01427; accession number KIS71533.1	Afu5	α-1,5-arabinanase/ RGI and II (GH43)	Cellvibrio japonicus Arb43A (overall identity 18%/identity w/o N-terminal signal peptide 17%) [Nurizzo, et al. 2002]; accession number WP_012486466	present	
umag_02356; accession number KIS69834.1	LacZ	ß-galactosidase/RGI, XG (GH42)	N/A	present	
umag_02204; accession number KIS69673.1	LacZ	ß-galactosidase/RGI, XG (GH42)	N/A	present	

Appendix xxxi

Appendices for Chapter 4

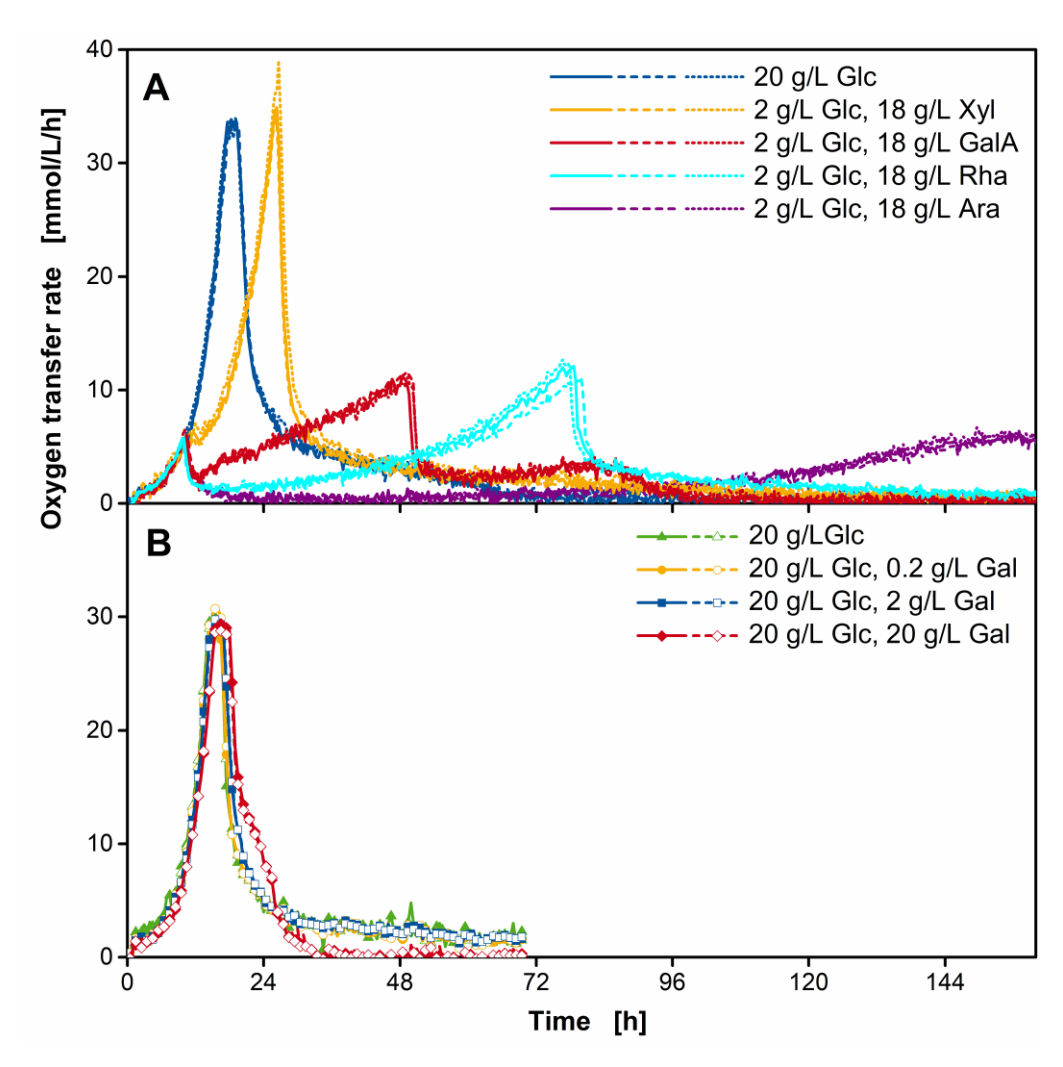


Figure A 10: Axenic cultivation of *U. maydis* AB33P5 Δ on different pectic sugars. A Cultivation in the μRAMOS device. A mixture of glucose (2 g/L) and 18 g/L of either xylose (yellow curves), GalA (red curves), rhamnose (turquoise curves) or arabinose (purple curves) was used as carbon source. A reference cultivation was grown on 20 g/L glucose (blue curves). OTR of biological triplicates, represented each as continuous, dotted and dashed line. Culture conditions: modified Verduyn medium, 0.1 M MES (replaced by MOPS buffer for GalA cultivations), pH 6.5, 48-well MTP (deep-well round), filling volume 0.8 mL, shaking frequency 1000 rpm, shaking diameter 3 mm, initial OD₆₀₀ = 0.1, temperature 30 °C. **B** Cultivation in the RAMOS device. A mixture of glucose (20 g/L) and varying amounts of galactose (0 to 20 g/L) was used as carbon source. OTR of biological duplicates. Culture conditions: modified Verduyn medium, 0.1 M MES, pH 6.5, 250 mL flask, filling volume 20 mL, shaking frequency 300 rpm, shaking diameter 50 mm, initial OD₆₀₀ = 0.1, temperature 30 °C

xxxii Appendix

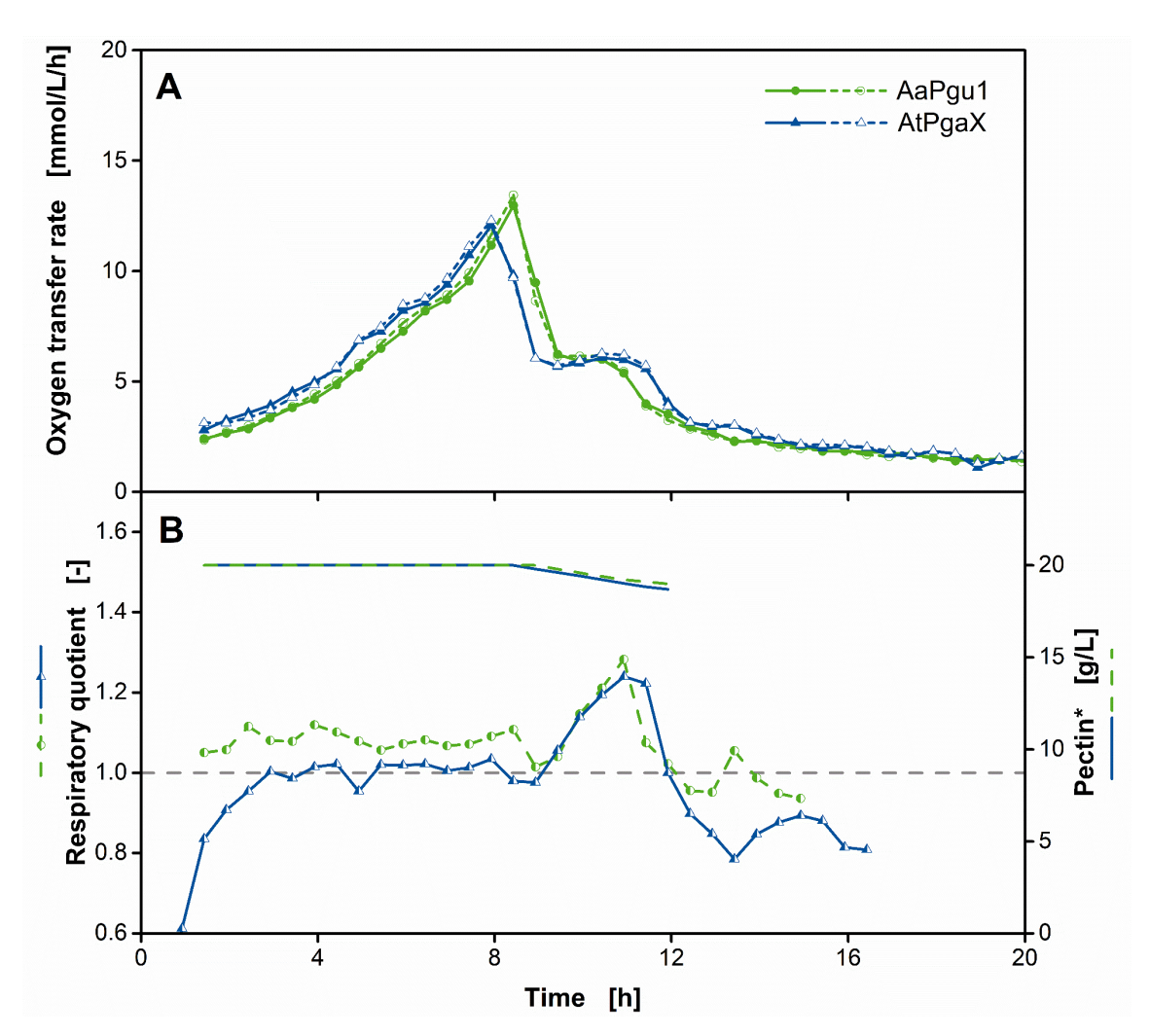


Figure A 11: Axenic cultivation of *U. maydis* AB33P5 Δ R/AaPgu1 and AB33P5 Δ R/AtPgaX on pectin SP-he. Strains AB33P5 Δ R/AaPgu1 (endo-polygalacturonase, green curves) and AB33P5 Δ R/AtPgaX (exopolygalacturonase, blue curves) were grown on a mixture of glucose (4 g/L) and SP-he (20 g/L) as carbon sources. A OTR of biological duplicates, represented each as line and dashed line. **B** Mean of biological duplicates of RQ (curves with symbols). For clarity reasons, the RQ is only shown for OTR > 2 mmol/L/h. Curves without symbols show the mean of biological duplicates of residual SP-he, calculated from the overall consumed oxygen as described in Chapter 3.2.9. End of SP-he consumption was defined by the RQ drop below 1. Culture conditions: modified Verduyn medium, 0.2 M MOPS, pH 6.0, 250 mL flask, filling volume 20 mL, shaking frequency 300 rpm, shaking diameter 50 mm, initial OD₆₀₀ = 0.6, temperature 30 °C

Appendix xxxiii

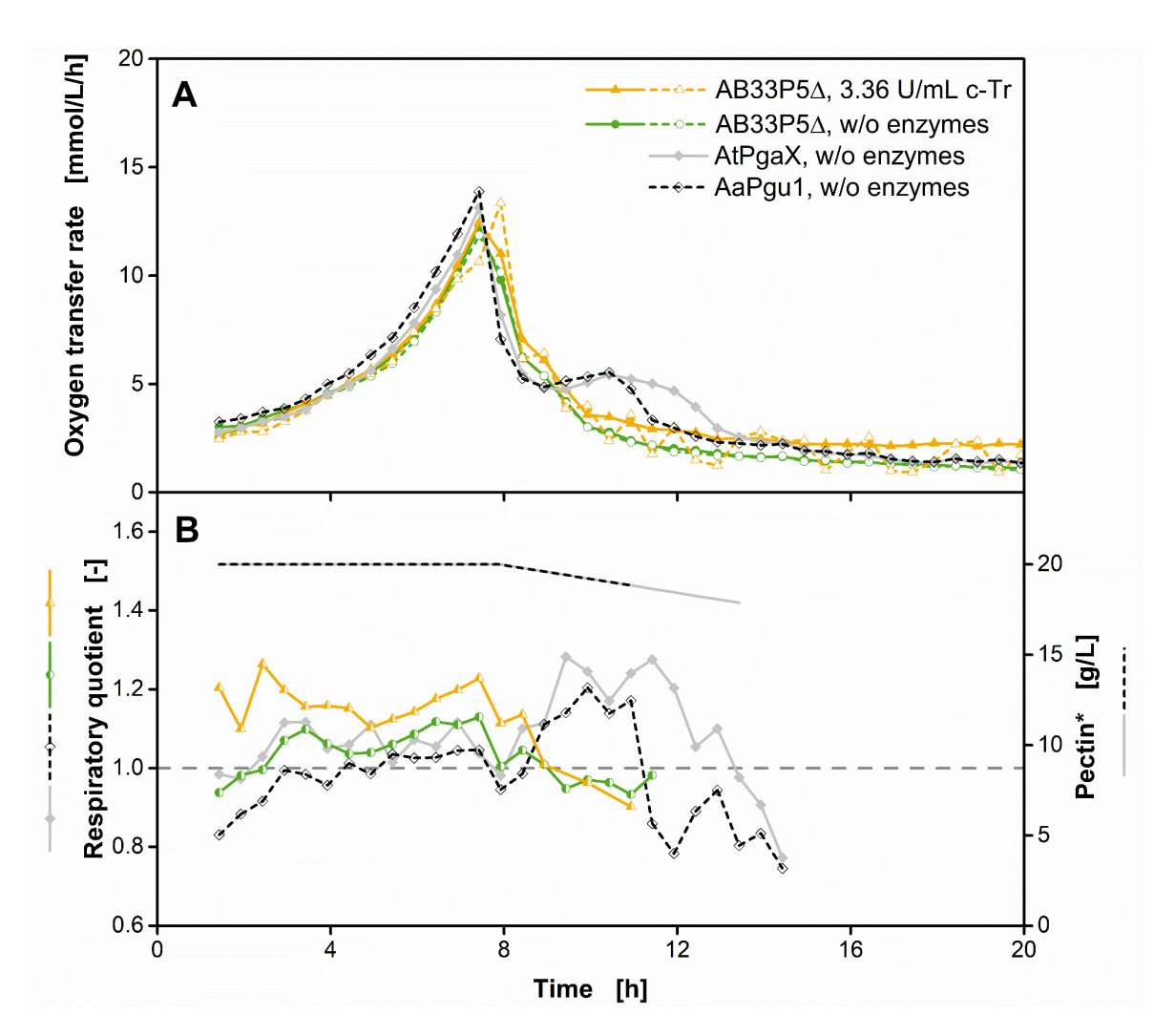


Figure A 12: Axenic cultivation of *U. maydis* **on pectin AP-he.** The strains AB33P5ΔR (green curves), AB33P5ΔR/AaPgu1 (endo-polygalacturonase, black curve) and AB33P5ΔR/AtPgaX (exo-polygalacturonase, grey curve) were grown on a mixture of glucose (4 g/L) and AP-he (20 g/L) as carbon sources. AB33P5Δ was supplemented with c-Tr (yellow curves). **A** OTR of biological duplicates (green and yellow curves). For clarity reasons, the RQ is only shown for OTR > 2 mmol/L/h. Black and grey curves without symbols show the residual AP-he, calculated from the overall consumed oxygen as described in Chapter 2. End of AP-he consumption was defined by the RQ drop below 1. Culture conditions: modified Verduyn medium, 0.2 M MOPS, pH 6.0, 250 mL flask, filling volume 20 mL, shaking frequency 300 rpm, shaking diameter 50 mm, initial OD₆₀₀ = 0.6, temperature 30 °C

xxxiv Appendix

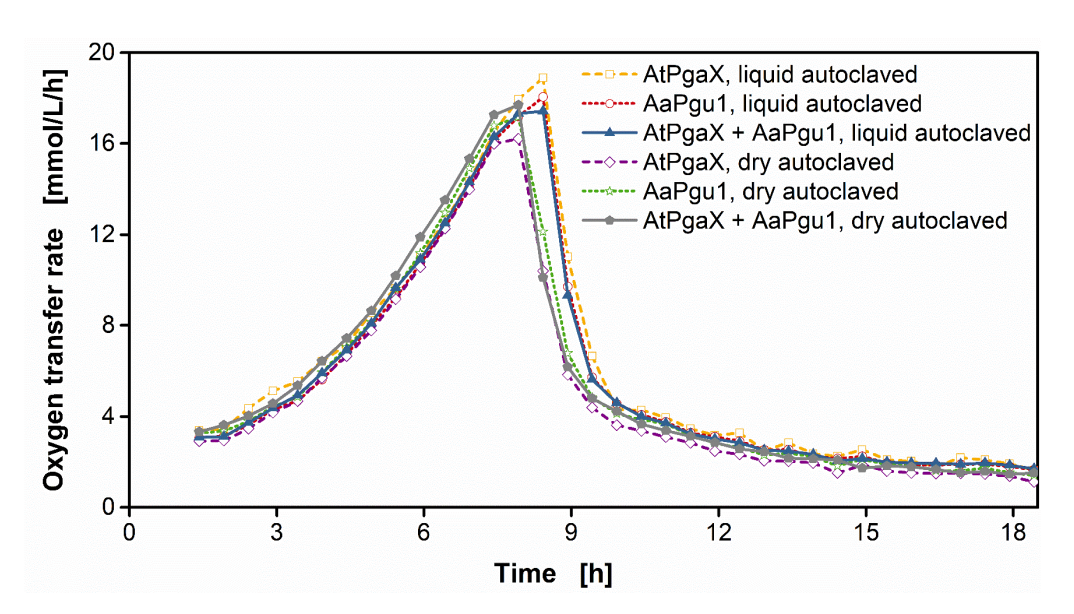


Figure A 13: Axenic and co-fermentation of *U. maydis* on differently pretreated sugar beet pulp. The strains AB33P5 Δ R/AaPgu1 (endo-polygalacturonase) and AB33P5 Δ R/AtPgaX (exo-polygalacturonase) were grown on a mixture of glucose (4 g/L) and sugar beet pulp (20 g/L) as carbon sources without addition of external enzymes. Sugar beet pulp was filled in shake flask and autoclaved either dry or with 10 mL of water. OTR over time. Culture conditions: modified Verduyn medium, 0.2 M MOPS, pH 6.0, 250 mL flask, filling volume 20 mL, shaking frequency 300 rpm, shaking diameter 50 mm, initial OD₆₀₀ = 0.6 (ratio 5:1 for AB33P5 Δ R/AtPgaX : AB33P5 Δ R/AaPgu1 co-fermentation), temperature 30 °C